Copyright Warning & Restrictions

The copyright law of the United States (Title 17, United States Code) governs the making of photocopies or other reproductions of copyrighted material.

Under certain conditions specified in the law, libraries and archives are authorized to furnish a photocopy or other reproduction. One of these specified conditions is that the photocopy or reproduction is not to be "used for any purpose other than private study, scholarship, or research." If a, user makes a request for, or later uses, a photocopy or reproduction for purposes in excess of "fair use" that user may be liable for copyright infringement,

This institution reserves the right to refuse to accept a copying order if, in its judgment, fulfillment of the order would involve violation of copyright law.

Please Note: The author retains the copyright while the New Jersey Institute of Technology reserves the right to distribute this thesis or dissertation

Printing note: If you do not wish to print this page, then select "Pages from: first page # to: last page #" on the print dialog screen

ABSTRACT

PERVAPORATION-ASSISTED ESTERIFICATION OF SALICYLIC ACID

by
Chaiya Chandavasu

The coupling of a pervaporation membrane unit with a reactor has been investigated as a means of improving the overall process efficiency. As model system, the esterification of salicylic acid with methanol in the presence of a homogeneous catalyst was studied in a unit consisting of a batch reactor externally coupled with a pervaporation module containing a composite poly(vinyl alcohol) membrane. The reaction was carried out at temperatures between 336 and 345 K. The catalyst was sulfuric acid at concentrations varying from 0.5 to 2.0 molar. Various initial molar ratios (θ_B) of methanol and salicylic acid, ranging from 8 to 50, were used. The by-product, water, was selectively and continuously removed from the reaction mixture by pervaporation. Consequently, the reaction processing time was reduced by about 60% compared to that in a conventional batch reactor. At 345 K, almost complete conversion was attained for an initial molar ratio of 8 within 10 h in the integrated system. Experiments performed at 341 K and $\theta_B = 8$ with different membrane areas showed that the processing time needed for 95% conversion of the salicylic acid drops from 30 h in the absence of the pervaporation membrane to 13 h with a membrane having a specific surface area of 66 m^{-1}.

A mathematical model, written in terms of operating variables and design parameters of the system, was developed to provide a fundamental understanding of the behavior of the pervaporation-integrated reactor. The mathematical model takes into

consideration details of the reaction kinetics. To validate the model, independent batch kinetic experiments were performed with different molar ratios (θ_B) and catalyst concentrations at different temperatures. The rate constant of the forward reaction was found to have a linear dependence on the catalyst concentration. The model was used successfully in describing the performance of the integrated (pervaporation-assisted) system. The validated model can now be used in simulation studies for parameter sensitivity and optimization purposes.

The coupling of the pervaporation unit with the chemical reactor was shown to be an efficient technique for enhancing performance of organic esterification processes. Moreover, it is easy to scale up and it contributes to pollution prevention by increasing conversion, and reducing the consumption of solvents and energy.

PERVAPORATION-ASSISTED ESTERIFICATION OF SALICYLIC ACID

by
Chaiya Chandavasu

A Thesis
Submitted to the Faculty of
New Jersey Institute of Technology
in Partial Fulfillment of the Requirements for the Degree of
Master of Science in Chemical Engineering

Department of Chemical Engineering,
Chemistry, and Environmental Science

October 1997

APPROVAL PAGE

PERVAPORATION-ASSISTED ESTERIFICATION OF SALICYLIC ACID

Chaiya Chandavasu

Dr. Kamalesh K. Sirkar, Thesis Advisor — Date
Professor of Chemical Engineering, Chemistry, and Environmental Science , NJIT

Dr. Basil C. Baltzis, Thesis Advisor — Date
Professor of Chemical Engineering, Chemistry, and Environmental Science , NJIT

Dr. Henry Shaw, Committee Member — Date
Professor of Chemical Engineering, Chemistry, and Environmental Science , NJIT

BIOGRAPHICAL SKETCH

Author: Chaiya Chandavasu

Degree: Master of Science in Chemical Engineering

Date: October 1997

Date of Birth: July 14, 1973

Place of Birth: Bangkok, Thailand

Undergraduate and Graduate Education:

- Master of Science in Chemical Engineering,
  New Jersey Institute of Technology, Newark, NJ, 1997

- Bachelor of Science in Chemistry,
  Mahidol University, Bangkok, Thailand, 1994

Major: Chemical Engineering

Presentations and Publications:

Chandavasu C., Poddar T. K., Baltzis B. C., and Sirkar K. K. "Pervaporation Assisted-Esterification of Salicylic Acid." *Engineering Foundation Conference on Clean Products and Processes*. San Diego, CA, 2 June 1997.

This thesis is dedicated to my beloved parents
for their love, encouragement, and unceasing support

ACKNOWLEDGMENT

The author wishes to express his sincere gratitude to his supervisors, Professor Kamalesh K. Sirkar and Professor Basil C. Baltzis, for their many suggestions and criticism throughout this research.

Special thanks to Professor Henry Shaw for serving as a member of the committee.

The author is grateful to the Novartis Pharmaceuticals Corporation for initial funding of the research, to the Emission Reduction Research Center and Membrane Separations Program at New Jersey Institute of Technology for providing further and continued funding for this project.

And finally, the author wishes to acknowledge the members of the Membrane Separations Laboratory at New Jersey Institute of Technology for their assistance and suggestions.

TABLE OF CONTENTS

TABLE OF CONTENTS
(Continued)

LIST OF TABLES

LIST OF TABLES
(Continued)

LIST OF FIGURES

LIST OF FIGURES
(Continued)

LIST OF FIGURES
(Continued)

LIST OF SYMBOLS

a	:	Rate reduction parameter, m^3/mol
A_m	:	Effective membrane area, m^2
C_i	:	Concentration of species i in reaction mixture, mol/m^3
C_i^*	:	Concentration of species i in membrane, mol/m^3
C_{A0}	:	Initial concentration of limiting reactant (salicylic acid), mol/m^3
d_f	:	Film thickness of gas chromatography capillary column, μm
D_i	:	Diffusivity of component i in membrane, m^2/s
E	:	Activation energy, J/mol
ΔG^*	:	Free energy of activation, J/mol
h	:	Planck's constant, J/s
ΔH°	:	Reaction enthalpy, J/mol
ΔH^*	:	Activation enthalpy, J/mol
J_i	:	Permeation flux through membrane, mol/(m^2.s)
$\boldsymbol{k}$	:	Boltzmann constant, J/K
k_0	:	Frequency factor of forward rate constant, m^3/(mol.h)
k_b	:	Backward reaction rate constant, m^3/(mol.s)
k_f	:	Forward reaction rate constant, m^3/(mol.s)
k_{f0}	:	Initial forward reaction rate constant, m^3/(mol.s)
K_1	:	Defined in equation 2.4
K_2	:	Defined in equation 2.5
K_e	:	Equilibrium constant, dimensionless

LIST OF SYMBOLS
(Continued)

M_i : Molcular weight of species *i*, g/mol

N_i : Amount of species *i* in reaction mixture, mol

P : Permeability coefficient, m/s

r : Reaction rate, mol/(m^3.s)

R : Gas constant, J/(mol.K)

ΔS° : Reaction entropy, J/(mol.K)

ΔS^* : Activation entropy, J/(mol.K)

t_{90} : Calculated time required to obtain 90% conversion of salicylic acid, h

t_{95} : Calculated time required to obtain 95% conversion of salicylic acid, h

T : Temperature, K

V : Volume of reaction mixture, m^3

V_0 : Initial volume of reaction mixture, m^3

x_i : Molar concentration of component *i* in the feed, mol/L

X_A : Conversion of salicylic acid, dimensionless

X_{Ae} : Equilibrium conversion of salicylic acid, dimensionless

y_i : Molar concentration of component *i* in the permeate, mol/L

Greek letters

α : Selectivity factor of membrane defined by equation 4.3

δ : Membrane thickness, m

LIST OF SYMBOLS
(Continued)

θ_i	:	Ratio of initial concentration of component *i* to initial concentration of the limiting reactant, dimensionless
ξ	:	Defined in equation 2.23
ρ_i	:	Density of species *i*, g/m^3
υ	:	Defined in equation 2.24

Subscripts

A	:	Salicylic acid (limiting reactant)
B	:	Methanol
cat	:	Catalyst (sulfuric acid)
E	:	Methyl salicylate
W	:	Water
i	:	A, B, E, or W

CHAPTER 1

INTRODUCTION

1.1 General

Although the active components of many pharmaceutical products are obtained via fermentation processes, the overwhelming majority of drugs in the marketplace are manufactured by synthetic organic processes. The chemical reactions employed in such synthesis processes are mostly heterogeneous; liquid-liquid and liquid-solid reactions dominate although gas-liquid reactions, including catalytic hydrogenations etc., are also encountered involving gaseous reagents and/or by-products. Achievement of appropriate reaction rates, selectivity and conversion requires consideration of a number of aspects regarding reactor design, mixing, product purity, product stability, reaction intermediates, etc. Novel reactor structures, such as integration of separation with reaction via membranes are expected to facilitate efficient production of desired products in larger scale organic syntheses in pharmaceutical industry via easy scale-up and concomitant pollution prevention.

In recent years, membrane separation processes have been combined with chemical reaction into a single process unit so as to enhance process performance. Various applications of membrane processes in reaction engineering are of interest. Extensive investigations have been carried out on hydrogen-permeable membrane reactors applied to reversible gas-phase reactions (Sun and Khang, 1988; Ioannides and Gavalas, 1993; Ziaka *et al.*, 1993a,b; Gao *et al.*, 1993, 1995; Gobina and Hughes, 1996). Nevertheless, relatively fewer recent applications have been reported on liquid-phase reversible reactions due to lack of suitable membranes having satisfactory permselectivity

and chemical resistance. Ultrafiltration membranes are too porous for efficient separation of small liquid molecules, while reverse osmosis membranes are likely to require a high operating pressure due to the high osmotic pressure of the reaction mixtures. Pervaporation, a novel membrane technique mainly used for dehydration of solvents, organic-organic separations, and recovery of volatile solvents from wastewater (Huang, 1991), appears to be an appropriate choice for this type of application.

Pervaporation is one of the membrane processes that can be employed for the separation of liquid mixtures that are difficult or not possible to separate by conventional methods. The pervaporation process can be considered as a unit operation with significant potential for various types of solutions. In the pervaporation process, the feed mixture is maintained in contact with one side of a permselective dense membrane and the permeate is continuously removed from the other side as a low-pressure vapor. The activity difference is generally maintained by creating a high vacuum on the permeate side in such a way that the pressure is kept below the vapor pressure of at least one component of the liquid in contact with the upstream phase of the membrane. A schematic of the pervaporation process is shown in Figure 1.1.

In this process volatile species in the reaction zone are selectively vaporized through a membrane which acts as a solid extracting phase. One of the potential applications of pervaporation process is to use it for driving an equilibrium-limited reaction. The separation membrane is a permselective barrier that allows selective permeation of the designated component from a liquid mixture. Thus, an idealized membrane reactor or its equivalent that integrates a membrane unit with a batch reactor, is expected to improve the conversion of kinetically or thermodynamically limited

reactions. The reaction enhancement occurs through controlled removal of one or more product species from the reaction zone. Like reactive distillation, the membrane reactor is another technique for achieving conversions above the equilibrium value.

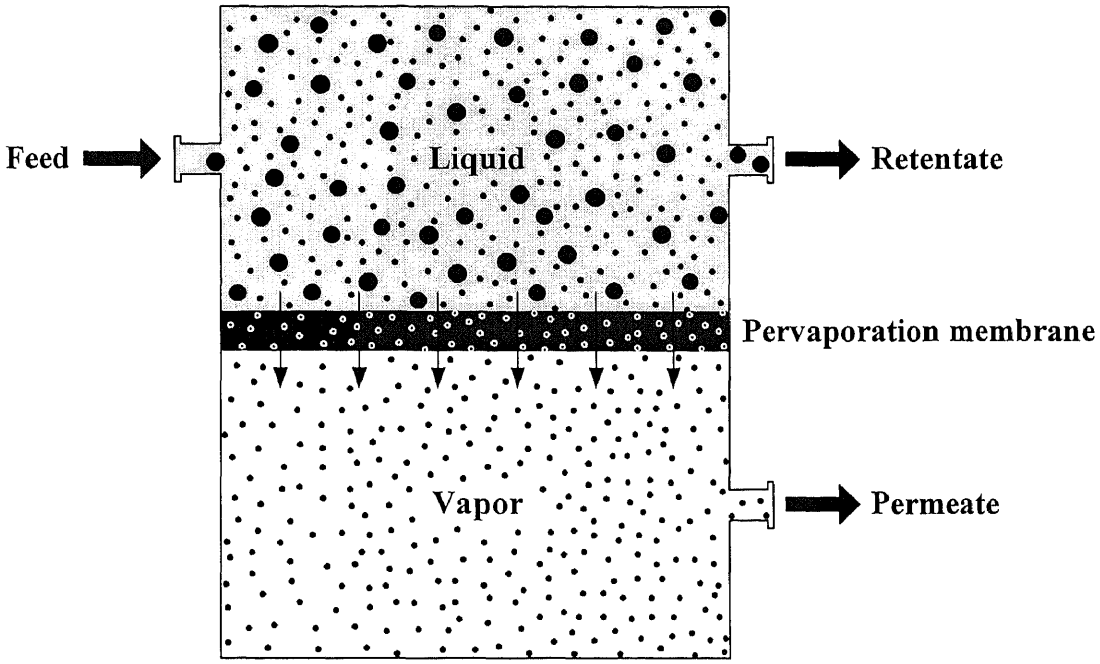

Figure 1.1 Schematic of the Pervaporation Process

In recent years, the pervaporation process has attracted attention due to the development of new and better polymeric or polymeric/composite type membranes, which are suitable for reaction engineering application. The availability of pervaporation membranes, which can withstand high temperature and severe chemical environments, has resulted in wide ranging applications utilizing the concept of membrane reactors.

In the pervaporation process, only the dense layer of the membrane contributes to separation of the mixture. Mass transport in pervaporation is generally described by a solution-diffusion mechanism which consists three consecutive steps: 1) selective sorption into the membrane on the feed side; 2) diffusion of the permeable molecules

through the membrane; 3) desorption of the permeate into a vapor phase at the downstream surface of the membrane. The driving force for permeation is the concentration gradient of the penetrants across the membrane. In this process the mass transport through the membrane is induced by maintaining a low vapor pressure on the downstream side, thereby eliminating the effect of osmotic pressure. The concept of using pervaporation to remove by-product species from reaction mixtures was proposed by Jennings and Binning (1960); however the interest in pervaporation-based membrane reactors was renewed recently when pervaporation proved to be a feasible separation technique in the chemical processes. Presently, pervaporation is best applied to dehydration of organic solvents, and the dehydration membranes normally work best when the water content in the feed mixture is not high. Thus, reversible reactions that produce by-product water are suitable applications of pervaporation for reaction rate enhancement.

Esterification of carboxylic acids with alcohols is a typical example of a reversible reaction that produces by-product water. The yield of the desired product for this type of reaction is generally low due to limits imposed by thermodynamic equilibrium. In some cases, reaction rates and extent of the equilibrium are limited by structures of the molecules.

Considering a catalytic esterification reaction scheme of the type:

$$A + B \overset{H^+}{\rightleftharpoons} C + D$$

where C is the desired ester product and D is the by-product water. By nature of this type of equilibrium-limited reaction, a conventional batch reactor will operate at a low

conversion for product C if the forward reaction-rate constant is of the same order of magnitude as the backward reaction rate constant. If, however, a membrane reactor is employed as shown in Figure 1.2 wherein the by-product water is removed through the permselective membrane from the reaction zone to the other side of the membrane, the reaction will proceed in the forward direction; therefore high conversion is expected to be attained in a reasonably short period.

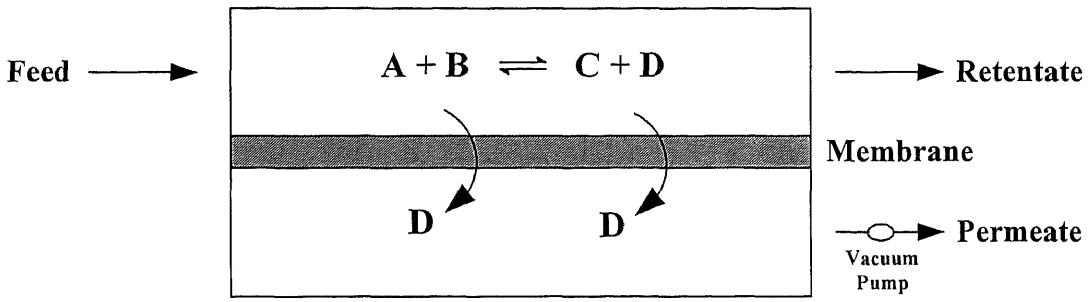

Figure 1.2 Membrane Reactor Schematic for By-product Withdrawal in a Reversible Reaction

To achieve a high ester yield, it is common to drive the position of the equilibrium to the ester side by either using a large excess of one of the reactants (usually the alcohol) or using other techniques such as reactive distillation to accomplish in situ removal of product(s) (Reid, 1952). The use of a large excess of reactant leads to an increase in cost for subsequent separation operations, while reactive distillation is only effective when the difference between the volatility of the product species and the reactant species is sufficiently large. Furthermore, distillation will require a substantial amount of energy due to the large reflux ratios needed when water is removed from low-boiling alcohols. In the cases where the reaction mixtures form an azeotrope, a simple reactive distillation configuration is insufficient. Besides, in reactive distillation the preferred temperature

range of reaction should match that for the distillation (deGarmo *et al.*, 1992). The optimum operating conditions cannot be determined generally by the reaction kinetics and/or thermodynamics, but are subject to the constraint of the temperature applicable for performing the distillation.

Due to the fact that in pervaporation-based membrane separation only the heat of vaporization of the permeating components has to be supplied, membrane separation can be considered to be more energy-efficient and economically competitive than conventional separation means such as distillation. This is due to the fact that, in practice, the process performance and energy consumption in reactive distillation are often dominated by distillation operations (Reid, 1952). Dams and Krug (1991) reported the production of ethyl acetate in a batch process; a pervaporation unit equipped with a 250-m^2 poly(vinyl alcohol)-based membrane was integrated with the reactor. The energy costs for different dehydration methods (Table 1.1) were estimated in comparison with a distillation-alone process. As shown in Table 1.1, dehydration in the pervaporation-integrated membrane reactor costs only 7% of that in conventional distillation.

Table 1.1 Relative Energy Costs for Dehydration by Different Configurations in the Esterification of Acetic Acid with Ethanol (Dams and Krug, 1991)

Configuration mode	Cost
Distillation only	100
Pervaporation + distillation	42
Pervaporation	22
Vapor permeation	22
Membrane-integrated reactor	7

In addition, membrane-integrated reactor operation becomes easier and continuous while membrane-unit scale-up problems are virtually eliminated since membrane units are modular.

Pervaporation-integrated reactors are expected to provide a favorable alternative due to the following considerations:

(1) Pervaporation technique with an appropriate membrane can be operated at a temperature that matches the optimal temperature for desired reaction.

(2) Pervaporation process provides a cost-effective means of separating the products. This is due to the fact that in pervaporation only a fraction of feed that permeates through the membrane undergoes phase change from liquid to vapor and, therefore, energy consumption is generally low as compared to conventional separation methods.

(3) Pervaporation is a rate-controlled separation process, and the separation efficiency is not limited by relative volatility as in distillation.

The last feature is characteristically important for reactions involving biological systems. For example, enzymatic esterifications normally have temperature constraints imposed by enzyme stability.

The reactor configuration and the nature of the membranes employed will depend on the system chosen, the reaction conditions, and the nature of the catalyst. Hydrophilic membranes that preferentially permeate water and retain small organic molecules can be employed in pervaporation processes. In recent years, many researchers have studied the feasibility of employing pervaporation membranes in reaction engineering. By utilizing the concept of membrane reactors, conversion in reversible reactions could be enhanced

and the processing time could be reduced substantially. In the case of acid-catalyzed esterification reactions, one can employ a hydrophilic membrane to remove water from an organic reaction mass by using vacuum-based pervaporation (Neel *et al.*, 1991). Various types of polymeric pervaporation membranes like polyimide, Chitosan, Nafion, etc. were tested in membrane reactors for esterification of oleic acid with ethanol (Kita *et al.*, 1987, 1988; Okamoto *et al.*, 1993). In addition, pervaporation membrane reactors have been studied for esterification of acetic acid with ethanol (Zhu *et al.*, 1996), tartaric acid with ethanol (Keurentjes *et al.*, 1994), oleic acid with butanol (Kwon *et al.*, 1995) and valeric acid with ethanol (Ni *et al.*, 1995) with various inorganic acids or lipases as catalysts. In some cases the membrane itself may act as a catalyst or the catalyst may be impregnated on the membrane (Bagnell *et al.*, 1994). Catalytically active pervaporation membranes have potential advantages. However their selectivity for alcohol over water make them still inapplicable for small molecular weight alcohols such as methanol. Waldburger *et al.* (1994) studied heterogeneously catalyzed acetic acid/ethanol esterification in a continuous flow reactor using a commercial poly(vinyl alcohol)-based membrane. After the whole reservoir volume had been recycled three times at 80°C (corresponding to a residence time of 15 h) the reactor conversion achieved was 98.7%. However, there was no attempt by the authors to mathematically model the experimental data.

Esterification is a complex reaction. The rate at which different acids are esterified as well as equilibrium conversion depend on the structure of the molecules and type of functional substituents of the acids and alcohols; therefore data on rates of

reaction, mechanisms, and the extent of reaction for specific reactions are essential for understanding the behavior of the pervaporation-coupled esterification.

The membrane in the pervaporation module, which is to be coupled with the reactor and separation unit, has to be suitable for the liquid mixture contacting the feed side of the membrane. Pervaporation membranes employed in this type of application usually are of the composite type (Figure 1.3) as they can combine very thin and highly selective separation layers with mechanically rigid and thermally stable backing layers.

Membranes add unique features to a membrane reactor. Membrane units provide very large surface area per unit volume of the device. As a result, overall transfer rates for separation through the membrane device can be very high, almost an order of magnitude larger than in conventional devices. The residence time of the reaction mixture can also be controlled easily over a wide range varying from a few seconds to much longer by controlling the flow rates through the membrane device.

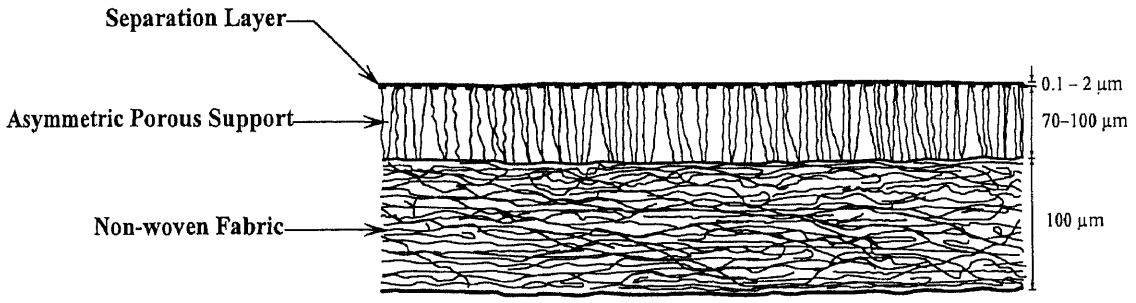

Figure 1.3 Cross-section of a Composite Pervaporation Membrane

A type of system of great relevance would be that shown in Figure 1.4. This type of system focuses on selective removal of a volatile product that could be water (as in

one-step esterification reaction) from the reaction system via a membrane. The volatile product is removed by pulling a vacuum on one side of the pervaporation membrane. This type of membrane-integrated reactor provides an illustration of the many capabilities of membrane-integrated reactors in synthetic pharmaceutical processes. Membrane-integrated reactors may be introduced profitably to improve productivity and yield while pollution prevention is achieved simultaneously in such a system and process.

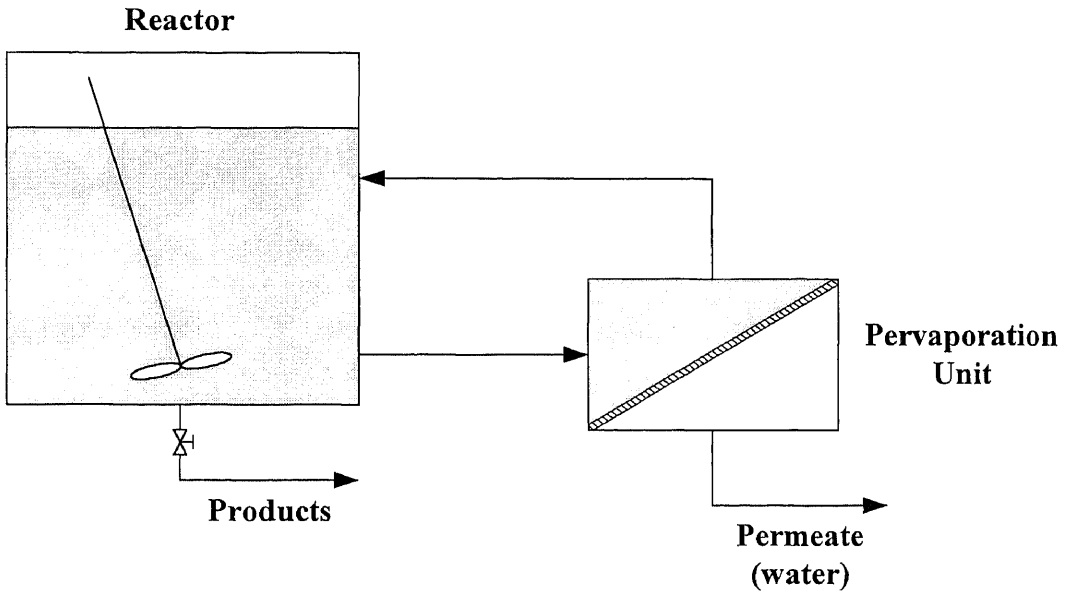

Figure 1.4 Schematic of the Pervaporation-Integrated Batch Reactor

1.2 Scope of the Thesis

A three-step approach has been adopted in this thesis:

a) Selection of reaction system and membrane.

b) Modeling of membrane-integrated reactors.

c) Experimental demonstration of membrane-integrated reactor performance and model validation.

Although, esterification reactions represent a significant group of reactions commonly found in the pharmaceutical industry, kinetic data on homogeneous esterification of aromatic carboxylic acids are relatively scarce in the literature. The acid-catalyzed esterification of salicylic acid with methanol (equation 1.1) was chosen to be the model reaction system for this study. This reaction system was selected because the desired ester product, methyl salicylate, is one of the most important esters in the pharmaceutical industry. Commercially, it is widely used as the pain-relieving ingredient in liniments.

One of the reactants in this esterification reaction, salicylic acid, is an aromatic carboxylic acid which is relatively less reactive than aliphatic carboxylic acids. Due to the fact that most aromatic carboxylic acids require long reaction periods and have low yields, new techniques that can improve process performance are of great importance.

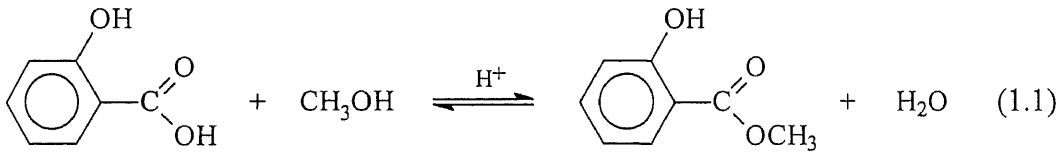

(1.1)

The aim of the research work was to obtain a better understanding of the behavior and kinetics of the esterification reaction between salicylic acid and methanol and a better understanding of the pervaporation-facilitated esterification between these two species. In order to obtain a clear picture of the influence of the different parameters, the systems, membranes, processes and reactors need to be studied along with synthetic organic processes.

The unit schematically shown in Figure 1.4 was used during the course of this study. During experiments various operating parameters (temperature, relative reactant composition, catalyst concentration) as well as design parameters (membrane surface area) were varied and their impact on process performance was investigated.

The process was described with a mathematical model which accounts for kinetic and mass transfer characteristics. In order to use and validate the model, kinetic constants were obtained from detailed, independent experiments under batch conditions. In these experiments, initial concentrations as well as temperature were varied. The model yielded a successful interpretation of the data obtained with the membrane integrated reactor. The model has led to a better understanding of the overall process and can be used in predicting desired regimes for the operating parameters.

In order to experimentally show the impact of the membrane integration on the process, experiments were also performed with the unit shown in Figure 1.4 in the absence of the membrane.

CHAPTER 2

MODEL DEVELOPMENT AND THEORETICAL CONSIDERATIONS

This chapter deals with the development of mathematical models for batch and pervaporation-assisted esterification processes, their numerical solutions and other theoretical considerations required to interpret the experimental results.

2.1 Kinetic Model for Batch Esterification Reaction

Esterification is a reversible reaction in which a carboxylic acid (*A*) reacts with an alcohol (*B*) in the presence of an acid catalyst to form the ester and water. This type of reaction can be written as

$$\underset{(A)}{RCOOH} + \underset{(B)}{R'OH} \overset{H^+}{\rightleftharpoons} \underset{(E)}{RCOOR'} + \underset{(W)}{H_2O} \qquad (2.1)$$

The reaction above involves a two-step mechanism when sulfuric acid is the catalyst used. The first step in esterification is the protonation of the carboxylic group of carboxylic acid to form a reaction intermediate, which cannot be separated:

$$A + H_2SO_4 \underset{k_2}{\overset{k_1}{\rightleftharpoons}} AH^+ \cdot HSO_4^- \qquad (2.2)$$

In the second step, which is the rate-determining one, the protonated carboxylic acid reacts with alcohol to form ester, water, and the regenerated catalyst:

$$AH^+ \cdot HSO_4^- + B \underset{k_4}{\overset{k_3}{\rightleftharpoons}} E + W + H_2SO_4 \qquad (2.3)$$

The concentration-based equilibrium constants of equations 2.2 and 2.3 can be written as

$$K_1 = \frac{C_{AH^+ \bullet HSO_4^-}}{C_A C_{H_2SO_4}} \tag{2.4}$$

$$K_2 = \frac{C_E C_W C_{H_2SO_4}}{C_{AH^+ \bullet HSO_4^-} C_B} \tag{2.5}$$

The rate of ester production according to equation 2.3 is

$$\frac{dC_E}{dt} = k_3 C_{AH^+ \bullet HSO_4^-} C_B - k_4 C_E C_W C_{H_2SO_4} \tag{2.6}$$

Rearranging equation 2.4 and substituting for the concentration of the intermediate into equation 2.6 gives

$$\frac{dC_E}{dt} = k_3 K_1 C_A C_B C_{H_2SO_4} - k_4 C_E C_W C_{H_2SO_4} \tag{2.7}$$

Combining k_3 and K_1 and setting it as k_5 leads to

$$\frac{dC_E}{dt} = C_{H_2SO_4} \left(k_5 C_A C_B - k_4 C_E C_W \right) \tag{2.8}$$

Setting $C_{H_2SO_4} k_5 = k_f$ and $C_{H_2SO_4} k_4 = k_b$, the rate expression can be written as

$$r = \frac{dC_E}{dt} = k_f C_A C_B - k_b C_E C_W = k_f \left(C_A C_B - \frac{1}{K_e} C_E C_W \right) \tag{2.9}$$

where k_f and k_b are the rate constants for the forward and backward reaction in equation 2.1 respectively, and K_e is the equilibrium constant which can be defined as the ratio of the forward and backward rate constants (equation 2.10). Subscripts A and B refer to the two reactants, acid and alcohol, and subscripts E and W refer to ester and water, respectively. The equation 2.9 is the power law model, which can be used to describe the reversible homogeneous reaction.

$$K_e = \frac{k_f}{k_b} = \frac{C_E C_W}{C_A C_B} \tag{2.10}$$

However, the esterification of salicylic acid with methanol in the presence of sulfuric acid does not follow the rate expression (equation 2.9) precisely. This implies that the real reaction mechanism is not given by equations 2.2 and 2.3. Water produced from the reaction reduces the reaction rate constant. Accordingly the effect of water produced on the reaction rate has to be taken into account. Okamoto *et al.* (1993) proposed that the forward rate constant is a function of water concentration in the reaction mixture. The expression for the forward rate constant can be written as

$$k_f = \frac{k_{f0}}{1 + aC_W} \tag{2.11}$$

where a is the reduction parameter, which is a function of temperature and molar ratio of reactants. Keurentjes *et al.* (1994) have suggested an alternative approach. They have described the reaction rate expressions in terms of activities; such rate expressions as well as the corresponding equilibrium constants are then related to those based on concentrations and additional factors containing activity coefficients. Estimates of activity coefficients were developed based on UNIFAC methods. Their model based on concentrations was better able to describe the data on tartaric acid esterification due to uncertainties in estimations of the activity coefficients.

2.2 Model for Pervaporation-Coupled Esterification

Considering the schematic of Figure 1.4 and assuming isothermal conditions, esterification in the membrane-integrated reactor can be described by the following material balances:

$$\frac{d(C_i V)}{dt} = -r_i V - J_i A_m \tag{2.12}$$

$$C_i \frac{dV}{dt} + V \frac{dC_i}{dt} = -r_i V - J_i A_m \tag{2.13}$$

where subscript i indicates species i, C_i is the molar concentration of species i, J_i is the permeation flux of species i through the membrane, r_i is the rate of disappearance of species i in the reactor due to chemical reaction (equation 2.9), and A_m is the effective membrane area in the pervaporation unit.

The volume of the reaction mixture, V, is given by equation 2.14 according to volume additivity:

$$V = \sum_i \frac{N_i M_i}{\rho_i} \tag{2.14}$$

where N_i is the number of moles of species i in the reaction volume, M_i and ρ_i are molecular weight and density of species i, respectively.

Assume the volume change of the reaction mixture in the system to be given by

$$\frac{dV}{dt} = -\sum_i \frac{J_i M_i}{\rho_i} A_m \tag{2.15}$$

The permeation flux of species i through a pervaporation membrane is usually concentration dependent. From Fick's first law, the permeation flux of species i is given by the expression

$$J_i = -D_i \frac{\partial C_i^*}{\partial \delta} \tag{2.16}$$

where D_i is the diffusivity of species i in the membrane and δ is the membrane thickness. Equations 2.9, 2.11, 2.13, 2.15, and 2.16 are the basic equations describing a batchwise pervaporation membrane-assisted reactor.

Considering the stoichiometry of equation 2.1 and assuming that only water goes through the membrane, one can write,

$$C_A = C_{A0}\frac{V_0}{V}(1 - X_A) \tag{2.17}$$

$$C_B = C_{A0}\frac{V_0}{V}(\theta_B - X_A) \tag{2.18}$$

$$C_E = C_{A0}\frac{V_0}{V}(\theta_E + X_A) \tag{2.19}$$

$$C_W = \frac{C_{A0}V_0(\theta_W + X_A) - \int_0^t J_W A_m dt}{V} \tag{2.20}$$

where X_A is the conversion of the salicylic acid (A) defined by the number of moles of A that have reacted per mole of A fed to the system, θ_B, θ_E, and θ_W are defined as the ratios of initial concentrations of species B, E, and W, respectively, to the initial concentration of A, and V_0 is the initial volume of the reaction mixture.

A material balance on the carboxylic acid yields

$$\frac{d(C_A V)}{dt} = -r_A V - J_A A_m \tag{2.21}$$

The pervaporation membrane does not allow the high molecular weight components pass through, thus the flux of the carboxylic acid, J_A is equal to zero. Rewriting equation 2.21 gives

$$\frac{d(C_A V)}{dt} = -r_A V$$

$$\frac{d[C_{A0}V_0(1-X_A)]}{dt} = -\left[k_f\left(C_A C_B - \frac{1}{K_e}C_E C_W\right)\right]\cdot V$$

$$C_{A0}V_0\frac{dX_A}{dt} = k_f\left[\frac{1}{V}C_{A0}V_0(1-X_A)C_{A0}V_0(\theta_B - X_A) - \frac{C_{A0}V_0(\theta_E + X_A)\cdot C_W}{K_e}\right]$$

$$\frac{dX_A}{dt} = k_f\left[C_{A0}\left(\frac{V_0}{V}\right)(1-X_A)(\theta_B - X_A) - \frac{(\theta_E + X_A)\cdot C_W}{K_e}\right] \qquad (2.22)$$

For the sake of simplicity, nondimensionalize variables C_W and V by defining

$$\xi = \frac{C_W}{C_{A0}} \qquad (2.23)$$

$$\upsilon = \frac{V}{V_0} \qquad (2.24)$$

Equation 2.22 is reduced to

$$\frac{dX_A}{dt} = k_f C_{A0}\left[\frac{(1-X_A)(\theta_B - X_A)}{\upsilon} - \frac{(\theta_E + X_A)\xi}{K_e}\right] \qquad (2.25)$$

Assume a "perfect" water permeable membrane, $J_A = J_B = J_E = 0$. Rewriting equation 2.15 gives

$$\frac{d\upsilon}{dt} = -\left(\frac{A_m}{V_0}\right)\cdot\left(\frac{J_W M_W}{\rho_W}\right) \qquad (2.26)$$

From the relation expressing the concentration of water in the reactor (equation 2.20),

$$C_W = \frac{C_{A0}V_0(\theta_W + X_A) - \int_0^t J_W A_m dt}{V}$$

$$\frac{d(C_W V)}{dt} = C_{A0}V_0 \frac{dX_A}{dt} - J_W A_m$$

$$V\frac{dC_W}{dt} + C_W \frac{dV}{dt} = C_{A0}V_0 \frac{dX_A}{dt} - J_W A_m$$

$$\frac{V}{C_{A0}V_0}\frac{dC_W}{dt} + \frac{C_W}{C_{A0}V_0}\frac{dV}{dt} = \frac{dX_A}{dt} - \frac{J_W A_m}{C_{A0}V_0}$$

$$\xi\frac{d\upsilon}{dt} + \upsilon\frac{d\xi}{dt} = \frac{dX_A}{dt} - \left(\frac{A_m}{V_0}\right)\frac{J_W}{C_{A0}}$$

$$\frac{d\xi}{dt} = \frac{1}{\upsilon}\left[\frac{dX_A}{dt} - \xi\frac{d\upsilon}{dt} - \left(\frac{A_m}{V_0}\right)\frac{J_W}{C_{A0}}\right] \tag{2.27}$$

The initial conditions are

$$\begin{aligned} &\text{at } t = 0, \ X_{A0} = 0 \\ &\text{at } t = 0, \ \upsilon_0 = 1 \\ &\text{at } t = 0, \ \xi_0 = 0 \end{aligned} \tag{2.28}$$

According to Fick's first law (equation 2.16), the permeation flux of water is given by the expression

$$J_W = -D_W \frac{\partial C_W^*}{\partial \delta} \tag{2.29}$$

where D_W is diffusivity of water in the membrane. However, the diffusivity of water is very difficult to determine in the case of pervaporation of the multicomponent mixture. It was reported by David *et al.* (1991) that in the case of pervaporation of an organic solvent containing low amount of water (less than 10% by weight) through a GFT membrane, an almost linear relationship was found between permeation flux and water concentration. In this study, the water concentration in the reaction mixtures is always less than 9.0% by weight, therefore, for the simplicity of analyses, the water flux is assumed to be proportional to the water concentration (equation 2.30).

$$J_W = P_W C_W \tag{2.30}$$

where P_W is the permeance of water.

The set of differential equations (equations 2.25, 2.26, and 2.27), along with equations 2.11, 2.18, 2.19, and 2.30 can be solved simultaneously by using the software package MATHEMATICA® (Wolfram Research, Inc.) to find the concentrations of all species as well as the volume of the reaction mixture as a function of time. Using this software package, a parametric study of this system was performed.

CHAPTER 3

EXPERIMENTAL

3.1 Chemicals

The following chemicals were used in the experiments: methanol, HPLC-grade; salicylic acid, analytical reagent (99.9%); sulfuric acid, reagent grade (96%). These chemicals were purchased from Fisher Scientific Co., Fairlawn, NJ.

3.2 Experimental Setup and Procedure

Two different types of experiments were conducted: (a) simple batch experiments to estimate the equilibrium constant (K_e) and the reaction rate constant (k_f) for the esterification of salicylic acid; (b) experiments with an integrated reactor to determine the effect of pervaporation on the overall process efficiency and the processing time of the reaction.

3.2.1 Batch Esterification

A 1-liter round-bottomed glass flask was used as the batch reactor. The reactor was equipped with a glass reflux condenser to prevent any loss of reaction mass, a long-stem mercury thermometer, a graduated feeding funnel, a sample port with a polytetrafluoroethylene (PTFE)-coated butyl rubber septum and an oil-bath having provision for oil circulation at a constant temperature. The setup was installed on top of a magnetic stirrer. The schematic of the experimental setup for the batch esterification experiments is shown in Figure 3.1. A number of batch esterification experiments between

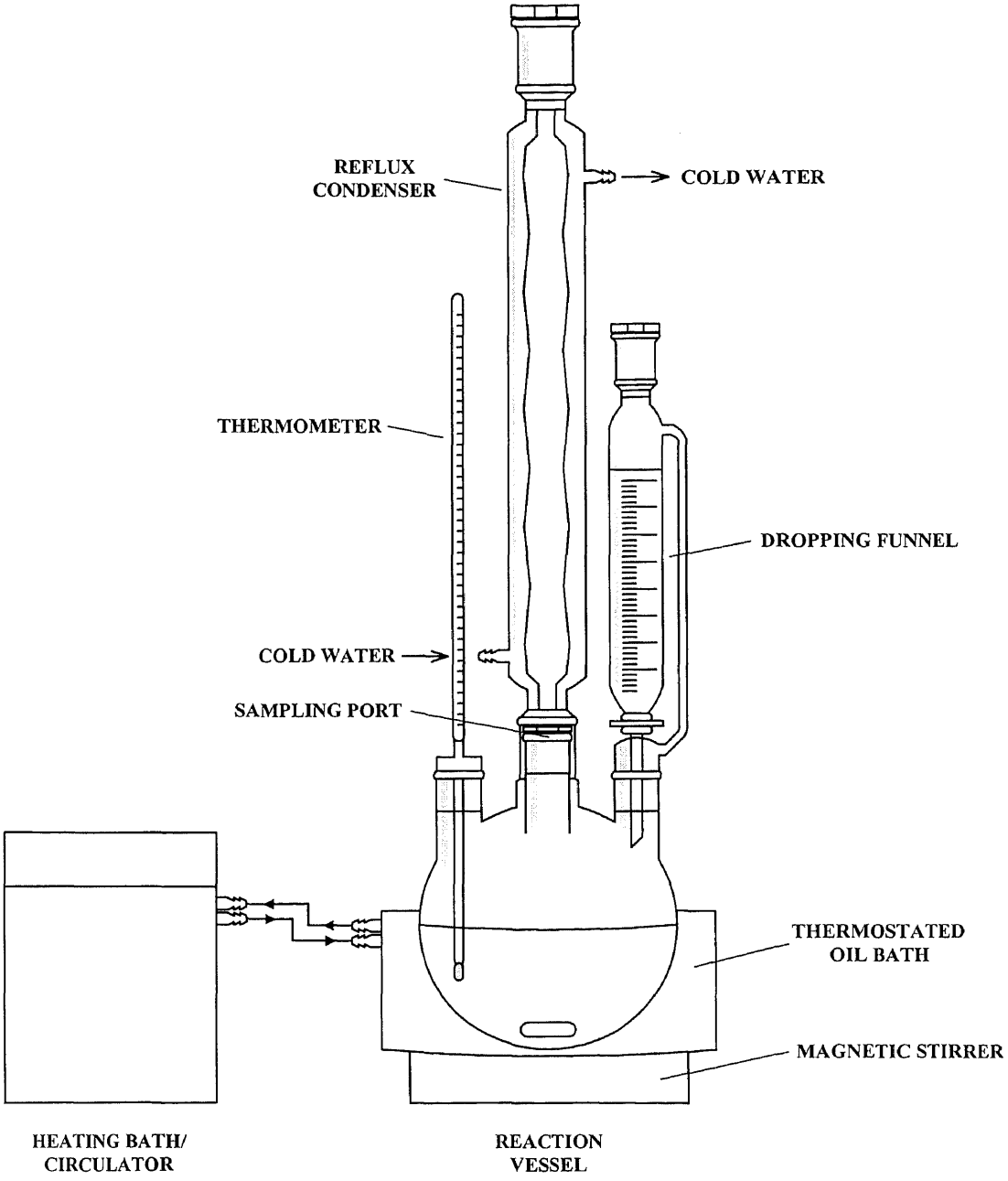

Figure 3.1 Schematic Diagram of the Experimental Apparatus for Esterification without Pervaporation

methanol and salicylic acid were carried out to generate time versus salicylic acid conversion data. These data were analyzed to determine the reaction rate constants.

A known mass of salicylic acid (measured with a chemical balance, Ohaus, Florham Park, NJ) was first taken in the round-bottomed flask. The required quantity of methanol (in excess of the stoichiometric amount) was added to the salicylic acid and the reaction mass was kept under stirring. The temperature of the reaction mass was first raised to a value of 15°C less than the actual reaction temperature, then a predetermined quantity of sulfuric acid was added to the reaction mass through the feeding funnel. Acid addition led to a temperature increase of the reaction mass therefore the rate of acid addition was adjusted to maintain the desired reaction temperature. Approximately 1 mL of reaction mass was collected at definite time intervals through the sample port by means of a syringe. The drawn sample was dispensed immediately into a 2-mL glass sample vial and sealed using a crimp cap. The sample vial was then stored quickly in the deep freezer to stop the reaction. The concentrations of the ester and salicylic acid were determined by a liquid chromatograph after appropriate dilution (4,000-10,000 times depending on reactant composition) of the sample with methanol. A typical batch run lasted for about 8 to 10 h. The sample collected before the addition of sulfuric acid was considered as the sample at time zero. The concentration of sample at time zero was then corrected for volume increment because of the addition of sulfuric acid. Reactions were carried out at different molar ratios of methanol to salicylic acid, temperatures, and catalyst concentrations (sulfuric acid).

3.2.2 Pervaporation-Coupled Esterification

The batch reactor setup described in the previous section was connected to a pervaporation cell via a Masterflex pump (model 7523-20, Cole-Parmer, Barrington, IL) equipped with a FTFE diaphragm pump head (model 7090-42, Bernant, Barrington, IL). All plastic tubing used in the experimental setup was Teflon TFE purchased from McMaster-Carr, New Brunswick, NJ. Type-K flow-through thermocouple probes connected with a digital thermometer (model HH22, Omega Engineering, Stamford, CT) were installed to measure the temperature of the liquid entering and exiting the pervaporation cell (Figure 3.2). An oilless vacuum pump (model UN7236.3, KNF Neuberger, Trenton, NJ) and a permeate condenser were connected to the downstream side of the cell (Figure 3.2). The pervaporation cells (model PTC-6, Carbone Lorraine, Salem, VA) and flat-sheet PVA membranes (model PERVAP 2001) were obtained from GFT, Neunkirchen-Heinitz, Germany. Two pervaporation cells were used for studying the effect of effective membrane area to initial volume ratio. The two cells had effective membrane areas of 130 and 184 cm^2. In early experiments, the pervaporation cell was well insulated to minimize heat losses without using a temperature control unit. In most of the subsequent experiments, the pervaporation unit was installed in a controlled-temperature bath filled with water as the heat carrier liquid. The membranes were cut to proper size to fit inside the cells over a sintered metal plate. The membranes were installed in the pervaporation cells and the vacuum pump was started. After installation of the membranes in the cell, the reaction mixture was fed into the reactor. The feed pump was started and the temperature controller was set at the operating temperature. A typical reaction mass was prepared in the way discussed before. The reaction mixture in the reactor was now heated to the desired temperature. The reaction mass was kept under

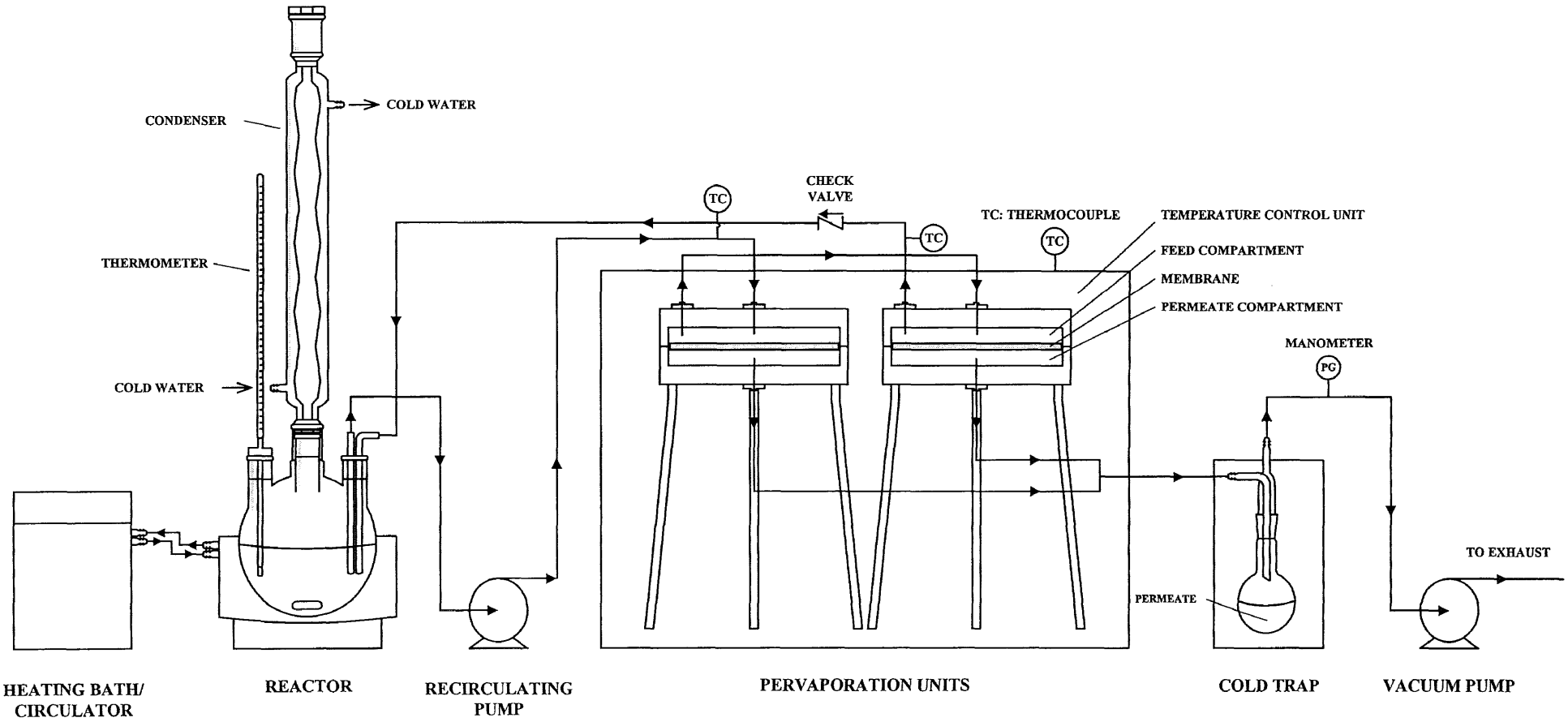

Figure 3.2 Schematic Diagram Showing the Setup for Pervaporation-Assisted Esterification

circulation through the pervaporation cells. The temperature of the reaction mass inside the pervaporation cells was maintained constant at a temperature same as that inside the reactor. When the reaction mass reached a temperature 15°C below the desired operating temperature, sulfuric acid addition was started. A similar sample collection procedure as in the case of simple batch experiments was followed. Although several runs lasted for periods of 22 to 26 h, most runs lasted 8 to 10 h. After the end of a particular run the reaction mass was allowed to cool to room temperature before the setup was dismantled. The membrane was rinsed with methanol followed by deionized water and then soaked with tissue paper to make it dry. A photograph of the setup is shown in Figure 3.3.

3.3 Measurement of the Concentrations of the Ester and Salicylic Acid

The concentrations of salicylic acid and methyl salicylate in the reaction mass were determined in a high performance liquid chromatograph (HPLC). A HP 1090 liquid chromatograph system (Hewlett-Packard, Palo Alto. CA) having an autosampler (model 728, Micromeritics, Norcross, GA), and a variable-wavelength absorbance detector (Hewlett-Packard) was used. A reverse-phase C-18 HPLC column (Chrompack, Raritan, NJ) suitable for the analysis of salicylic acid and methyl salicylate was used in the HPLC device. The specifications of the column used in the investigation are as follows:

Packing material	: Hypersil octadecylsilane (ODS)
Typical particle size	: 5 μm
Length	: 100 mm
Internal diameter	: 3 mm
Outside diameter	: 9 mm
Column material	: glass

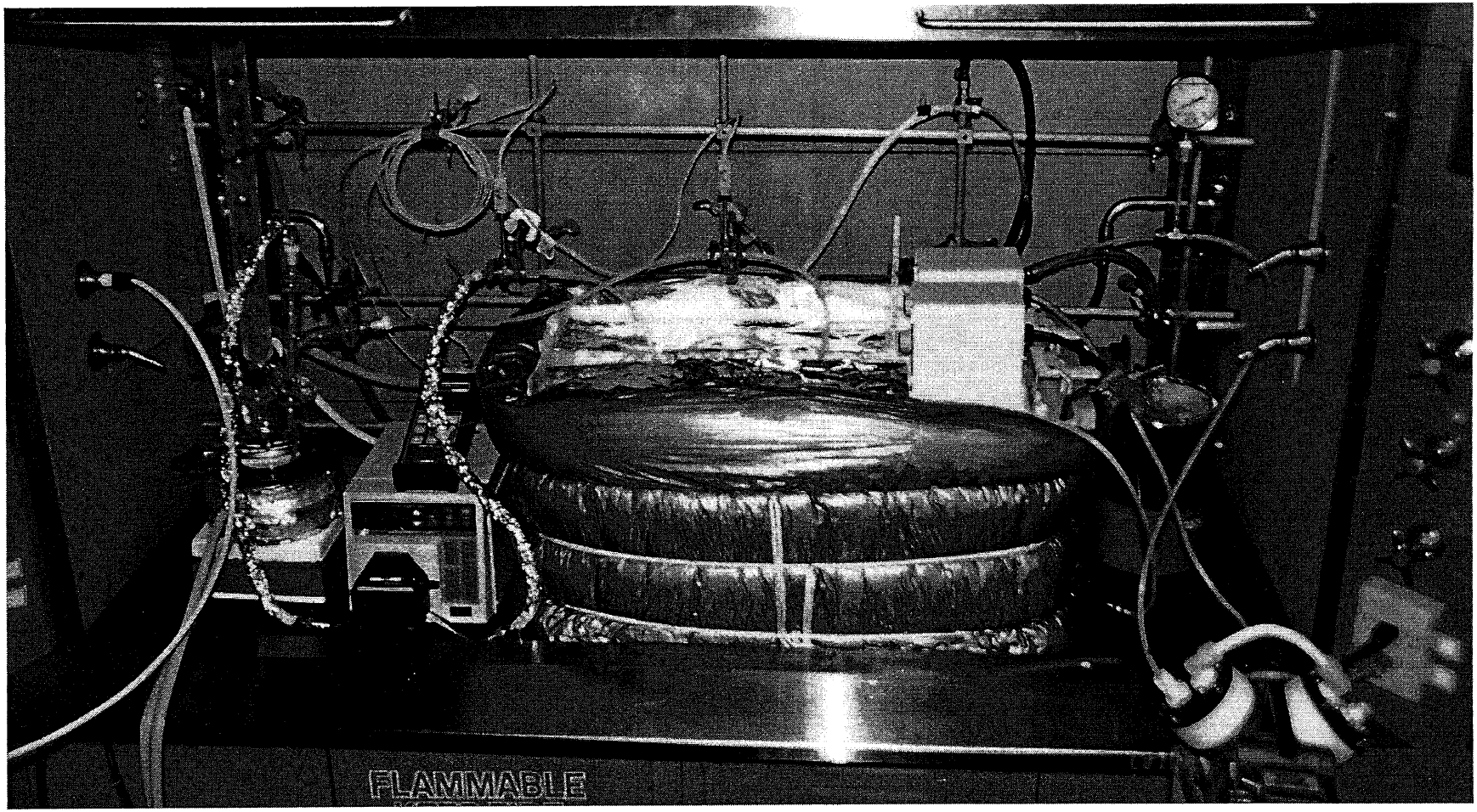

Figure 3.3 Photograph of the Experimental Setup for Pervaporation-Assisted Esterification

A sample from the experiment collected at a definite time was properly diluted with methanol and injected into the analytical column employing the autosampler. Salicylic acid and methyl salicylate components were separated in the column and after the separation, the sample was carried to the detector, where UV absorbance of each component was measured at 280-nm wavelength. Salicylic acid and methyl salicylate were qualitatively determined and their concentrations quantified under the following conditions:

Mobile phase (v/v)	: 60% methanol/ 40% water
Pressure	: 8.2 MPa
Flow rate	: 0.40 cm^3/min
Temperature	: ambient

The conditions were optimized to obtain good chromatographic separation of the salicylic acid and the methyl salicylate peaks. Retention time of each component was determined through comparison with standards. The retention times for standard salicylic acid and methyl salicylate solutions were 1.0 and 3.0 min respectively. An integrator (model 3390A, Hewlett-Packard) incorporated with the HPLC setup calculated the peak areas of the individual compounds. Calibration curves were prepared from fresh standard solutions for both salicylic acid and methyl salicylate to relate their concentrations with the peak areas obtained from the integration unit. The calibrations were checked at intervals separated by 2 to 3 experimental runs. The calibrations of standard salicylic acid and methyl salicylate solutions are shown in Figure 3.4 and 3.5 respectively.

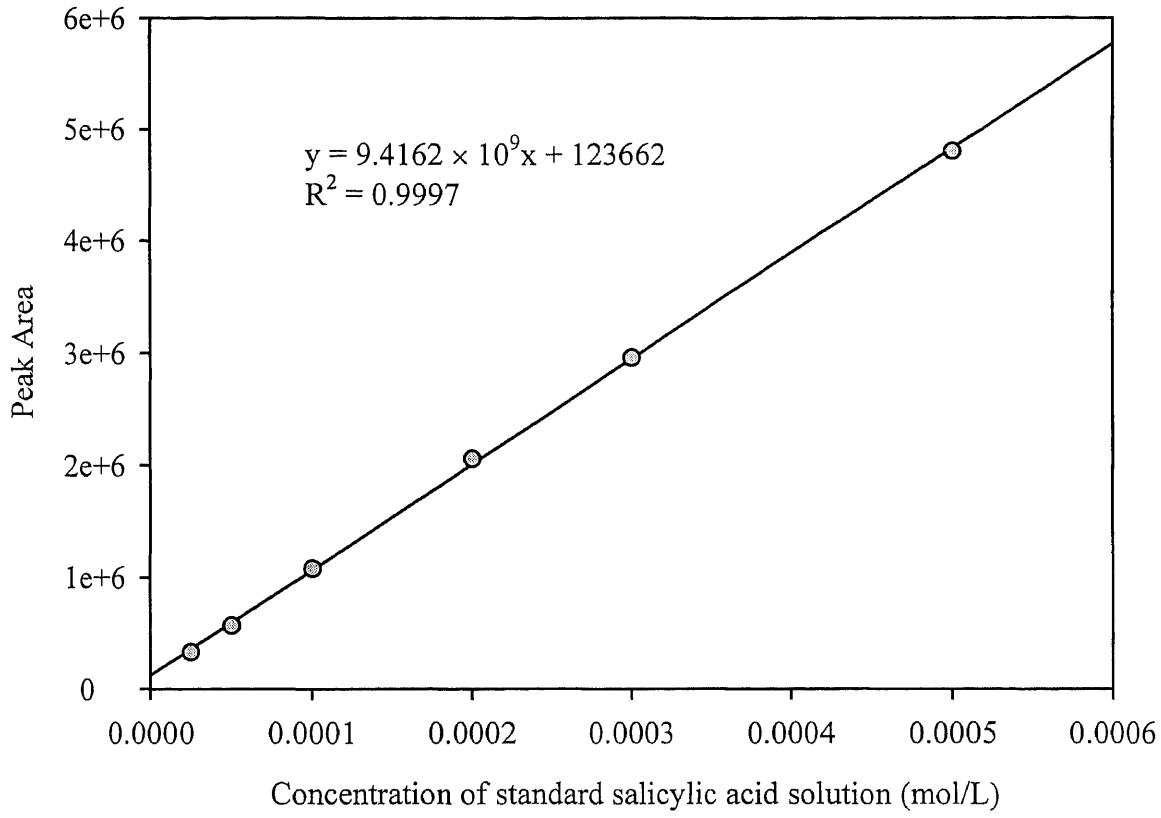

Figure 3.4 Calibration of Standard Salicylic Acid Solution (Peak Area vs. Concentration in mol/L)

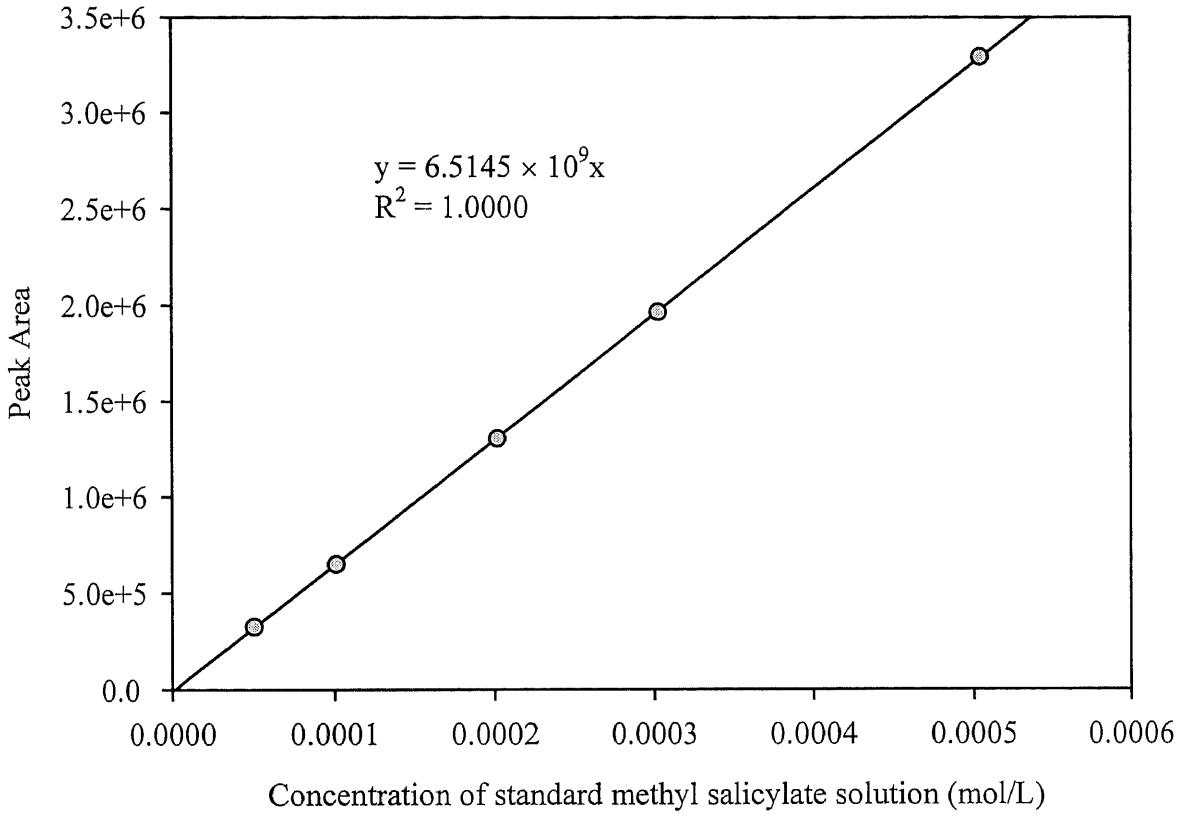

Figure 3.5 Calibration of Standard Methyl Salicylate Solution (Peak Area vs. Concentration in mol/L)

3.4 Permeate Analysis

Analysis of permeate samples was performed using the headspace technique and a HP 5890 Series II gas chromatograph (Hewlett-Packard) equipped with a pressure-programmable, cool on-column injector. A flame ionization detector (FID) operated at 250°C was employed. The headspace gas chromatography (GC) is based on a sampling technique in which the sample is placed in a closed vessel that is equilibrated at an elevated temperature. As a result, volatile and semivolatile compounds that are present in the sample are vaporized and enriched in the volume of gas above the sample (the so-called headspace). An aliquot of the headspace gas is injected into a gas chromatograph. There are two main advantages of this sampling technique. Firstly, by thermostating the sample, volatile compounds are separated from the matrix, which may be a complex mixture of nonvolatile components that are unsuitable for injection into a gas chromatograph. Secondly, volatile compounds are enriched in the gas phase above the sample, enabling the detection of trace-level substances. This technique was applied to determine the methanol content in the permeate samples.

The following procedure was used: A piece of deactivated fused-silica tubing (80 cm × 0.32 mm) (Hewlett-Packard) was pushed through the disk septum of the pressure-programmable, on-column injector. It was passed through the injector into a 5 m × 0.53 mm, Hydroguard FS, capillary precolumn (Hewlett-Packard), and the other end of the deactivated fused-silica tubing was connected to a needle which was pushed through the disk septum of the sample vial (Figure 3.6). The 20-mL headspace vial containing the sample was closed using a PTFE-coated butyl rubber septum (with a star spring and a crimp cap) and thermostated in a heating bath filled with water. After the sample was

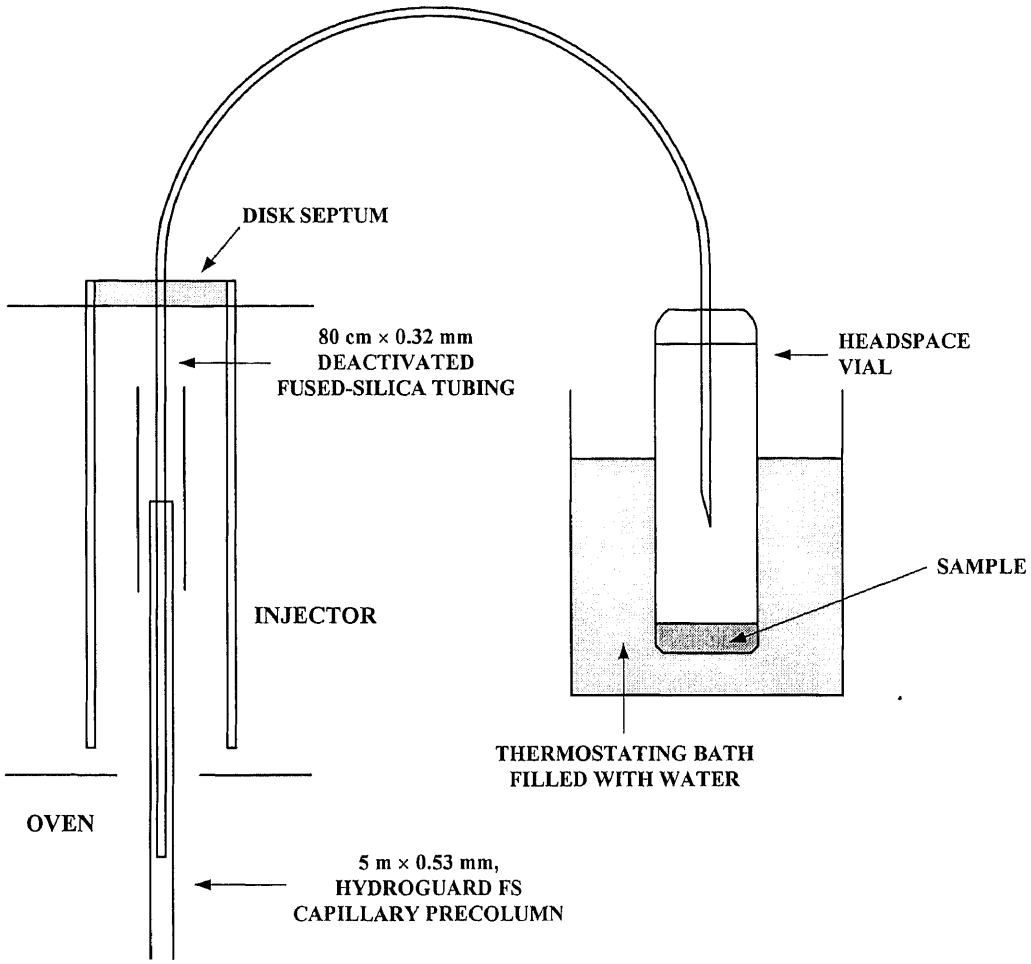

Figure 3.6 Schematic of the Instrumental Setup for Pressure-Balanced Sampling Using the Electronic-Pressure-Controlled, On-Column Injection

equilibrated at the operating temperature, the needle was removed from the septum of an empty vial where it had been in standby position during thermostating and pushed through the septum cap of the sample vial. The carrier gas flowed through the deactivated fused-silica tubing into the headspace of the sample vial and increased the head pressure. After pressurizing the sample for 3 min, the pressure was temporarily decreased by activating a pressure program in the programmable on-column injector. Consequently, the pressure on the column temporarily was lower than the pressure in the headspace vial. Because the sample vial was connected to the column by the deactivated fused-silica tubing, headspace gas containing sample analytes flowed out of the pressurized headspace directly onto the column. The separation was performed utilizing a 30 m × 0.32 mm, 1.0-μm d_f crossbond trifluoropropylmethyl poly(siloxane), fused-silica column that was connected to the precolumn by a glass-seal capillary column connector (both from Hewlett-Packard). The separation column was connected to the FID detector (Hewlett-Packard), where methanol was detected. The following is an overview of the experimental conditions for pressure-balanced headspace GC analyses used in the investigation:

Head pressure (constant)	: 180 kPa
Pressure program	: 180 kPa, 680 kPa/min, 170 kPa, 0.02 min, 680 kPa/min, 180kPa
Oven temperature	: 60°C, 14 min
Thermostating temperature	: 80°C
Thermostating time	: 15 min
Column gas flow rate	: 2.82 mL/min
Sample	: 1 cm^3 of diluted sample
Retention time	: 4.0 min

There was an attempt to optimize the conditions used for the permeate analysis. The method developed here by using pressure balance headspace sampling was successfully used for identification of methanol and other compounds present in the sample. However the method was not quite successful for quantitation of methanol in the methanol-water system due to the small difference in boiling points of the two compounds. The methanol concentration in the permeate obtained by the analysis developed here has an error within 9% range.

CHAPTER 4

RESULTS AND DISCUSSION

In order to describe, from a theoretical viewpoint, the behavior of the coupling between the batch reactor and the pervaporation unit, independent kinetic information from the batch reactor of the studied reaction is essential. To validate the model for the pervaporation-coupled batch reactor, the kinetic parameters from the batch studies were incorporated into the model.

Batch experiments were performed at different operating conditions to study the effect of each parameter on the reaction kinetics. The batch experiments were performed at different temperatures with various concentrations of catalyst and initial molar ratios of salicylic acid to methanol.

Pervaporation-integrated batch experiments were carried out at different values of the membrane area to initial solution volume ratio (A_m/V_0) and temperature to study effects of these parameters on the performance of the integrated unit. The kinetic parameters from the batch experiments were employed in simulations of the pervaporation-integrated batch runs.

Two different methods were used to determine the apparent rate constants of each experiment.

- Slope at the origin of the conversion versus time plot. In this approach, the water and ester concentrations in the reactor were considered to be very small with respect to the alcohol and acid concentrations, and the second term in the kinetic equation (equation 2.9) was therefore neglected. The initial rate constant of the forward

reaction (k_{f0}) obtained from this method was used as an initial guess for the value determined by the following step.

- Integration of the set of differential equations (equations 2.25, 2.26, and 2.27) along with algebraic equations (equations 2.11, 2.18, 2.19, and 2.30) and numerical optimization of the rate constants by using the estimated k_{f0} value from the initial slope method as the starting value to get the best fitting of the experimental conversion data versus time profiles to the model. The detailed calculations of the initial rate constant are provided in Appendix A.

4.1 Effect of Reaction Temperature on Batch Esterification

Batch experiments were carried out at different reaction temperatures (325 to 341 K) to study the temperature dependence of kinetics of the esterification reaction (Figure 4.1). The experimental conversion data for 325, 331, 336, and 341 K are provided in Tables 4.1-4.4. Concentration-based equilibrium constants were measured experimentally at different temperatures ranging from 331 to 341 K. The equilibrium constants were determined from the equilibrium concentrations of each component in the reaction mixture. From experimental results, the reaction temperature affected the equilibrium constant. With an increase in reaction temperature, the equilibrium constant increased as shown in Figure 4.2.

4.1.1 Activation Energy and Frequency Factor

It was found from the experiments that reaction temperature affected the rate constant of the forward reaction. The parameters of the Arrhenius equation (equation 4.1), activation

energy (E), and frequency factor (k_0) were determined for the forward reaction from batch experiments carried out at different temperatures.

$$k_{f0} = k_0 \exp\left(-\frac{E}{RT}\right) \tag{4.1}$$

Values of ln k_{f0} against $1/T$ (provided in Table 4.5) were fitted by linear regression and the result of this procedure is plotted in Figure 4.3. The values of k_0 and E obtained

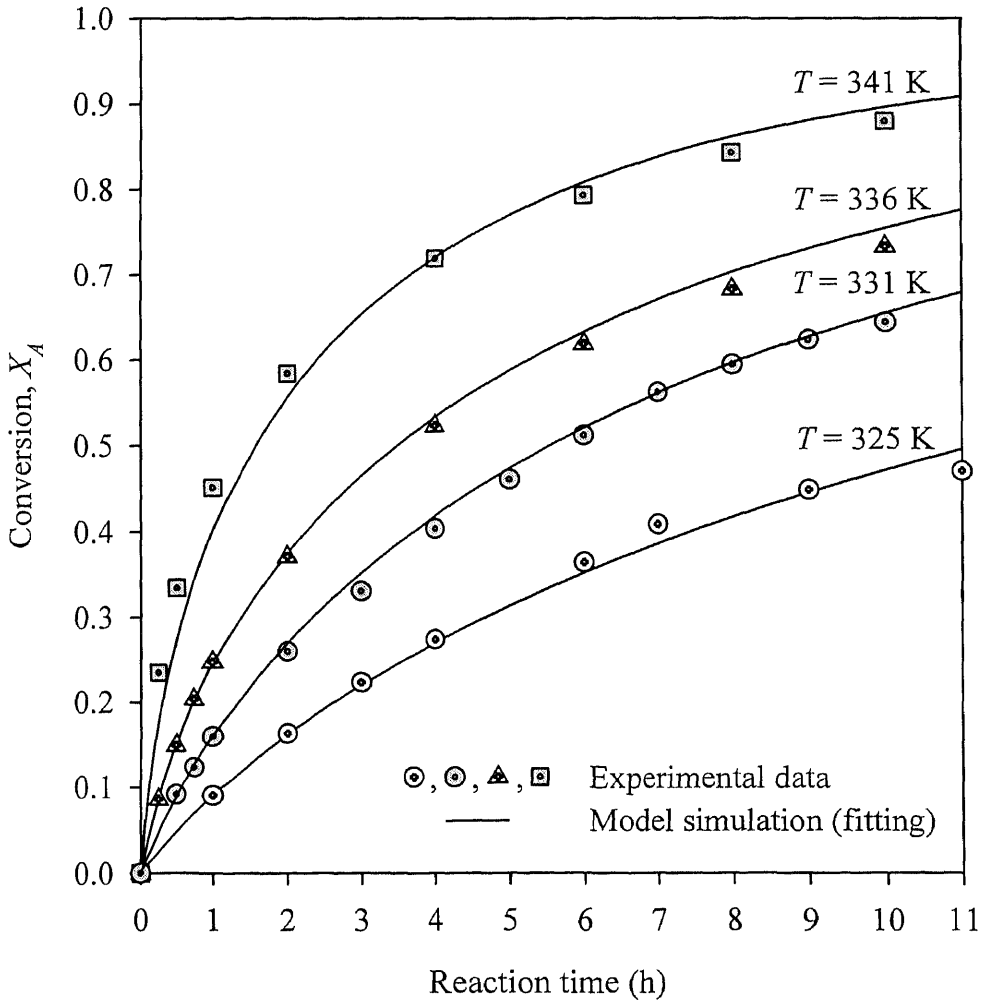

Figure 4.1 Effect of Reaction Temperature on Batch Esterification (without Pervaporation): $\theta_B = 8$, $C_{cat} = 1.10$ M

Table 4.1 Experimental and Calculated Conversions for Batch Esterification at $T = 325$ K

Reaction time (h)	X_A, *exp.* (%)	X_A, *calc.* (%)
0.0	0.00	0.00
1.0	9.04	9.07
2.0	16.27	16.15
3.0	22.30	22.00
4.0	27.37	26.98
6.0	36.38	35.17
7.0	40.84	38.62
9.0	44.84	44.56
11.0	46.99	49.53

Experimental conditions: $\theta_B = 8.0$, $C_{cat} = 1.10$ M

Table 4.2 Experimental and Calculated Conversions for Batch Esterification at T = 331 K

Reaction time (h)	X_A, *exp.* (%)	X_A, *calc.* (%)
0.00	00.00	0.00
0.50	09.20	8.96
0.75	12.35	12.67
1.00	15.95	16.02
2.00	25.94	26.91
3.00	33.06	35.20
4.00	40.34	41.86
5.00	46.09	47.38
6.00	51.16	52.06
7.00	56.18	56.10
8.00	59.42	59.62
9.00	62.33	62.72
10.00	64.38	65.46

Experimental conditions: $\theta_B = 8.0$, $C_{cat} = 1.10$ M

Table 4.3 Experimental and Calculated Conversions for Batch Esterification at T = 336 K

Reaction time (h)	X_A, *exp.* (%)	X_A, *calc.* (%)
0.00	0.00	0.00
0.25	8.60	8.80
0.50	14.91	15.25
0.75	20.37	20.43
1.00	24.71	24.82
2.00	37.10	37.77
4.00	52.30	53.59
6.00	61.86	63.51
8.00	68.21	70.46
10.00	73.24	75.60

Experimental conditions: $\theta_B = 8.0$, $C_{cat} = 1.10$ M

Table 4.4 Experimental and Calculated Conversions for Batch Esterification at T = 341 K

Reaction time (h)	X_A, *exp.* (%)	X_A, *calc.* (%)
0.00	0.00	0.00
0.25	23.50	17.45
0.50	33.45	27.31
1.00	45.11	40.20
2.00	58.43	55.65
4.00	71.88	72.00
6.00	79.27	80.79
8.00	84.27	86.14
10.00	87.94	89.59

Experimental conditions: $\theta_B = 8.0$, $C_{cat} = 1.10$ M

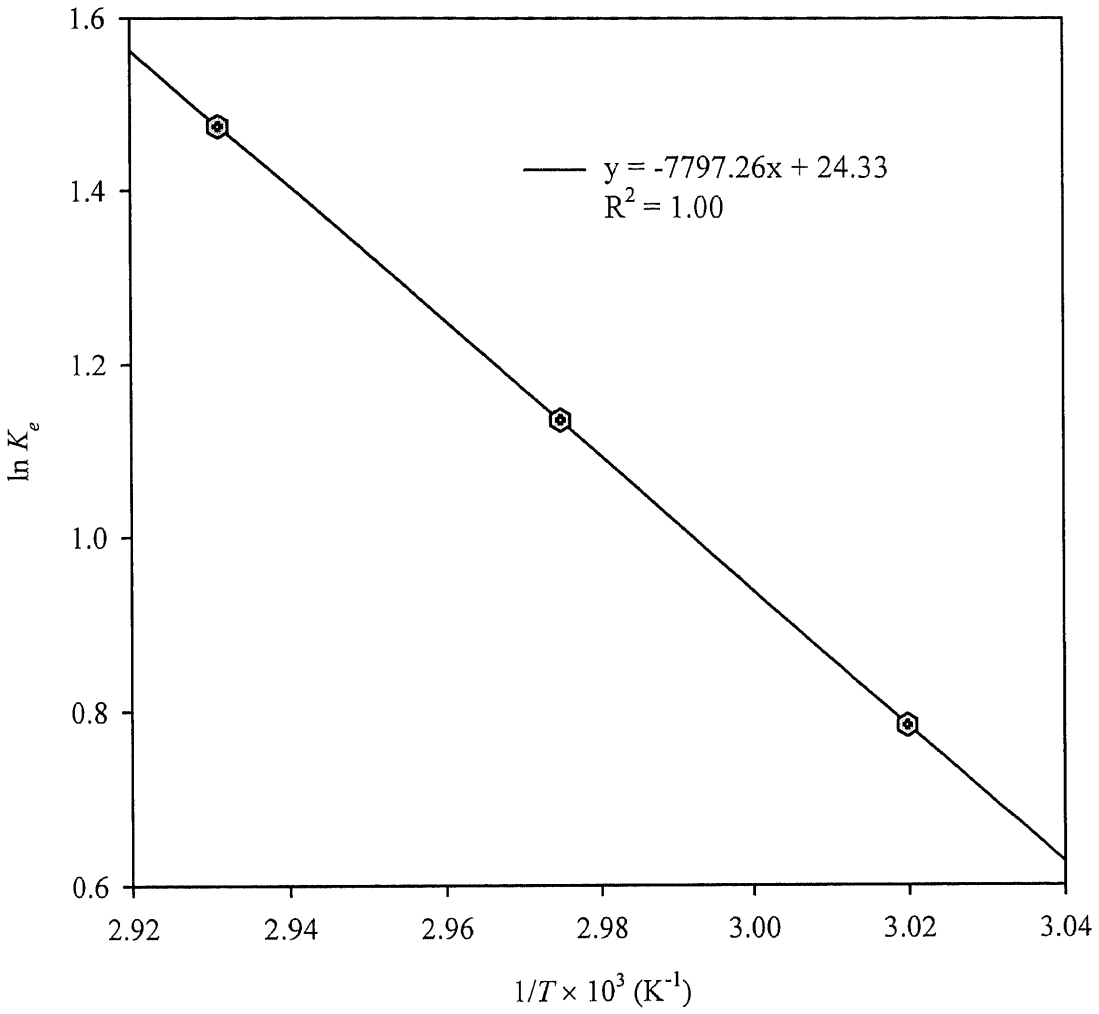

Figure 4.2 Variation of Natural Logarithm of Equilibrium Constant with the Reciprocal of Absolute Temperature

Table 4.5 Relationship between Temperature and Initial Forward Reaction Rate Constant

T (K)	$k_{f0} \times 10^2$ (mol/L)$^{-1}$(h)$^{-1}$
325	0.58
331	1.22
336	2.33
341	6.72

Experimental conditions: $\theta_B = 8.0$, $C_{cat} = 1.10$ M

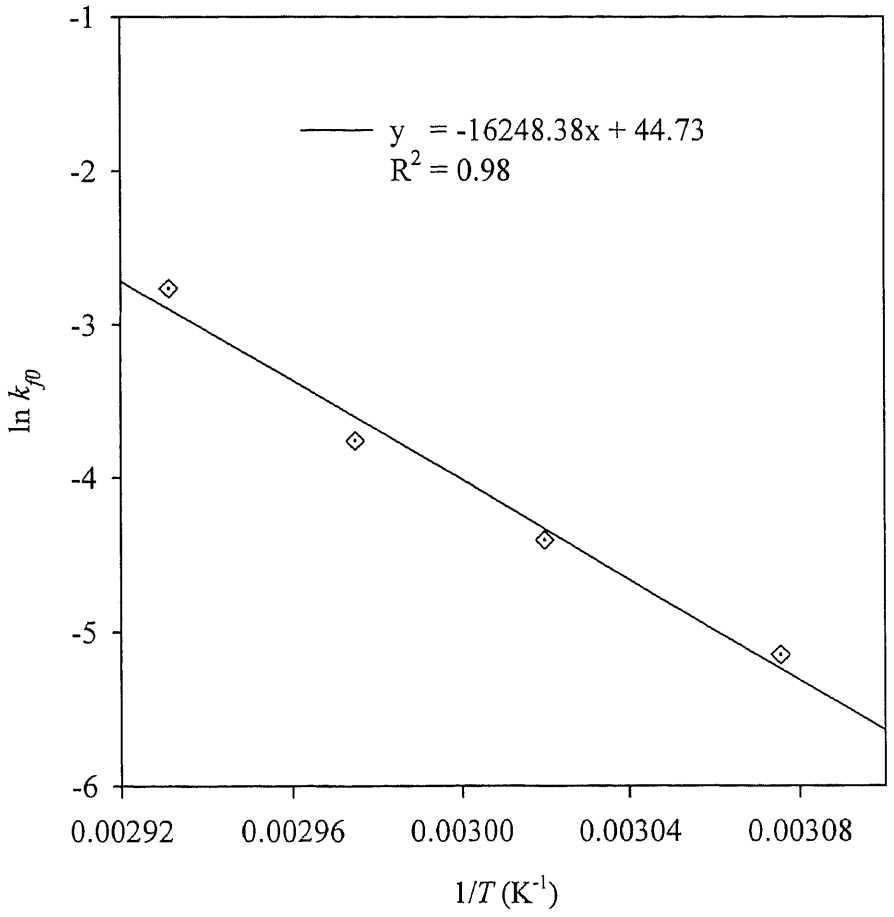

Figure 4.3 Arrhenius Plot for Determination of Activation Energy of Esterification: $\theta_B = 8.0$, $C_{cat} = 1.10$ M

from the Arrhenius plot were 2.667×10^{19} L/(mol.h) and 135.09 kJ/mol, respectively, using the least-squares method.

4.1.2 Reaction Enthalpy and Reaction Entropy

Reaction enthalpy at standard conditions can be used to indicate whether a reaction is endothermic or exothermic. It can be determined either from the formation enthalpy of each reactant and product or by the equilibrium constants. The reaction enthalpy and reaction entropy can be determined from the following equation

$$\ln K_e = -\frac{\Delta H^\circ}{RT} + \frac{\Delta S^\circ}{R} \tag{4.2}$$

According to equation 4.2, the reaction enthalpy and reaction entropy can be estimated by plotting ln K_e against $1/T$ as shown in Figure 4.2. By using the least-squares method, the reaction enthalpy (ΔH°) was calculated as 64.83 kJ/mol. The positive value of ΔH° shows that the reaction is endothermic. The value of the reaction entropy can also be evaluated from the slope of ln K_e vs $1/T$ plot and was found to be 202.28 J/(mol.K). Values of K_e for different temperatures are provided in Table 4.6 at specified θ_B and C_{cat} values.

4.1.3 Activation Enthalpy

The values of the activation energy (E) and the frequency factor (k_0) provide a full description of the kinetic data; however it may be desirable to express the results in terms

of the activation enthalpy ΔH^* to interpret the mechanism of the reaction. According to the transition state theory, the forward rate constant can be expressed as

$$k_{f0} = \frac{\mathbf{k}T}{h} e^{-\Delta G^*/RT} \tag{4.3}$$

$$k_{f0} = \frac{\mathbf{k}T}{h} e^{-\Delta H^*/RT} \cdot e^{\Delta S^*/R} \tag{4.4}$$

In conformity with equation 4.4, the activation enthalpy of the forward reaction can be approximately obtained from the Eyring plot by plotting $\ln(k_{f0}/T)$ against $1/T$. The slope of such a plot will yield the value of $-\Delta H^*/R$. The Eyring plot is shown in Figure 4.4 and the value of ΔH^* was calculated as 132.32 kJ.mol^{-1}. The estimated ΔH^* value is presented here for the sake of completeness of the thermodynamic data for the studied reaction. No attempt was made in using ΔH^* in interpreting the possible exact reaction mechanism.

Table 4.6 Relationship between Reaction Temperature and Equilibrium Constant

T (K)	K_e
331	2.19
336	3.11
341	4.37

Experimental conditions: $\theta_B = 8.0$, $C_{cat} = 1.10$ M

4.1.4 Temperature Dependence of the Reduction Parameter

According to the experimental data, the reduction parameter (a) used in the model depended only on temperature and the initial methanol to salicylic acid molar ratio. It was found that the value of a increased with increasing temperature (Table 4.7). The value of

a did not increase significantly in the lower temperature range. On the other hand, *a* was a strong function of reaction temperature in the high temperature range (331-341 K), (Figure 4.5). The value of *a* was determined during the course of fitting the data to the model as shown in Figure 4.1.

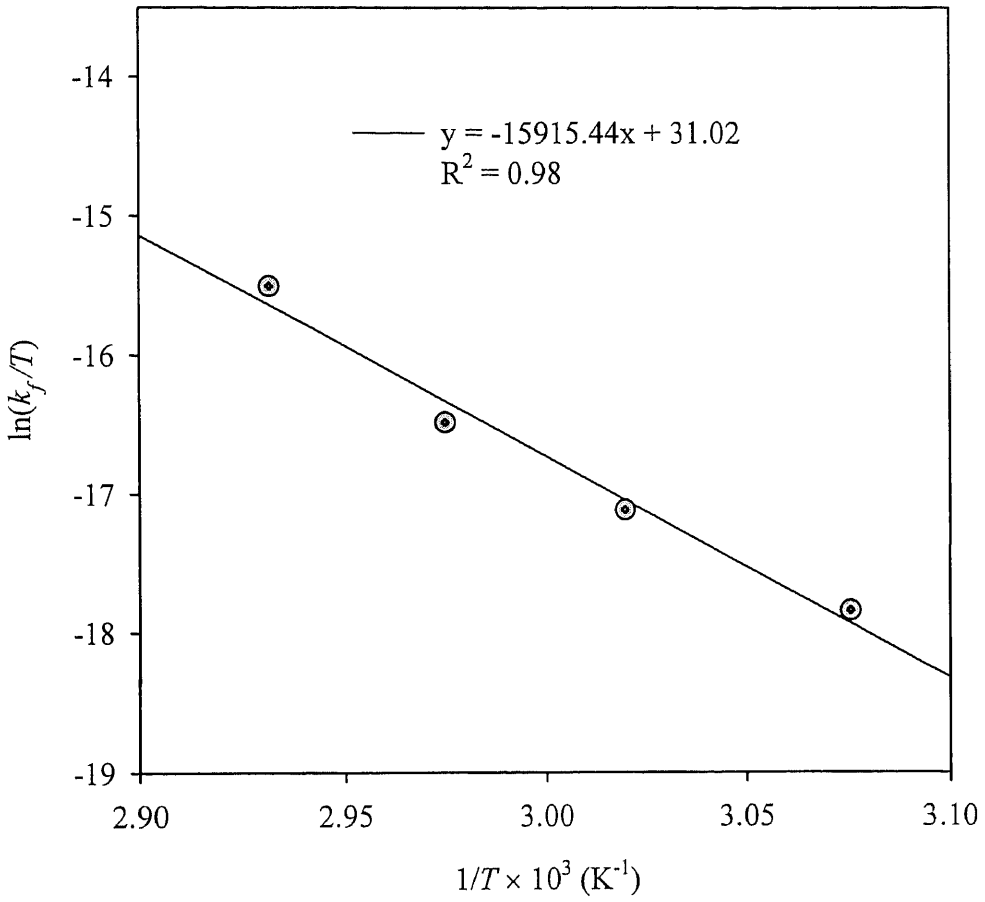

Figure 4.4 Eyring Plot for Determination of Activation Enthalpy: θ_B = 8.0, C_{cat} = 1.10 mol/L

Table 4.7 Dependence of Reduction Parameter (a) on Reaction Temperature

T (K)	a (L/mol)
325	0.96
331	1.03
336	1.62
341	2.33

Experimental conditions: $\theta_B = 8.0$, $C_{cat} = 1.10$ M

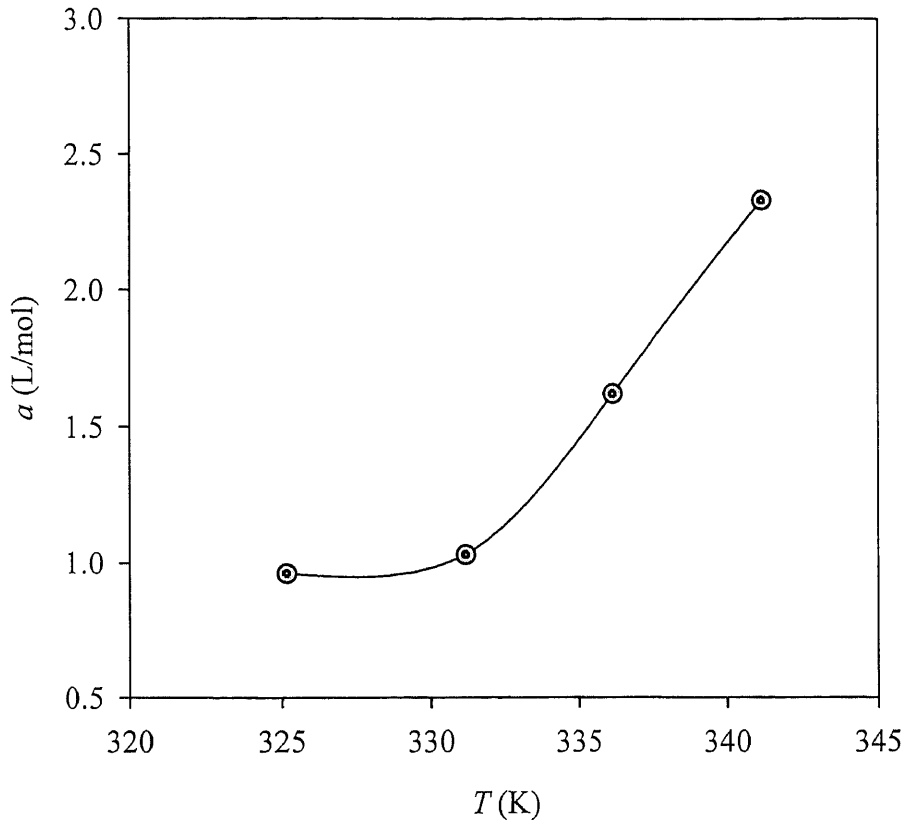

Figure 4.5 Dependence of Reduction Parameter (a) on Reaction Temperature

4.1.5 Effect of Reaction Temperature on Time Required to Attain 90% Conversion

To illustrate the effect of reaction temperature on the processing time, the calculated time needed to achieve 90% conversion of salicylic acid (t_{90}) is used. The plot of t_{90} against reaction temperature is illustrated in Figure 4.6; the numerical values are provided in Table 4.8. It is clear that t_{90} decreased with increase in temperature. For a θ_B = 8 and C_{cat} = 1.10 M, t_{90} was reduced from 90.0 to 10.3 h when the temperature was increased from 325 to 341 K. This information on temperature dependence is essential for adjusting the operating parameters in the pervaporation-assisted esterification process. The appropriate temperature for reaction and pervaporation unit attached to the batch reactor should be 341 K; the pervaporation process also requires a high temperature feed to increase the transmembrane flux of the higher permeable component. Temperatures exceeding 341 K cannot be used since the boiling point of the reaction mixture is 343 K.

4.2 Effect of Catalyst Concentration on Batch Esterification

Experiments were conducted with various concentrations of sulfuric acid in the range of 0 to 2.0 molar at constant values of reaction temperature to study the effect of catalyst concentration on reaction kinetics of the esterification. The data are provided in Tables 4.9 to 4.13. The effect of catalyst concentration is shown in Figure 4.7. An increase in catalyst concentration accelerates the production of ester; therefore an increase in the amount of catalyst may be an alternative way to accelerate the ester production. In other words, the establishment of equilibrium was accelerated with an increase in catalyst concentration. However, by using a high concentration of catalyst, it will be more difficult

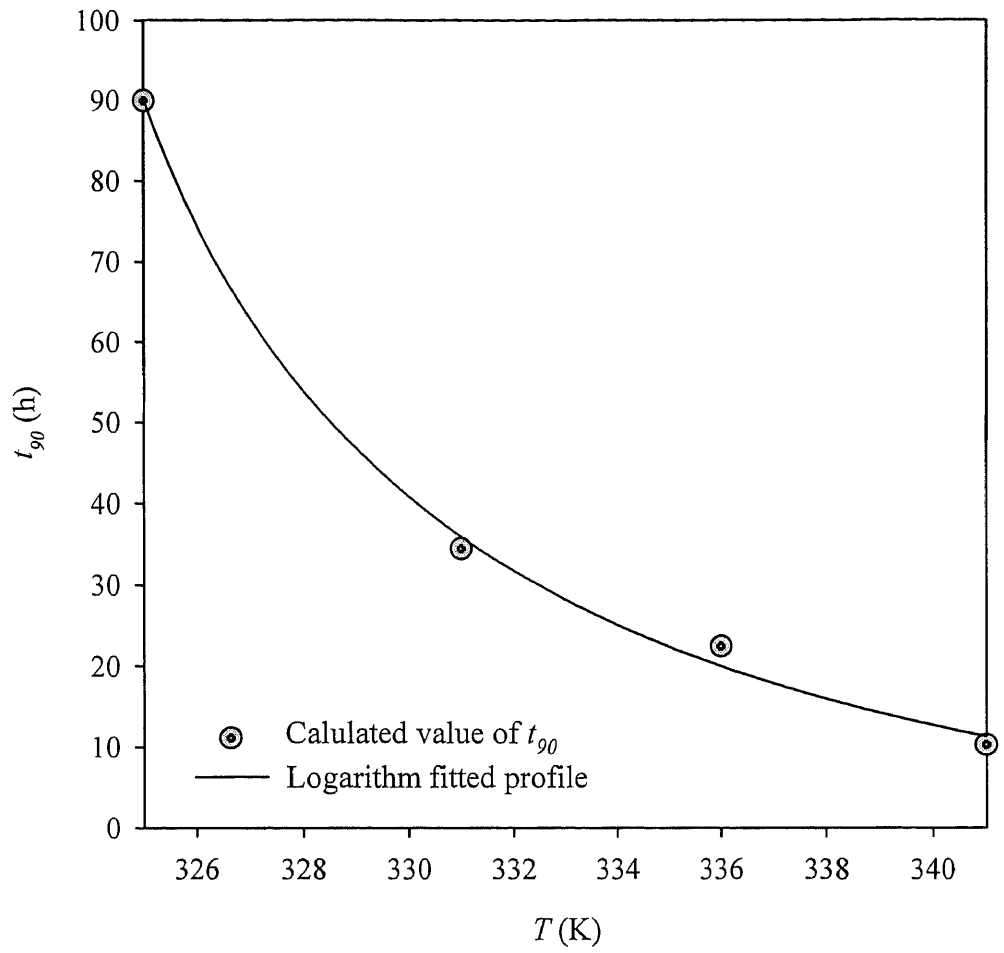

Figure 4.6 Effect of Temperature on t_{90} for Batch Esterification (without Pervaporation): $\theta_B = 8.0$, $C_{cat} = 1.10$ M

Table 4.8 Effect of Temperature on t_{90} (Batch Experiments)

T (K)	t_{90} (h)
325	89.98
331	34.49
336	22.51
341	10.31

Experimental conditions: $\theta_B = 8.0$, $C_{cat} = 1.10$ M

and cost-intensive to remove a large amount of sulfuric acid from the reaction mixture by neutralization after the reaction is completed. As the catalyst concentration is increased, the forward rate constant increases. Values of k_{f0} for different catalyst concentrations are provided in Table 4.14 for specified T and θ_B values. From the experimental results, the initial rate constant of forward reaction was found to have a linear dependence on the catalyst concentration in the range of investigation (Figure 4.8). A reaction run without catalyst was carried out at 336 K for several hours and methyl salicylate was not detected. It was apparent that there was essentially no reaction when there was no catalyst in the system.

Table 4.9 Experimental and Calculated Conversions for Batch Esterification when C_{cat} = 0.50 mol/L

Reaction time (h)	X_A, *exp.* (%)	X_A, *calc.* (%)
0.00	0.00	0.00
0.25	5.25	4.71
0.50	9.65	8.70
0.75	14.81	12.18
1.00	17.93	15.28
2.00	25.41	25.20
3.00	32.23	32.69
5.00	42.06	43.79
7.00	51.05	51.90

Experimental conditions: T = 336 K, θ_B = 10.0

Table 4.10 Experimental and Calculated Conversions for Batch Esterification when C_{cat} = 1.00 mol/L

Reaction time (h)	X_A, *exp.* (%)	X_A, *calc.* (%)
0.00	0.00	0.00
0.25	7.36	8.51
0.50	16.00	14.97
0.75	19.86	20.26
1.00	24.28	24.75
2.00	33.30	38.17
3.00	44.31	47.50
5.00	57.26	60.23
7.00	66.93	68.72

Experimental conditions: T = 336 K, θ_B = 10.0

Table 4.11 Experimental and Calculated Conversions for Batch Esterification when C_{cat} = 1.10 mol/L

Reaction time (h)	X_A, *exp.* (%)	X_A, *calc.* (%)
0.00	0.00	0.00
0.25	8.57	9.37
1.00	24.39	26.70
2.00	39.19	40.68
3.00	48.00	50.25
5.00	59.47	63.11
6.50	65.18	69.69
7.00	67.43	71.51
8.00	70.20	74.70
9.00	73.51	77.42

Experimental conditions: T = 336 K, θ_B = 10.0

Table 4.12 Experimental and Calculated Conversions for Batch Esterification when C_{cat} = 1.50 mol/L

Reaction time (h)	X_A, *exp.* (%)	X_A, *calc.* (%)
0.00	0.00	0.00
0.25	14.99	12.44
0.50	25.90	21.03
0.75	31.73	27.71
1.00	35.89	33.22
2.00	47.93	48.77
3.00	57.61	58.89
5.00	68.72	71.70
7.00	78.22	79.48

Experimental conditions: T = 336 K, θ_B = 10.0

Table 4.13 Experimental and Calculated Conversions for Batch Esterification when C_{cat} = 2.00 mol/L

Reaction time (h)	X_A, *exp.* (%)	X_A, *calc.* (%)
0.00	0.00	0.00
0.25	16.67	15.38
0.50	26.91	25.34
0.75	33.01	32.86
1.00	37.14	38.93
2.00	54.22	55.47
3.00	64.10	65.74
5.00	77.80	78.03
7.00	85.73	84.95

Experimental conditions: T = 336 K, θ_B = 10.0

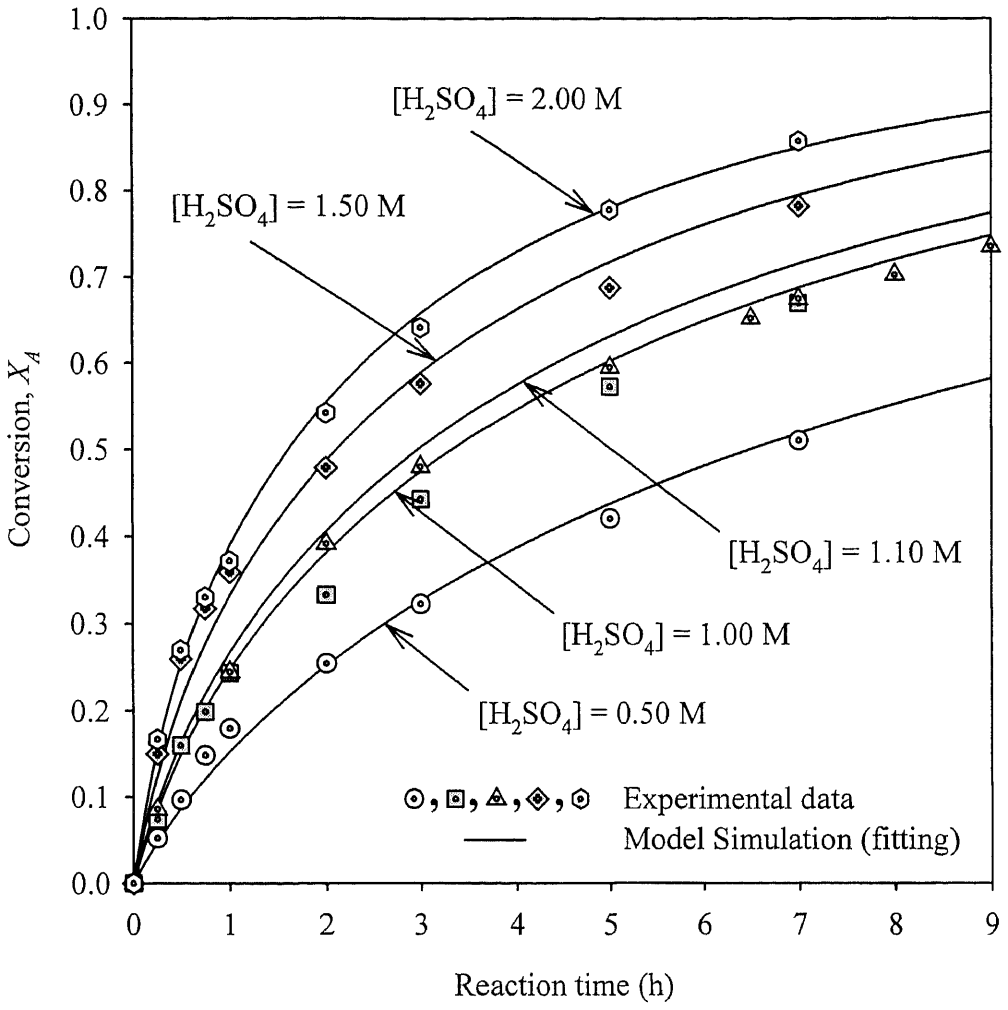

Figure 4.7 Effect of Catalyst Concentration on Conversion Profiles of Batch Esterification (without Pervaporation): T = 336 K, θ_B = 10.0

Table 4.14 Relationship between Catalyst Concentration and Initial Forward Reaction Rate Constant

C_{cat}	$k_{f0} \times 10^2$ (mol/L)$^{-1}$(h)$^{-1}$
0.00	0.00
0.50	1.37
1.00	2.67
1.10	2.99
1.50	4.22
2.00	5.53

Experimental conditions: $T = 336$ K, $\theta_B = 10.0$

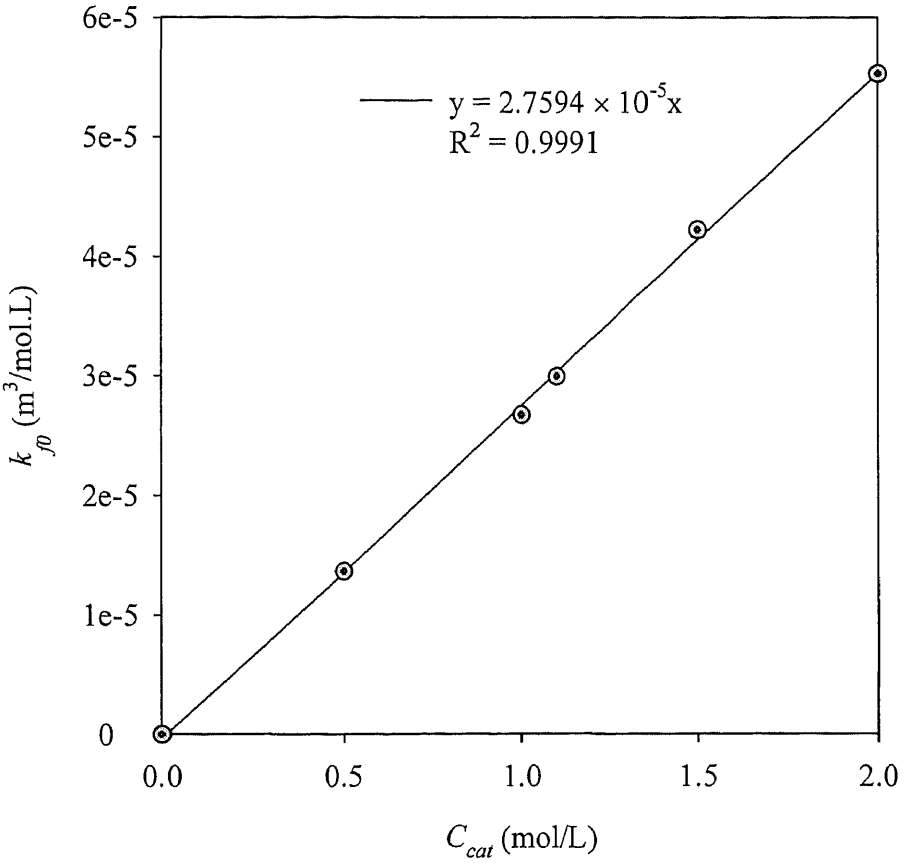

Figure 4.8 Relationship between Initial Rate Constant of Forward Reaction and Temperature for Batch Esterification (without Pervaporation): $\theta_B = 8.0$, $C_{cat} = 1.10$ M

It was found that the reduction parameter (a) did not depend upon the catalyst concentration. Model-fitted profiles by employing the same value of a (= 1.62) for different catalyst concentrations appeared to be in good agreement with experimental data (Figure 4.7). The calculated time required to achieve 90% conversion (t_{90}) was reduced by about 75% when the catalyst concentration was increased from 0.5 M to 2.0 M (Figure 4.9). Values of t_{90} for different catalyst concentrations are provided in Table 4.15 for the specified T and θ_B values.

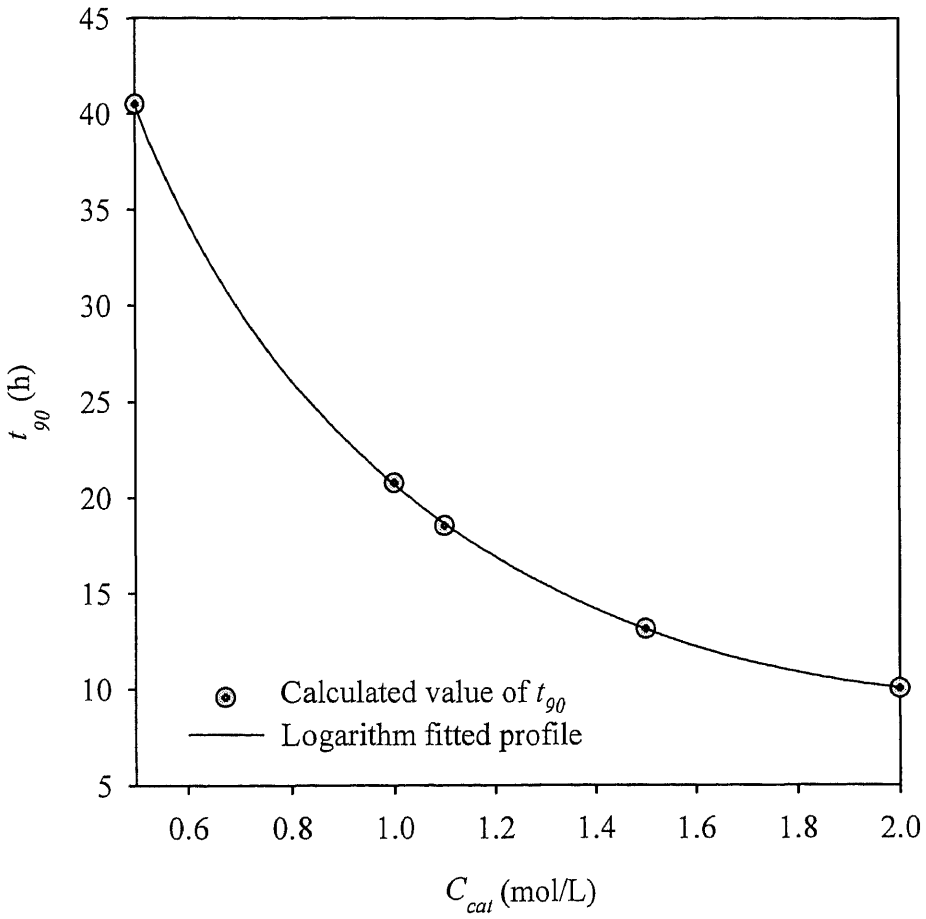

Figure 4.9 Effect of Catalyst Concentration on t_{90} for Batch Esterification (without Pervaporation): T = 336 K, θ_B = 10.0

Table 4.15 Effect of Catalyst Concentration on t_{90} (Batch Experiments)

C_{cat} (mol/L)	t_{90} (h)
0.50	40.51
1.00	20.79
1.10	18.56
1.50	13.15
2.00	10.04

Experimental conditions: $T = 336$ K, $\theta_B = 10.0$

4.3 Effect of Initial Molar Ratio of Alcohol to Carboxylic Acid

It is well known that a sufficiently high ratio of methanol to salicylic acid leads to a quasi-complete conversion of the acid even without pervaporation. However, by using a excess of methanol to drive the reaction is cost-intensive and makes it difficult to separate the desired products out of the reaction mixture when the reaction is completed.

To validate the theoretical model for the pervaporation-integrated batch reactor, information on the dependence of process performance on the molar ratio of methanol to salicylic acid (θ_B), which is a parameter in the model, is needed. Therefore, the experiments were conducted at different initial molar ratios of alcohol to acid in a range of 8 to 50. Due to the fact that salicylic acid has a limited solubility in methanol, the minimum molar ratio that could be used was 8. Conversion data for different θ_B values are provided in Tables 4.16 to 4.19. The experimental data were nicely fitted to the model (Figure 4.10) which confirms the validity of the model developed for the batch esterification. Tables 4.20 and 4.21 provide, respectively, the dependence of t_{95} and a on θ_B. A summary of the kinetic information obtained from the batch experiments at different temperatures with different values of θ_B is given in Table 4.22.

Table 4.16 Experimental and Calculated Conversions for Batch Esterification when $\theta_B = 8.0$

Reaction time (h)	X_A, *exp.* (%)	X_A, *calc.* (%)
0.00	0.00	0.00
0.25	8.60	8.80
0.50	14.91	15.25
0.75	20.37	20.43
1.00	24.71	24.82
2.00	37.10	37.77
4.00	52.30	53.59
6.00	61.86	63.51
8.00	68.21	70.46
10.00	73.24	75.60

Experimental conditions: $T = 336$ K, $C_{cat} = 1.10$ M

Table 4.17 Experimental and Calculated Conversions for Batch Esterification when $\theta_B = 10.0$

Reaction time (h)	X_A, *exp.* (%)	X_A, *calc.* (%)
0.00	0.00	0.00
0.25	8.57	9.00
0.50	11.44	15.60
0.75	20.37	20.91
1.00	24.39	25.40
2.00	39.19	38.66
3.00	48.00	47.83
4.00	54.72	54.79
5.00	59.47	60.33
6.00	65.18	64.88
7.00	67.43	68.68
8.00	71.61	71.90
9.00	73.51	74.67

Experimental conditions: $T = 336$ K, $C_{cat} = 1.10$ M

Table 4.18 Experimental and Calculated Conversions for Batch Esterification when $\theta_B = 21.0$

Reaction time (h)	X_A, *exp.* (%)	X_A, *calc.* (%)
0.00	0.00	0.00
0.30	7.44	11.59
1.00	26.36	28.10
2.00	41.18	42.58
3.00	49.43	52.46
4.00	57.74	59.85
5.00	66.14	65.64
6.00	70.39	70.32
7.00	74.10	74.17
8.00	78.08	77.39

Experimental conditions: $T = 336$ K, $C_{cat} = 1.10$ M

Table 4.19 Experimental and Calculated Conversions for Batch Esterification when $\theta_B = 50.0$

Reaction time (h)	X_A, *exp.* (%)	X_A, *calc.* (%)
0.00	0.00	0.00
0.25	12.34	10.54
0.50	20.22	18.26
0.75	25.46	24.44
1.00	29.25	29.63
2.00	43.06	44.78
4.17	62.40	63.68
6.17	74.43	73.90
8.00	80.97	80.24
10.00	86.23	85.15

Experimental conditions: $T = 336$ K, $C_{cat} = 1.10$ M

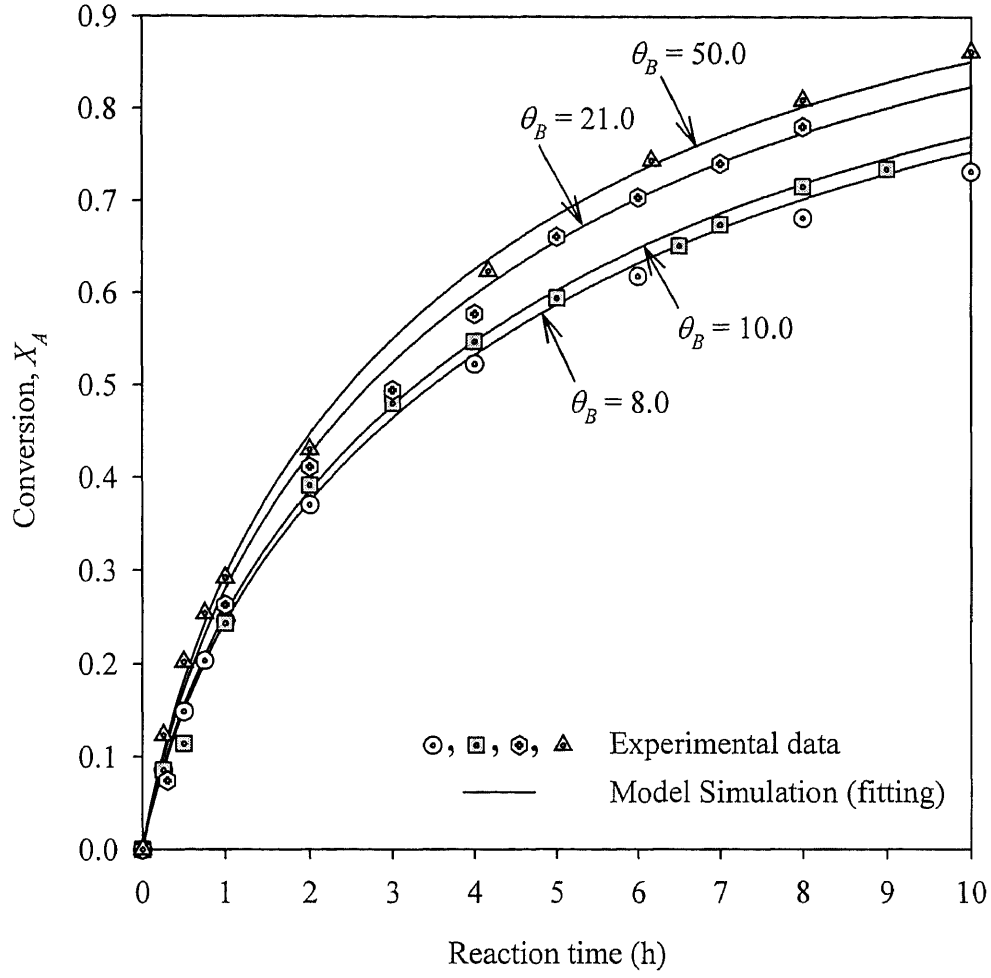

Figure 4.10 Effect of Initial Molar Ratio of Methanol to Salicylic Acid (θ_B) on Conversion Profiles of Batch Esterification (without Pervaporation): T = 336 K, C_{cat} = 1.10 M

Table 4.20 Effect of Initial Molar Ratio of Methanol to Salicylic Acid on Calculated t_{95} for Batch Esterification

θ_B	t_{95} (h)
8.0	44.89
10.0	34.65
21.0	22.33
50.0	18.54

Experimental conditions: T = 336 K, C_{cat} = 1.10 M

Table 4.21 Dependence of Reduction Parameter (a) on Initial Molar Ratio of Methanol to Salicylic Acid (θ_B)

θ_B	a (L/mol)
8	1.62
10	1.92
21	3.21
50	6.70

Experimental conditions: $T = 336$ K, $C_{cat} = 1.10$ M

The reduction parameter, a, was found to have a linear relationship with θ_B. The reduction parameter increased when θ_B increased (Figure 4.11). The information on dependence of the reduction parameter on the molar ratio from batch experiments allows the computation of conversion profiles in pervaporation-assisted esterification at different alcohol/acid ratios. The salicylic acid conversions as a function of time show (Figure 4.10) that, with an increase θ_B, the ester formation is significantly accelerated. Time required to achieve 95% conversion of salicylic acid was reduced from 44.9 to 18.5 h by increasing θ_B from 8 to 50 (Figure 4.12). From the t_{95}-θ_B plot, without economic considerations, the optimal value for θ_B for batch esterification was concluded to be about 20. This is due to the fact that the reaction performance was not improved substantially when θ_B values beyond 20 were used.

Table 4.22 Kinetic Information of the Batch Reactions

T (K)	Molar Ratio, θ_B (C_{B0}/C_{A0})	C_{cat} (mol/L)	X_{Ae} (%)	K_e	k_{f0} $(mol/L)^{-1}(h)^{-1}$	k_b $(mol/L)^{-1}(h)^{-1}$
331	8.00	1.10	94.25	2.191	0.0122	5.568×10^{-3}
336	8.00	1.10	95.81	3.114	0.0233	7.482×10^{-3}
341	8.00	1.10	96.94	4.369	0.0672	1.538×10^{-2}
336	8.00	1.10	95.81	3.114	0.0233	7.482×10^{-3}
336	21.00	1.10	98.43	3.082	0.0233	7.560×10^{-3}
336	50.00	1.10	99.34	3.063	0.0233	7.607×10^{-3}

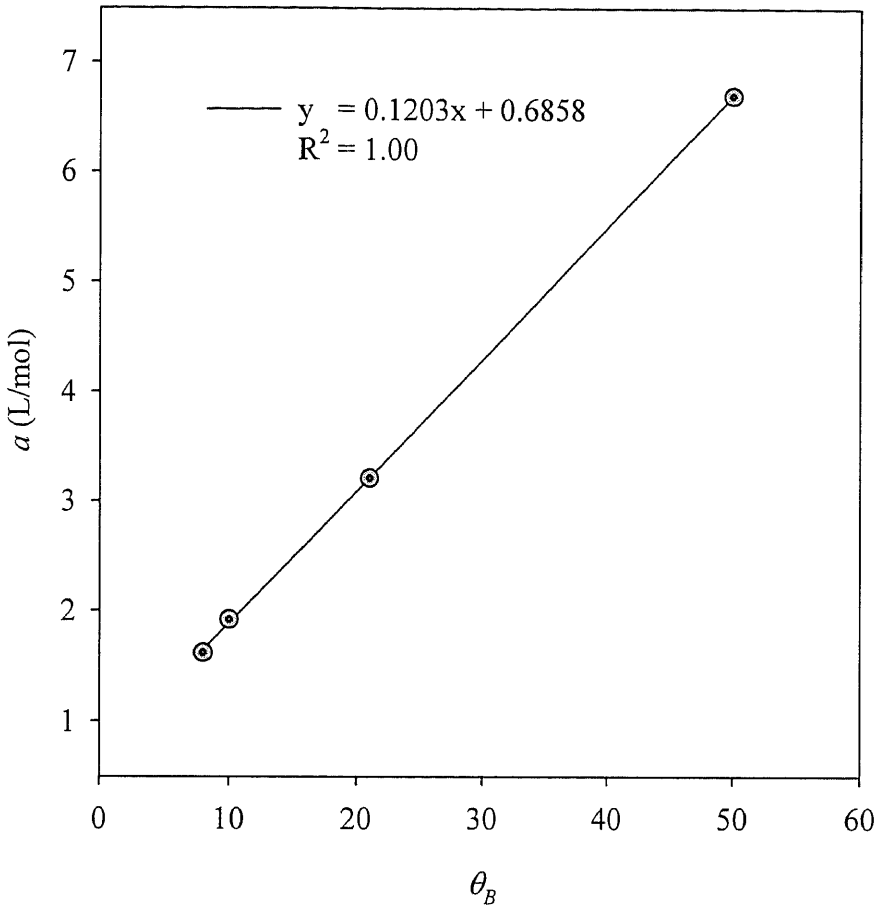

Figure 4.11 Dependence of Reduction Parameter (*a*) on Initial Methanol to Salicylic Acid Molar Ratio

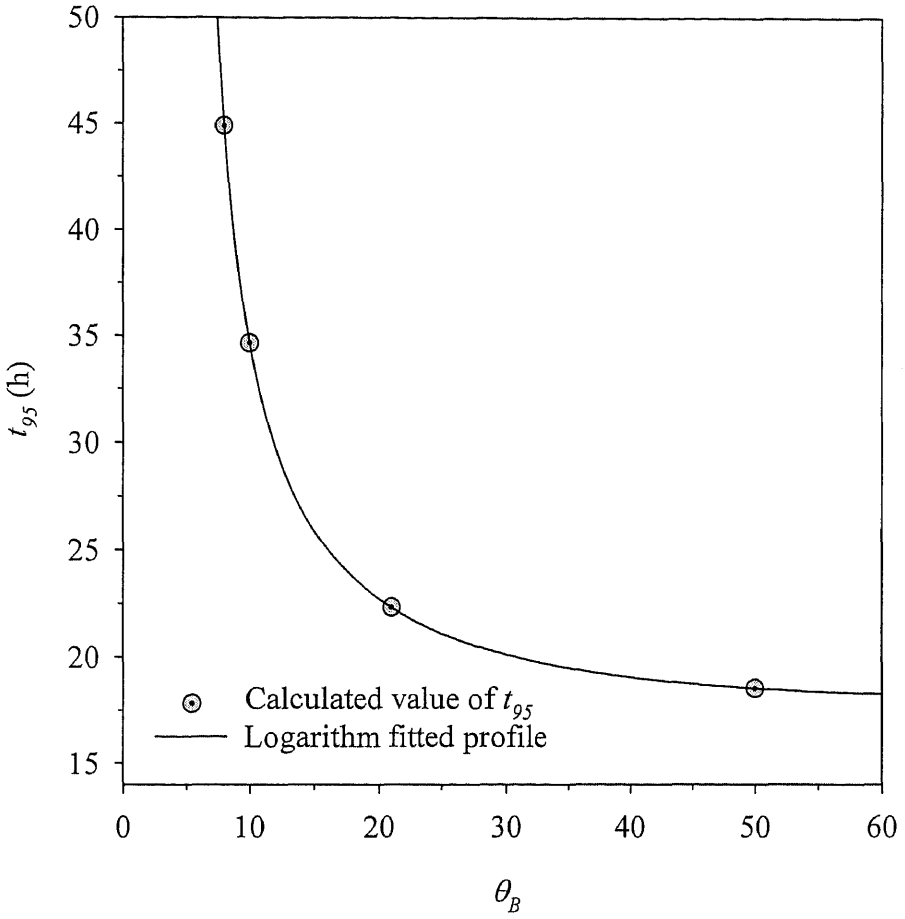

Figure 4.12 Effect of Initial Molar Ratio (θ_B) on t_{95} for Batch Esterification (without Pervaporation): $T = 336$ K, $C_{cat} = 1.10$ M

4.4 Effect of the Effective Membrane Area to Solution Volume Ratio, A_m/V_0

The ratio A_m/V_0 is an important parameter for determining the water separating capacity of the pervaporation-integrated system. Due to the fact that the catalyst concentration has an influence only on the reaction kinetics and not on the pervaporation rates, the pervaporation experiments were carried out at a constant catalyst concentration of 1.10 mol/L to study the effect of A_m/V_0 ratio. To study the effect of A_m/V_0, the effective membrane area was varied while keeping the initial reaction volume constant. In this study, A_m/V_0 was varied in the range of 27-66 m^{-1}. The operating temperature of the reactor and the pervaporation unit was set at 341 K. However, due to heat losses in transfer lines between the reactor and the pervaporation unit, an average system temperature was lower than the set temperature. A detailed discussion regarding the temperature discrepancy is provided in Appendix C of the thesis.

A blank experiment was carried out by using the integrated system without the membrane (curve 1 in Figure 4.13) to obtain k_{f0} value at the average system temperature. The obtained k_{f0} value was used in the mathematical model to simulate predicted profiles for pervaporation-assisted esterification. The experimental conversion-time curves are shown in Figure 4.13; the data are provided in Table 4.23. The influence of A_m/V_0 ratio on the process can be predicted from the model. Figure 4.13 shows computed curves of conversion rate for different A_m/V_0 ratios for a constant permeance ($P_W = 2.95\times10^{-3}$ $m.h^{-1}$). The model-predicted profiles appear to be in good agreement with the experimental data (Figure 4.13).

In a pervaporation-integrated batch reactor, water can be removed more rapidly by increasing the ratio of the membrane area to solution volume (A_m/V_0). A variation of

the A_m/V_0 ratio, while keeping other parameters constant, increases the permeation flux of water through the membrane. Experiments at 341 K and $\theta_B = 8$ with different membrane areas were performed and showed that the processing time needed for 95% conversion of the salicylic acid drops from 30 h in the absence of the pervaporation membrane to 13 h with a membrane having a specific surface area of 65.9 m^{-1} (Figure 4.14). Values of t_{95} for different A_m/V_0 ratios are provided in Table 4.24 at specified T, θ_B and C_{cat} values.

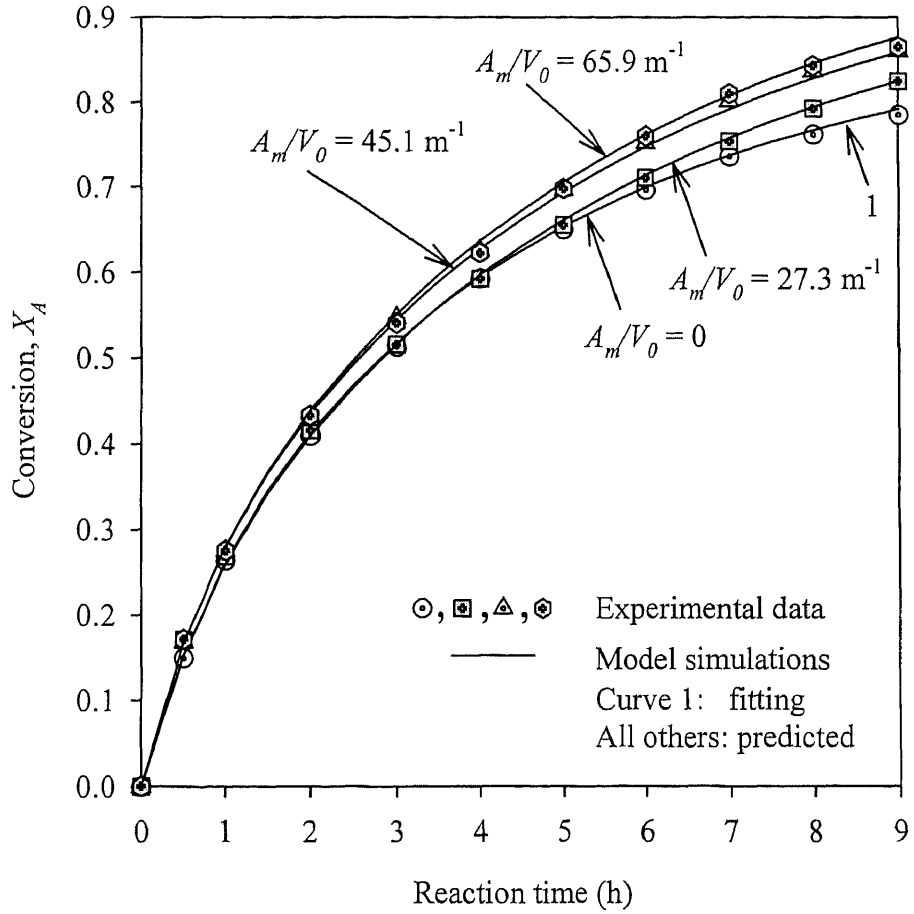

Figure 4.13 Effect of Effective Membrane Area to Initial Solution Volume Ratio (A_m/V_0) on Conversion Profiles of Pervaporation-Assisted Esterification: T = 341 K, $\theta_B = 8$, $C_{cat} = 1.10$ M

Table 4.23 Experimental and Calculated Conversions for Pervaporation-Assisted Esterification at Different Membrane Area to Initial Solution Volume Ratios (A_m/V_0), T = 341 K, θ_B = 8, C_{cat} = 1.10 M

Reaction time (h)	$A_m/V_0 = 0$		$A_m/V_0 = 27.3$ m^{-1}		$A_m/V_0 = 45.1$ m^{-1}		$A_m/V_0 = 65.9$ m^{-1}	
	X_A, *exp.* (%)	X_A, *calc.* (%)	X_A, *exp.* (%)	X_A, *calc.* (%)	X_A, *exp.* (%)	X_A, *calc.* (%)	X_A, *exp.* (%)	X_A, *calc.* (%)
0.0	0.00	0.00	0.00	0.00	0.00	0.00	0.00	0.00
0.5	14.95	15.23	17.05	15.27	16.81	16.76	17.13	16.78
1.0	26.36	25.81	26.86	25.95	27.51	28.00	27.54	28.09
2.0	40.97	40.56	41.59	41.01	42.81	43.57	43.34	43.92
3.0	51.29	50.80	51.56	51.65	54.67	54.50	54.08	55.15
4.0	59.26	58.47	59.20	59.76	62.57	62.82	62.30	63.77
5.0	65.06	64.48	65.54	66.21	69.68	69.42	69.86	70.64
6.0	69.69	69.31	71.09	71.46	75.23	74.78	76.03	76.22
7.0	73.63	73.27	75.39	75.80	80.16	79.19	81.04	80.79
8.0	76.20	76.56	79.25	79.44	83.67	82.84	84.35	84.56
9.0	78.48	79.32	82.46	82.51	86.00	85.88	86.51	87.65

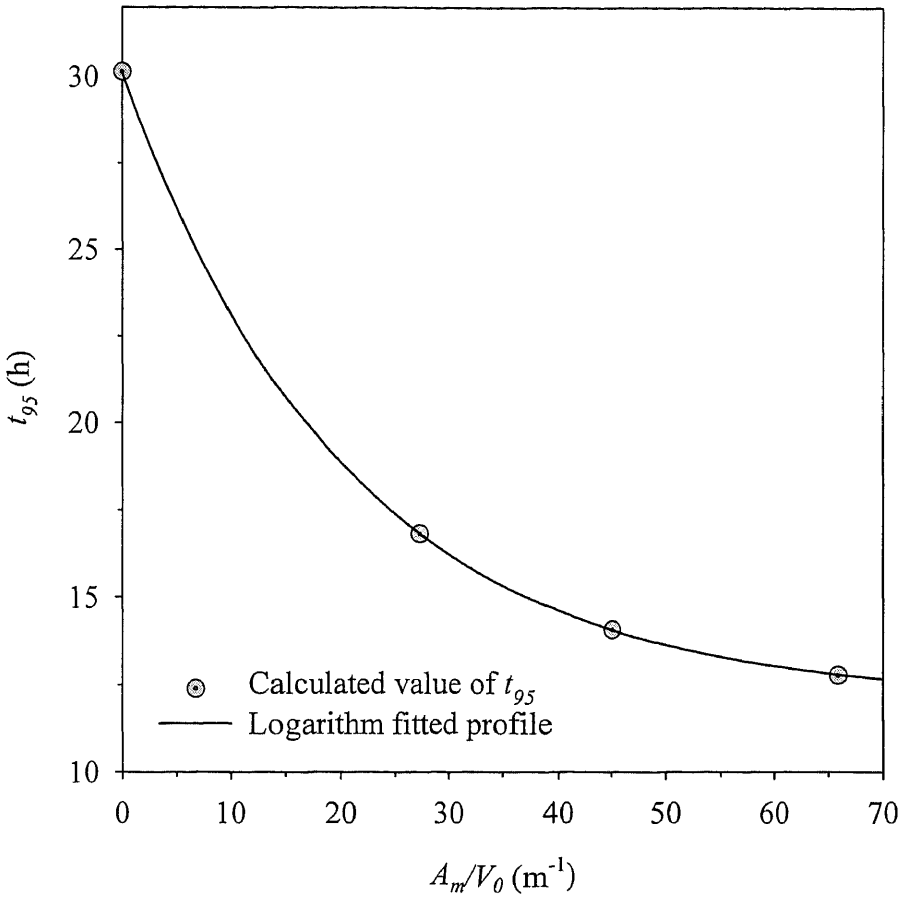

Figure 4.14 Effect of Effective Membrane Area to Initial Solution Volume Ratio (A_m/V_0) on t_{95} for Pervaporation-Assisted Esterification: T = 341 K, θ_B = 8, C_{cat} = 1.10 M

Table 4.24 Effect of Effective Membrane Area to Initial Volume Ratio (A_m/V_0) on t_{95} for Pervaporation-Assisted Esterification

A_m/V_0 (m^{-1})	t_{95} (h)
0.0	30.14
27.3	16.82
45.1	14.09
65.9	12.79

Experimental conditions: T = 341 K, θ_B = 8, C_{cat} = 1.10 M

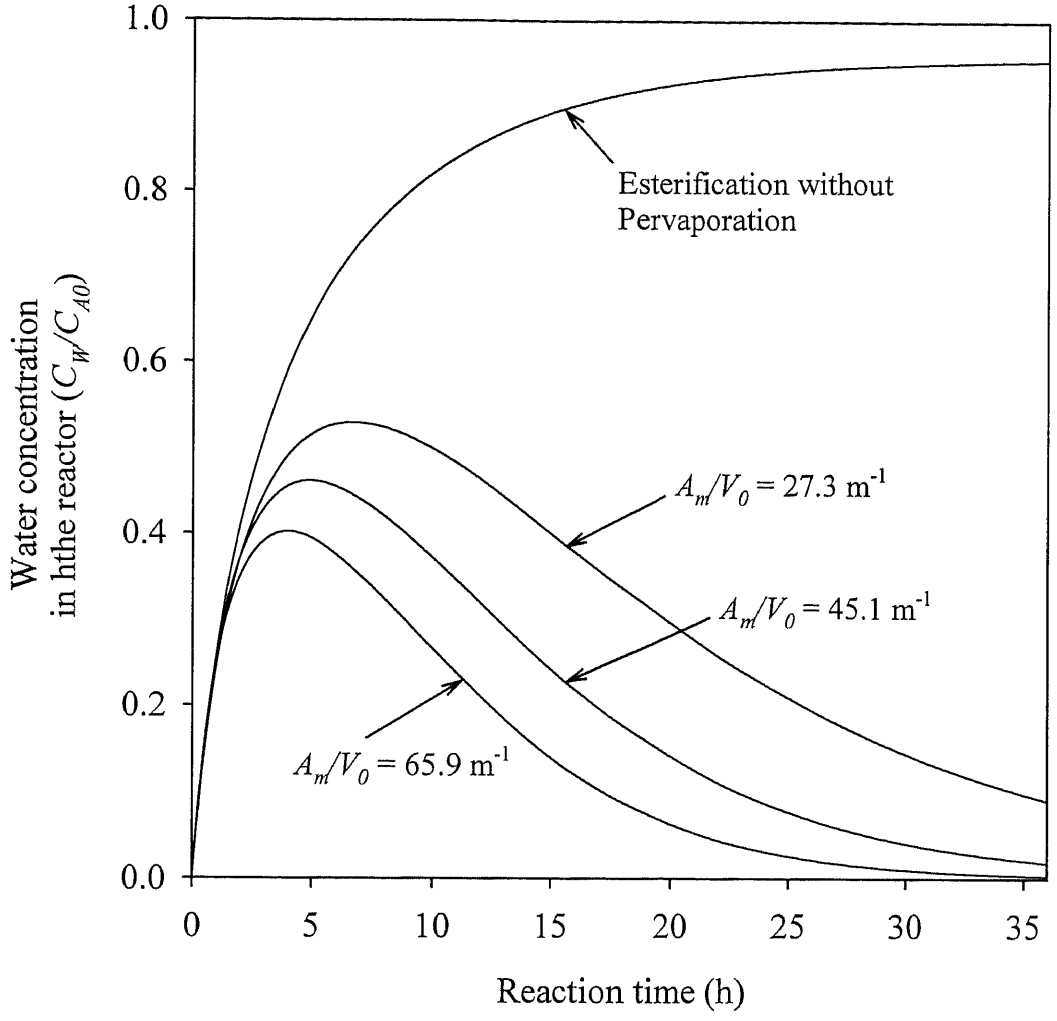

Figure 4.15 Effect of Effective Membrane Area to Initial Solution Volume Ratio (A_m/V_0) on Water Concentration in the Pervaporation-Integrated Batch Reactor: T = 341 K, θ_B = 8, C_{cat} = 1.10 M

The calculated concentrations of water at different A_m/V_0 ratios shown in Figure 4.15 illustrate how water concentration changes with reaction time in the pervaporation-integrated reactor. It can be seen that when the membrane is used to enhance the reaction performance, water concentration undergoes a maximum as reaction proceeds. The

increase in A_m/V_0 ratio leads to a faster conversion of acid and alcohol to ester, and to a decrease in the areas under the curves, i.e. to a lesser accumulation of water in the reactor; this lower accumulation favors increased forward reaction because it reduces the ester hydrolysis.

The existence of a maximum in the water concentration versus time plots is caused by two competing effects: one is the water formation due to the reaction, which tends to cause water build-up in the reactor, and the other water removal by pervaporation, which tends to lower water concentration in the reactor. During the early period of reaction, the rate of chemical reaction is high, whereas water concentration is low and so is the rate of water removal from the reactor. Consequently, water concentration gradually increases until it reaches a maximum when its formation and removal rates become equal. Thereafter the rate of water removal is faster than the rate of formation, resulting in depletion of water from the reactor. Naturally, for a given reaction system, the larger the value of A_m/V_0, the shorter the time required for water to reach the maximum concentration and the smaller the magnitude of the maximum water concentration, as shown in Figure 4.15.

4.5 Selectivity of the Poly(vinyl alcohol)-based Composite (GFT) Membrane

The analysis of permeate indicated the presence of two components, water and methanol. The average concentration of methanol was found to be 7.71% by volume. The selectivity of water over methanol of the GFT membrane can be calculated according to equation 4.3:

$$\alpha_{W/B} = \frac{y_W / y_B}{x_W / x_B} \tag{4.3}$$

where y_W and y_B are the molar concentrations of water and methanol in the permeate and x_W and x_B are the molar concentrations of water and methanol in the feed. The average selectivity of the GFT membrane was found to be 568. The poly(vinyl alcohol)-based membrane has a high selectivity for water over the alcohol; however this polymeric material contains secondary alcohol groups which could also be esterified by the carboxylic acid in the presence of the catalyst. It was found that the membrane performance deteriorated after contacting with the reaction mixture at high temperature for 24 h. A physical change that could be observed was a change of the membrane color, which became darker compared to a fresh (unused) membrane.

In the mathematical model, it was assumed that the pervaporation membrane allows only water to pass through. The assumption means the methanol flux (J_B) is equal to zero. According to the experimental results, the assumption is reasonable because the errors caused by it are always less than –0.04%. A detailed discussion regarding the impact of methanol flux on calculated conversion-time profiles of pervaporation-assisted esterification is provided in Appendix D of the thesis.

4.6 Effect of Temperature on the Pervaporation-Integrated System

Experimental results (Figure 4.16) show that an increase in temperature causes, as expected, an acceleration of esterification but also an acceleration of pervaporation. Detailed values are provided in Table 4.25. The corresponding water contents in the reactor during the reaction are shown in Figure 4.17. The water concentration increases and decreases much faster at higher temperature. The maximum points of water concentrations shift towards shorter times when the temperature increases. This indicates

a stronger acceleration of the water removal rate by the pervaporation. The temperature affected the pervaporation by an increase in the transmembrane flux of the more permeable component (water). Besides, the partial vapor pressure of water was increased by an increase in temperature.

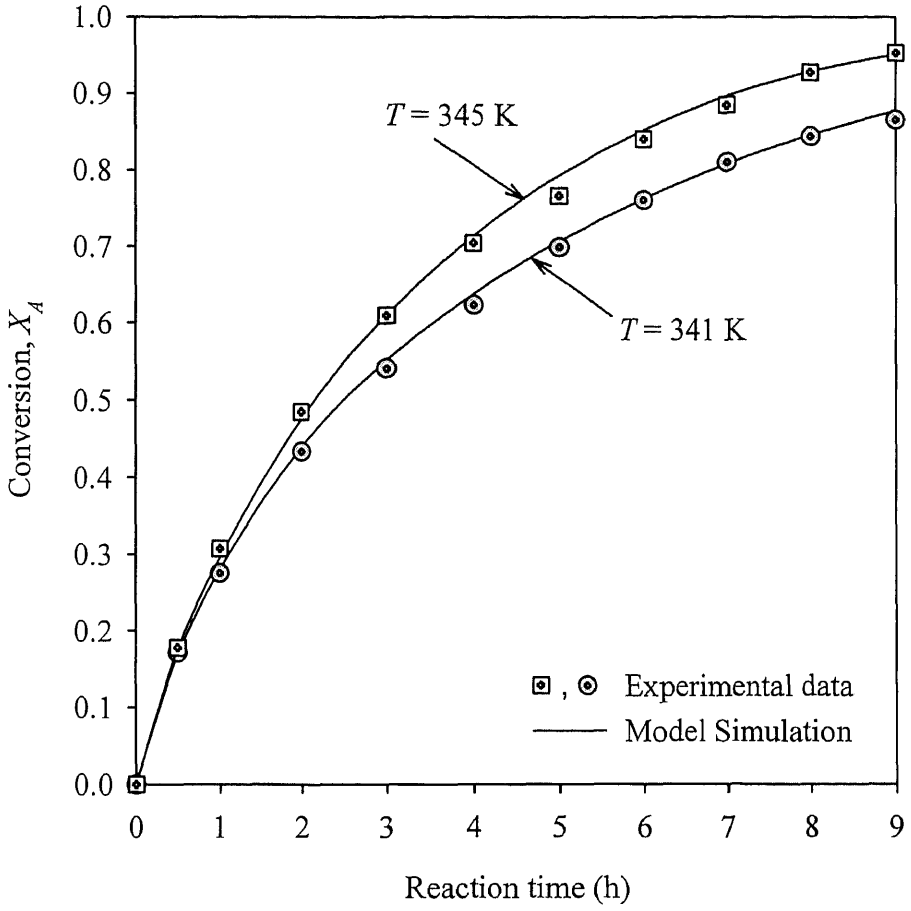

Figure 4.16 Effect of Reaction Temperature on Pervaporation-Assisted Esterification: $\theta_B = 8.0$, $C_{cat} = 1.10$ M, $A_m/V_0 = 65.9$ m^{-1}

Table 4.25 Experimental and Calculated Conversions for Pervaporation-Assisted Esterification at $T = 341$ and $T = 345$ K

Reaction time (h)	$T = 341$ K		$T = 345$ K	
	X_A, *exp.* (%)	X_A, *calc.* (%)	X_A, *exp.* (%)	X_A, *calc.* (%)
0.0	0.00	0.00	0.00	0.00
0.5	17.13	16.78	17.82	17.56
1.0	27.54	28.09	30.76	29.63
2.0	43.34	43.92	48.49	47.59
3.0	54.08	55.15	60.93	61.00
4.0	62.30	63.77	70.42	71.34
5.0	69.86	70.64	76.59	79.26
6.0	76.03	76.22	84.03	85.22
7.0	81.04	80.79	88.44	89.63
8.0	84.35	84.56	92.72	92.82
9.0	86.51	87.65	95.29	95.08

Experimental conditions: $\theta_B = 8.0$, $C_{cat} = 1.10$ M, $A_m/V_0 = 65.9$ m^{-1}

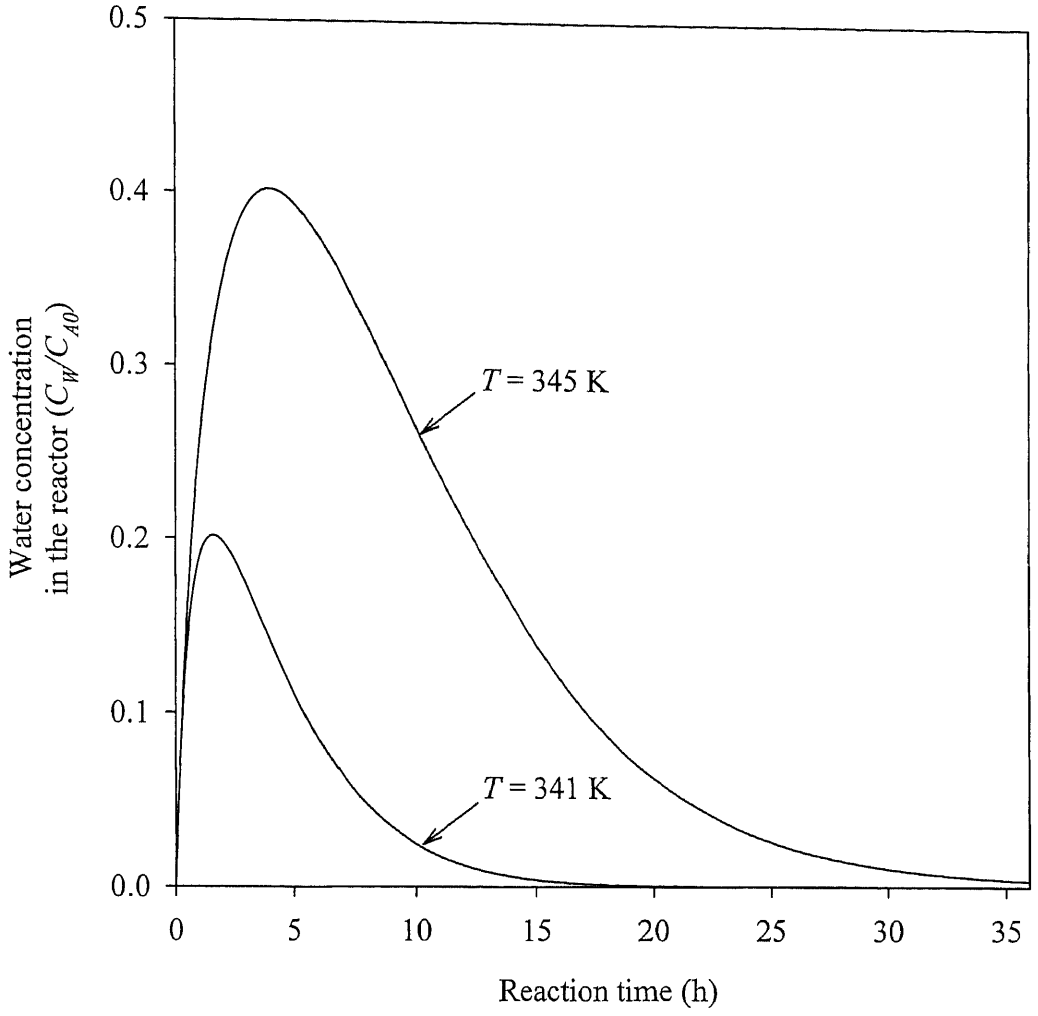

Figure 4.17 Effect of Reaction Temperature on Water Concentration in the Pervaporation-Integrated Batch Reactor: θ_B = 8, C_{cat} = 1.10 M, A_m/V_0 = 65.9 m^{-1}

4.7 Comparison between the Effect of the Process Parameters (Temperature, Catalyst Concentration, θ_B, and A_m/V_0)

The effects of the process parameters, T, C_{cat}, θ_B, and A_m/V_0, are interrelated, and can be used to predict optimum operating conditions for the production process. These four parameters can be categorized into three groups:

- Factors affecting only the esterification kinetics: catalyst concentration, and initial molar ratio of methanol to salicylic acid.
- Factors affecting only the pervaporation kinetics: ratio of effective membrane area to volume of reaction mixture.
- Factors affecting both the esterification and pervaporation kinetics: temperature.

To compare the effect of these different factors, the calculated time needed to achieve certain values of salicylic acid conversion (t_{90} and t_{95}) were used. All curves obtained from the calculated values of t_{90} and t_{95} have the same pattern (Figure 4.18). In the case of the two parameters, initial molar ratio (θ_B) and A_m/V_0, without any economic consideration, it appears that there is an optimum value of each parameter for a fast conversion of salicylic acid. The optimum values for θ_B was about 20. This is due to the fact that there was not much reduction of the t_{95} beyond θ_B equal to 20. For A_m/V_0 ratio, it was found that the optimum value would be about 45 m^{-1}, which gives rise to 95% of conversion in 14 hours. However, a simultaneous cost optimization may yield other optimum values.

Temperature has the strongest impact on the performance of the integrated process because it influences both the esterification and pervaporation rates.

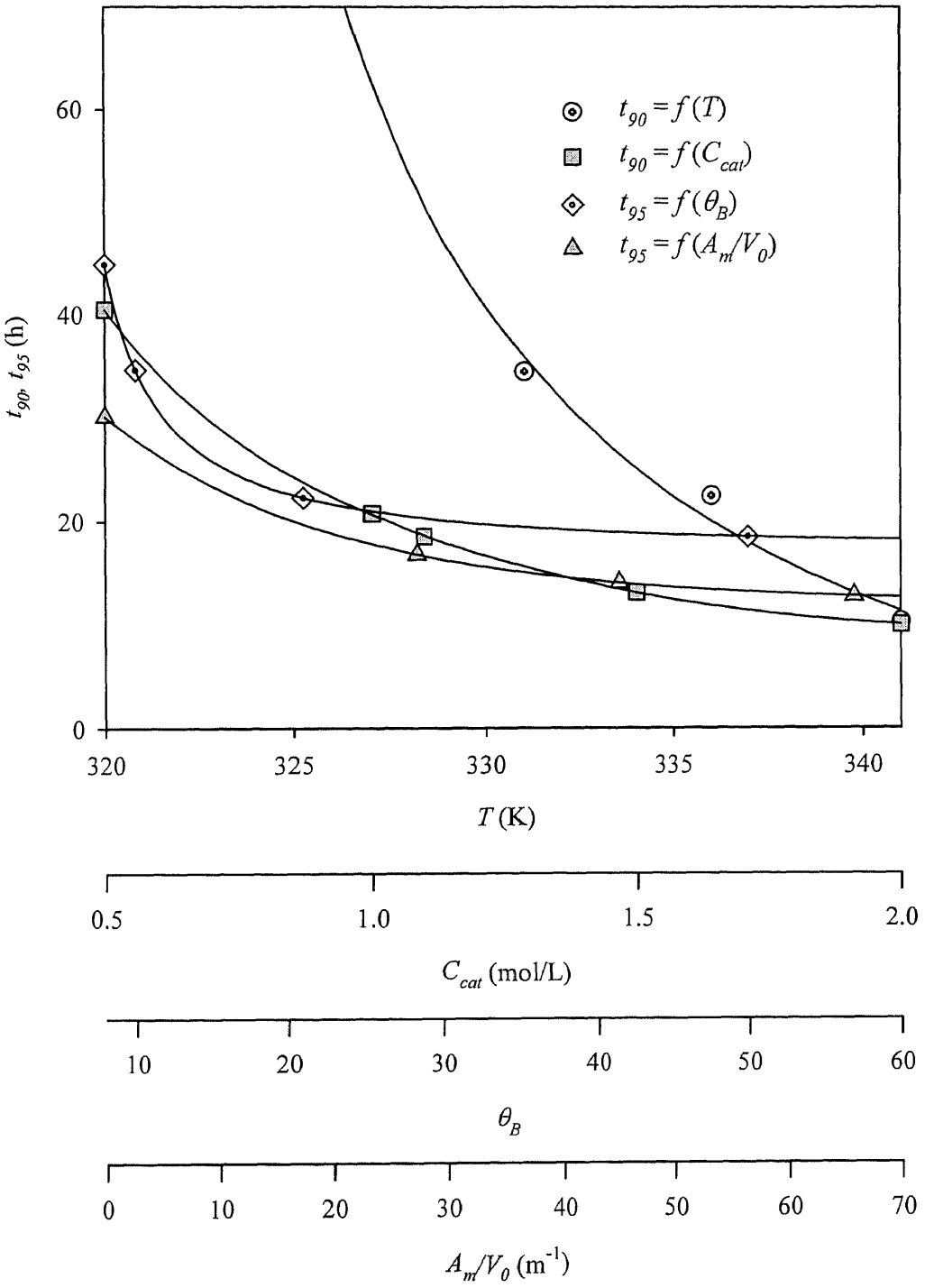

Figure 4.18 Comparison of the Effect of T, C_{cat}, θ_B, and A_m/V_0 on t_{90} and t_{95}

The catalyst concentration is the second most effective parameter. Although it affects only the kinetics of esterification it is rather efficient. It has been discussed earlier that the separation cost in downstream processes may affect significantly the economy of the overall process by using a large amount of catalyst.

The ratio of membrane area to reaction volume and the initial molar ratio of methanol to salicylic acid appeared to have the same influence on the time required to attain a certain value of conversion. However, as mentioned before, there are several disadvantages of using a θ_B value to drive the reaction. First, by using a high θ_B, a large amount of waste of the unreacted feed component will be generated; it has to be separated from the desired product which increases the operational cost for separation. Second, the production cost will increase due to the use of a large amount of reactant.

CHAPTER 5

CONCLUSIONS AND RECOMMENDATIONS

5.1 Conclusions

Pervaporation was shown to be an effective means for dehydration of reaction mixtures in esterification processes. By integrating a pervaporation unit to a conventional batch reactor, the production rate of the esterification process can be increased substantially. Likewise, the reaction equilibrium can be significantly shifted towards the final products. Experimental data obtained with poly(vinyl alcohol)-based membranes as well as modeling results for esterification in the presence and absence of pervaporation support such claims.

This study has shown that the esterification externally coupled with pervaporation is governed by four main parameters: temperature, catalyst concentration, initial molar ratio of alcohol to acid, and A_m/V_0 ratio. The effect of these parameters on the conversion rate for ester production was investigated experimentally and modeled. Their impact can be classified according to the order: temperature > catalyst concentration > initial molar ratio of methanol to salicylic acid ≈ effective membrane area to reaction volume ratio.

The process was described by a detailed mathematical model, which takes into consideration details of the reaction kinetics. To validate the model, independent batch kinetic experiments were performed with different initial molar ratio of the reactants (θ_B) and catalyst concentrations at different temperatures. The catalyst was sulfuric acid at concentrations varying from 0.5 to 2.0 molar. Based on batch kinetic experiments, the

rate constant of the forward reaction was found to have a linear dependence on the catalyst concentration.

The mathematical model described successfully the performance of the integrated (pervaporation-assisted) system. The validated model can be used in simulation studies for parameter sensitivity and optimization purposes. However, cost optimization would be needed if an industrial operation is considered.

5.2 Recommendations for Further Research

It is recommended to proceed with a modification of the model presented in this thesis to include the influence of the reaction mechanism of this specific reaction between salicylic acid and methanol in the presence of sulfuric acid as a catalyst. The acid-catalyzed esterification reaction is a complicated reaction and it is more complex than that given by the usual equation. According to the reaction kinetics included in the present model, the reaction between salicylic acid and methanol was assumed to be of the bimolecular-type (Figure 5.1). However, due to the fact that salicylic acid is an ortho-substituted aromatic carboxylic, it could react with methanol by the $A_{AC}1$ mechanism (unimolecular) (Figure 5.2). For the best prediction, the theoretical rate equation should be derived based on the true mechanisms of this specific reaction. A fundamental understanding of the mechanistic viewpoint of this specific reaction is necessary for calculation, simulation, and design of the process.

As mentioned above, the use of large amounts of sulfuric acid as a catalyst in the esterification leads to an increase in the operational cost for subsequent separations at downstream processes; it would be advantageous if heterogeneous catalytic materials could

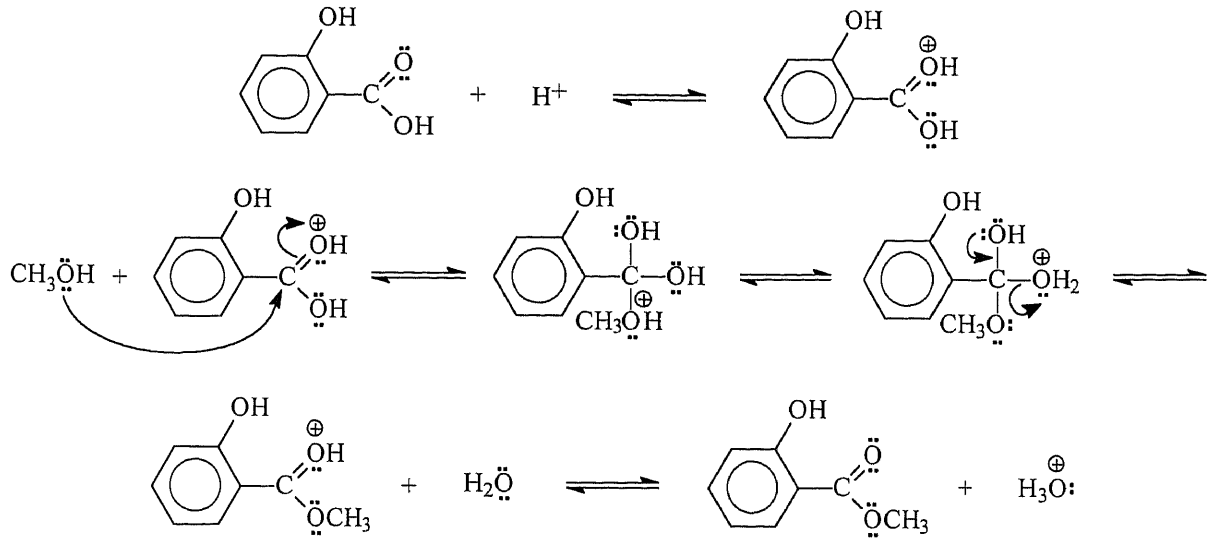

Figure 5.1 $A_{AC}2$ (Acid-Catalyzed, Acyl-Oxygen Cleavage, *Bimolecular*) Mechanism

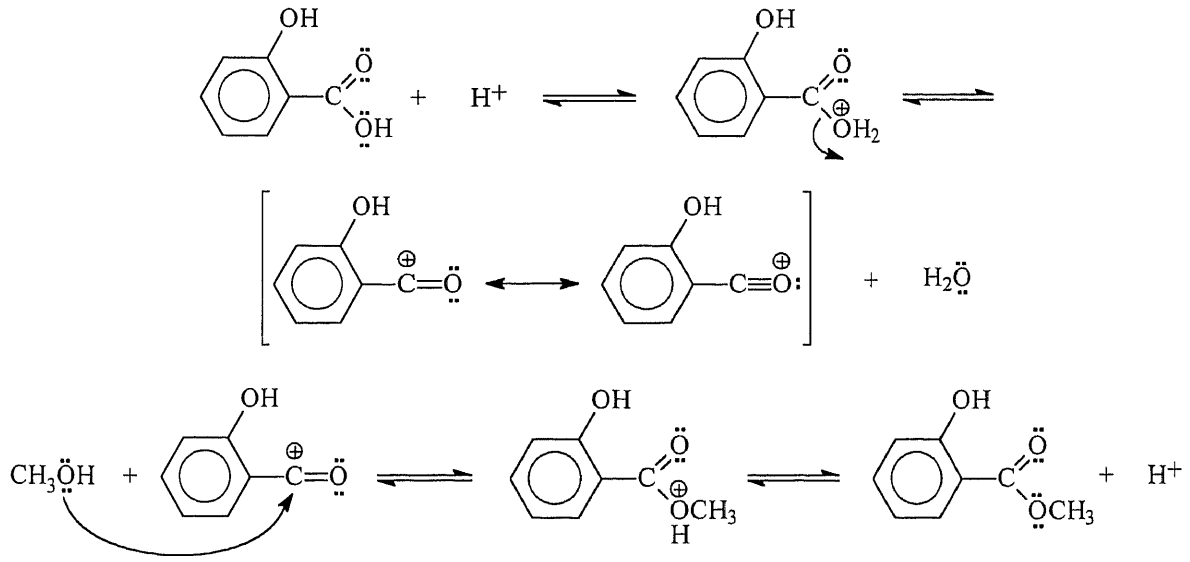

Figure 5.2 $A_{AC}1$ (Acid-Catalyzed, Acyl-Oxygen Cleavage, *Unimolecular*) Mechanism

be applied to this specific reaction. It is recommended to study an alternative process for synthesis of methyl salicylate by using an acid ion exchange resin. By the immobilization of protons in this polymeric material, no acid is dissolved in the reaction mass and therefore no neutralization is necessary. Once the system is developed, one can apply the pervaporation unit into the process to enhance the reaction performance. It will be useful to develop the mathematical model including the kinetics of heterogeneous catalysis and membrane performance, which could be used for optimization of the process design.

From the engineering design viewpoint, the membrane stability is one of the most important issues that have to be considered. The ability of a membrane to maintain both the permeability and selectivity under specific system conditions for an extended period of time is important for the process design.

By employing the poly(vinyl alcohol)-based membranes in esterification process, the membrane is exposed to concentrated acids at high temperature. As discussed earlier in the thesis, salicylic acid in the presence of sulfuric acid in the reaction mixture can esterify the membranes. Consequently, the life of the membrane is shorter than hoped for. To use pervaporation as economically as possible, a factor that has to be considered is the membrane life. Besides the high transmembrane flux and selectivity, the pervaporation membrane selected for the process should have a longer life span. A membrane with longer life span needs to be replaced less often and therefore results in lower operating costs. For the studied system, water has to be separated from the reaction mixture that has a high concentration of methanol. Due to the small size of methanol molecules, the selected membrane must have a high selectivity of water over methanol. There is no alternative other than poly(vinyl alcohol) composite membrane for this case. However,

for other esterification systems using higher molecular weight alcohols such as butanol, one might consider other membranes as alternatives. A type of membranes that can be considered as an option to use with esterification processes is a perfluorinated membrane such as a Nafion-like membrane. Nafion is a perfluorinated ion-exchange membrane endowed with both catalytic and separative properties, which is useful to facilitate esterification processes. Although the Nafion-like membranes are not highly selective for water over alcohols (especially lower molecular weight ones such as methanol), they can be used for esterification of carboxylic acids with higher molecular weight alcohols such as butanol. An advantage of the Nafion-like membranes over the poly(vinyl alcohol) composite membranes is their stability. Since the Nafion-like membranes do not have secondary alcohol groups, they will not get esterified by carboxylic acid in the presence of catalyst. Moreover, The Nafion-like membranes are a group of polymeric materials that contain fluorocarbon backbones, therefore, they will be able to withstand high temperature and severe chemical environments better than the poly(vinyl alcohol)-based membranes. It is an interesting area of research to explore the possibilities of applying this type of membranes to pervaporation-facilitated processes.

APPENDIX A

RATE CONSTANT DETERMINATION METHODOLOGY AND SAMPLE SIMULATIONS OF BATCH ESTERIFICATION PROCESS

Esterification of salicylic acid with methanol is represented by the following stoichiometric equation:

$$\underset{(A)}{RCOOH} + \underset{(B)}{R'OH} \underset{k_b}{\overset{k_f}{\rightleftharpoons}} \underset{(E)}{RCOOR'} + \underset{(W)}{H_2O} \qquad \text{(A.1)}$$

where k_f is the forward reaction rate constant and k_b is the reverse reaction rate constant.

The rate expression according to equation A.1 is

$$-\frac{dC_A}{dt} = k_f C_A C_B - k_b C_E C_W \qquad \text{(A.2)}$$

Considering the stoichiometry of equation A.1, the concentration of any species at any instant for the constant-volume system can be written as

$$C_A = C_{A0}(1 - X_A) \qquad \text{(A.3)}$$

$$C_B = C_{A0}(\theta_B - X_A) \qquad \text{(A.4)}$$

$$C_E = C_{A0}(\theta_E + X_A) \qquad \text{(A.5)}$$

$$C_W = C_{A0}(\theta_W + X_A) \qquad \text{(A.6)}$$

Substitute equation A.3 to A.6 into equation A.2 yields

$$\frac{dX_A}{dt} = C_{A0}\left[k_f(1 - X_A)(\theta_B - X_A) - k_b X_A^2\right] \qquad \text{(A.7)}$$

Figure A.1 shows one example of data fitting for a particular experiment performed at $T = 336$ K, $\theta_B = 8.0$ and $C_{cat} = 1.10$ M. The experimental conversion data up

to 1 h are provided in Table A.1. The set of parameters used in the sample calculation is as follows:

C_{A0}	2.324 mol/L
k_{f0}	2.33×10^{-2} L/(mol.h)
K_e	3.114
a	1.62 L/mol
V_0	272.1 mL

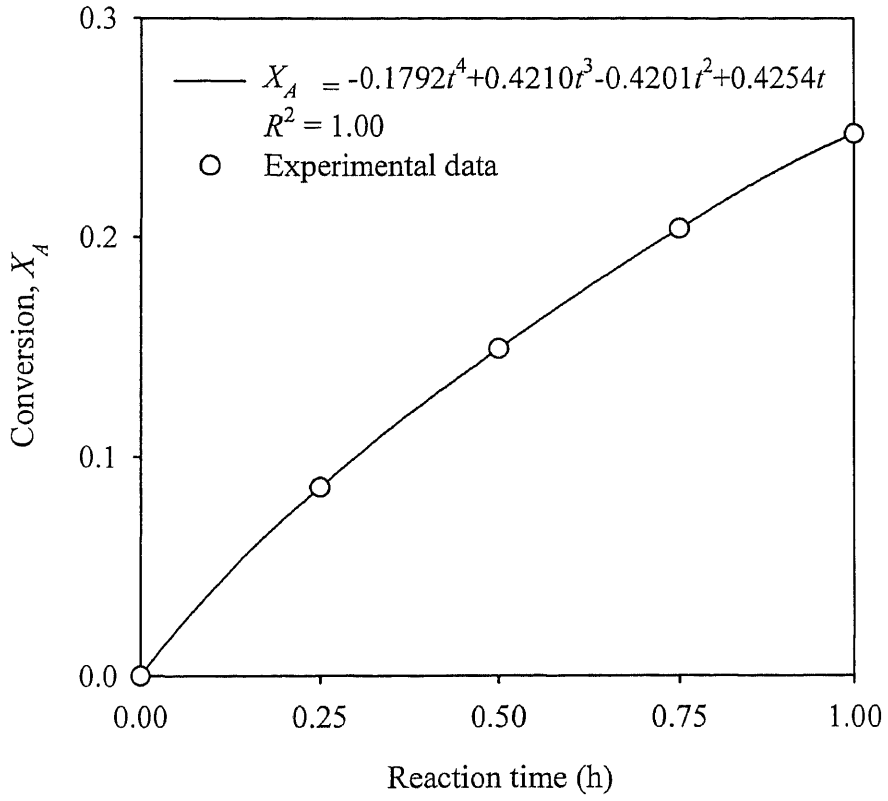

Figure A.1 Conversion-Time Curve of Batch Esterification at $T = 336$ K when $\theta_B = 8.0$ and $C_{cat} = 1.10$ M

Table A.1 Experimental Conversions for Batch Esterification at $T = 336$ K when $\theta_B = 8.0$ and $C_{cat} = 1.10$ M

Reaction time (h)	X_A, *exp.* (%)
0.00	0.00
0.25	8.60
0.50	14.91
0.75	20.37
1.00	24.71

Initial forward rate constant can be determined from equation A.7. Rearranging equation A.7 gives

$$k_f = k_{f0} = \frac{\left.\frac{dX_A}{dt}\right|_{t=0}}{C_{A0}\theta_B} \tag{A.8}$$

where $\left.\frac{dX_A}{dt}\right|_{t=0}$ is a slope at the origin of the plot of conversion versus time (Figure A.1) which can be determined by differentiating the fitted polynomial curve with respect to time and setting X_A equal to zero.

$$\left.\frac{dX_A}{dt}\right|_{t=0} = -0.7168t^3\Big|_{t=0} + 1.2630t^2\Big|_{t=0} - 0.8402t\Big|_{t=0} + 0.4254$$
$$= 0.4254 \text{ h}^{-1}$$

Consequently, k_{f0} can be calculated from equation A.8 as

$$k_{f0} = \frac{0.4254}{2.324 \times 8.0} = 2.288 \times 10^{-2} \text{ (mol/L)}^{-1}\text{(h)}^{-1}$$

The set of differential and algebraic equations was solved through numerical integration technique by using this calculated k_{f0} as an initial value in the model. Results

of the integrations were compared with experimental data either graphically or quantitatively*, and used to estimate value for k_{f0} which best fit the mathematical model to the data. The final value of k_{f0} was calculated as 2.330×10^{-2} $(mol/L)^{-1}(h)^{-1}$. This final value of k_{f0} was used to simulate the model-fitted conversion-time profile as shown in Figure 4.1.

MATHEMATICA® software codes for the batch simulation performed at $T = 336$ K when $\theta_B = 8.0$ and $C_{cat} = 1.10$ M. are provided in the next pages.

* (based on differences between experimental and calculated values from fitting)

Simulations of Batch Esterification Process

$T = 336$ K, $m_0 = 8.0$, $C_{cat} = 1.10$ M

```
In[1]:= C_A0 = 2324 (* mol/m^3 *)

Out[1]= 2324

In[2]:= k_f0 = 2.33 x 10^-5 (* m^3/(mol.h) *)

Out[2]= 0.0000233

In[3]:= a = 1.62 / 1000 (* m^3/mol *)

Out[3]= 0.00162

In[4]:= k_f = k_f0 / (1 + a C_A0 ξ[t]) (* m^3/(mol.h) *)

Out[4]= 0.0000233 / (1 + 3.76488 ξ[t])

In[5]:= K_e = 3.114

Out[5]= 3.114

In[6]:= Θ_B = 8

Out[6]= 8

In[7]:= Θ_E = 0

Out[7]= 0

In[8]:= Θ_w = 0

Out[8]= 0

In[9]:= M_A = 0.13812 (* kg/mol *)

Out[9]= 0.13812

In[10]:= M_B = 0.03204 (* kg/mol *)

Out[10]= 0.03204

In[11]:= M_E = 0.15215 (* kg/mol *)

Out[11]= 0.15215

In[12]:= M_W = 0.018016 (* kg/mol *)

Out[12]= 0.018016
```

```
In[13]:= ρA = 1443  (* kg/m^3 *)

Out[13]= 1443

In[14]:= ρB = 791.4  (* kg/m^3 *)

Out[14]= 791.4

In[15]:= ρE = 1181  (* kg/m^3 *)

Out[15]= 1181

In[16]:= ρW = 978  (* kg/m^3 *)

Out[16]= 978

In[17]:= V0 = 272.1 × 10^-6 (* m^3 *)

Out[17]= 0.0002721

In[18]:= X'[t] == kf CA0 (((1 - X[t]) (ΘB - X[t])) - ((ΘE + X[t]) ξ[t])/Ke)

Out[18]= X'[t] == (0.0541492 ((1 - X[t]) (8 - X[t]) - 0.32113 X[t] ξ[t]))/(1 + 3.76488 ξ[t])

In[19]:= Sol1 = NDSolve[{X'[t] == kf CA0 (((1 - X[t]) (ΘB - X[t])) - ((ΘE + X[t]) ξ[t])/Ke),
           υ'[t] == 0,
           ξ'[t] == (X'[t] - ξ[t] υ'[t])/υ[t], X[0] == 0, ξ[0] == 0, υ[0] == 1},
           {X[t], ξ[t], υ[t]}, {t, 0, 50}]

Out[19]= {{X[t] → InterpolatingFunction[{{0., 50.}}, <>][t],
           ξ[t] → InterpolatingFunction[{{0., 50.}}, <>][t],
           υ[t] → InterpolatingFunction[{{0., 50.}}, <>][t]}}
```

```
In[20]:= Result1 = Table[{t, Evaluate[X[t] /. Sol1]}, {t, 0, 10, 0.5}];
         TableForm[Result1]
```

Out[20]//TableForm=

0	0.
0.5	0.152475
1.	0.248185
1.5	0.319957
2.	0.377719
2.5	0.426062
3.	0.467552
3.5	0.503792
4.	0.535861
4.5	0.564525
5.	0.590352
5.5	0.613774
6.	0.635132
6.5	0.654695
7.	0.672686
7.5	0.689287
8.	0.704649
8.5	0.718903
9.	0.732159
9.5	0.744512
10.	0.756045

```
In[21]:= Simulation1 = Plot[Evaluate[X[t] /. Sol1], {t, 0, 10},
         PlotRange → {0, 1}]
```

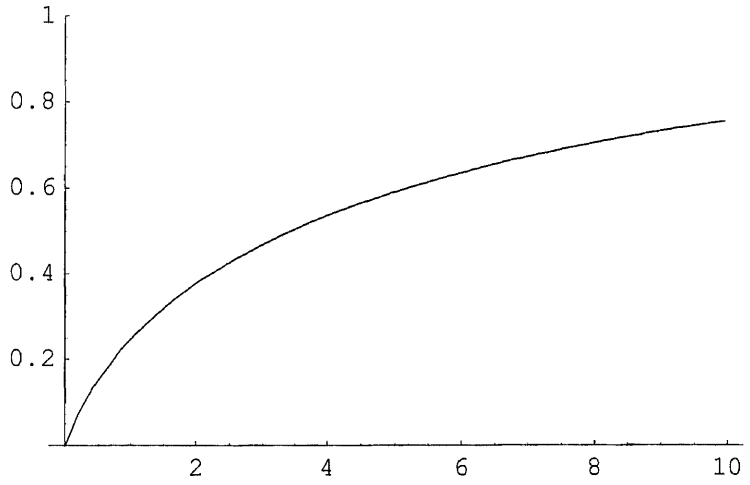


```
Out[21]= - Graphics -
```

```
In[22]:= data1 =
          {{0, 0}, {0.25, 0.0860}, {0.5, 0.1491}, {0.75, 0.2037}, {1, 0.2471},
           {2, 0.3710}, {4, 0.5230}, {6, 0.6186}, {8, 0.6821}, {10, 0.7324}}
```

```
Out[22]= {{0, 0}, {0.25, 0.086}, {0.5, 0.1491}, {0.75, 0.2037}, {1, 0.2471},
          {2, 0.371}, {4, 0.523}, {6, 0.6186}, {8, 0.6821}, {10, 0.7324}}
```

```
In[23]:= dataplot1 = ListPlot[data1, Prolog -> AbsolutePointSize[4]];
```

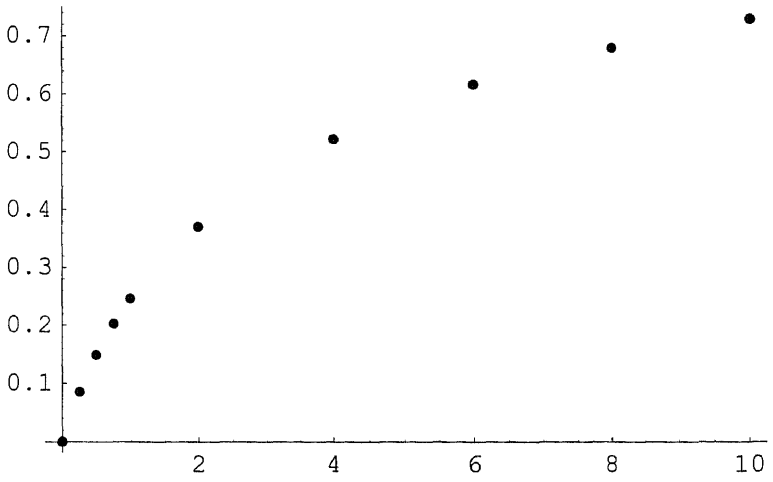


```
In[24]:= Show[dataplot1, Simulation1]
```

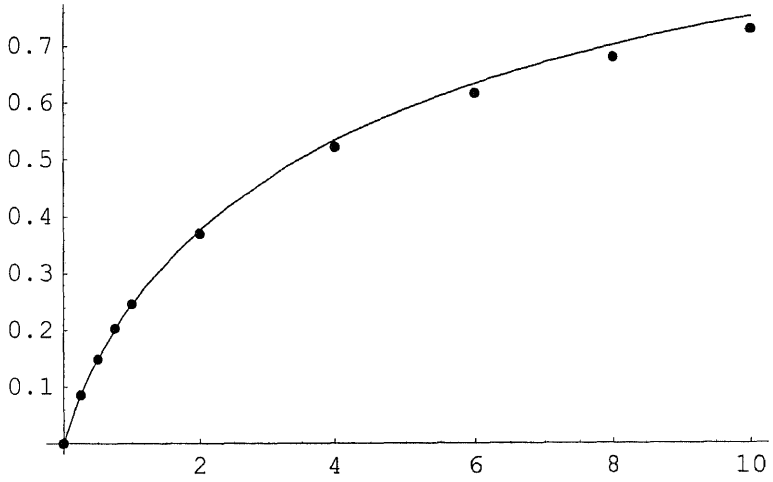


```
Out[24]= - Graphics -
```

APPENDIX B

SAMPLE SIMULATIONS OF PERVAPORATION-ASSISTED ESTERIFICATION PROCESS BY MATHEMATICA® SOFTWARE PACKAGE

Simulations of an arbitrary pervaporation-assisted esterification process by MATHEMATICA® software package are provided here. MATHEMATICA® codes for the simulation are corresponding to the experiment performed at $T = 336$ K when $\theta_B = 8.0$, $C_{cat} = 1.10$ M. and $A_m/V_0 = 65.9$ m^{-1}. The set of parameters used in the sample calculation is as follows:

C_{A0}	2.191 mol/L
k_{f0}	2.52×10^{-2} L/(mol.h)
K_e	4.37
a	1.025 L/mol
V_0	476.2 mL

Simulations of Pervaporation-Assisted Esterification Process

$T = 341$ K, $C_{cat} = 1.10$ M, $m_0 = 8.0$, $A_m/V_0 = 65.9$ m^{-1}

```
In[1]:= A_m = 314 × 10^-4  (* m^2 *)

Out[1]= 157/5000

In[2]:= C_A0 = 2191 (* mol/m^3 *)

Out[2]= 2191

In[3]:= k_f0 = 2.52 × 10^-5 (* m^3/(mol.h) *)

Out[3]= 0.0000252

In[4]:= a = 1.025 / 1000 (* m^3/mol *)

Out[4]= 0.001025

In[5]:= k_f = k_f0 / (1 + a C_A0 ξ[t]) (* m^3/(mol.h) *)

Out[5]= 0.0000252 / (1 + 2.24577 ξ[t])

In[6]:= K_e = 4.37

Out[6]= 4.37

In[7]:= θ_B = 8

Out[7]= 8

In[8]:= θ_E = 0

Out[8]= 0

In[9]:= θ_w = 0

Out[9]= 0

In[10]:= M_A = 0.13812  (* kg/mol *)

Out[10]= 0.13812

In[11]:= M_B = 0.03204  (* kg/mol *)

Out[11]= 0.03204
```

In[12]:= $M_E = 0.15215$ (* $\frac{kg}{mol}$ *)

Out[12]= 0.15215

In[13]:= $M_W = 0.018016$ (* $\frac{kg}{mol}$ *)

Out[13]= 0.018016

In[14]:= $\rho_A = 1443$ (* $\frac{kg}{m^3}$ *)

Out[14]= 1443

In[15]:= $\rho_B = 791.4$ (* $\frac{kg}{m^3}$ *)

Out[15]= 791.4

In[16]:= $\rho_E = 1181$ (* $\frac{kg}{m^3}$ *)

Out[16]= 1181

In[17]:= $\rho_W = 978$ (* $\frac{kg}{m^3}$ *)

Out[17]= 978

In[18]:= $J_A = 0$ (* $\frac{mol}{m^2 \cdot h}$ *)

Out[18]= 0

In[19]:= $J_B = 0$ (* $\frac{mol}{m^2 \cdot h}$ *)

Out[19]= 0

In[20]:= $J_E = 0$ (* $\frac{mol}{m^2 \cdot h}$ *)

Out[20]= 0

In[21]:= $P_W = 0.00295$ (* $\frac{m}{h}$ *)

Out[21]= 0.00295

In[22]:= $V_0 = 476.2 \times 10^{-6}$ (* m^3 *)

Out[22]= 0.0004762

In[23]:= $\frac{A_m}{V_0}$ (* $\frac{1}{m}$ *)

Out[23]= 65.9387

In[24]:= $J_W = P_W C_{A0} \xi[t]$ (* $\frac{mol}{m^2 \cdot h}$ *)

Out[24]= 6.46345 ξ[t]

```
In[25]:= X'[t] == k_f C_A0 ( ((1 - X[t]) (θ_B - X[t])) / υ[t] - ((θ_E + X[t]) ξ[t]) / K_e )

Out[25]= X'[t] == (0.0552132 (-0.228833 X[t] ξ[t] + ((1-X[t]) (8-X[t])) / υ[t])) / (1 + 2.24577 ξ[t])

In[26]:= υ'[t] == -(A_m (J_A M_A / ρ_A + J_B M_B / ρ_B + J_E M_E / ρ_E + J_W M_W / ρ_W)) / V_0

Out[26]= υ'[t] == -0.00785099 ξ[t]

In[27]:= ξ'[t] == (X'[t] - ξ[t] υ'[t] - A_m J_W / (V_0 C_A0)) / υ[t]

Out[27]= ξ'[t] == (-0.194519 ξ[t] + X'[t] - ξ[t] υ'[t]) / υ[t]

In[28]:= Sol_1 = NDSolve[{X'[t] == k_f C_A0 ( ((1 - X[t]) (θ_B - X[t])) / υ[t] - ((θ_E + X[t]) ξ[t]) / K_e ),
           υ'[t] == -(A_m (J_A M_A / ρ_A + J_B M_B / ρ_B + J_E M_E / ρ_E + J_W M_W / ρ_W)) / V_0,
           ξ'[t] == (X'[t] - ξ[t] υ'[t] - A_m J_W / (V_0 C_A0)) / υ[t], X[0] == 0, ξ[0] == 0, υ[0] == 1},
           {X[t], ξ[t], υ[t]}, {t, 0, 50}]

Out[28]= {{X[t] → InterpolatingFunction[{{0., 50.}}, <>][t],
           ξ[t] → InterpolatingFunction[{{0., 50.}}, <>][t],
           υ[t] → InterpolatingFunction[{{0., 50.}}, <>][t]}}
```

```
In[29]:= Result1 = Table[{t, Evaluate[X[t] /. Sol1]}, {t, 0, 10, 0.5}];
         TableForm[Result1]
```

Out[29]//TableForm=

0	0.
0.5	0.167849
1.	0.280925
1.5	0.367992
2.	0.439178
2.5	0.499401
3.	0.55147
3.5	0.597159
4.	0.63767
4.5	0.67386
5.	0.706364
5.5	0.735672
6.	0.76217
6.5	0.78617
7.	0.80793
7.5	0.82767
8.	0.845575
8.5	0.86181
9.	0.876517
9.5	0.889827
10.	0.901855

```
In[30]:= Simulation1 = Plot[Evaluate[X[t] /. Sol1], {t, 0, 10},
           PlotRange → {0, 1}]
```

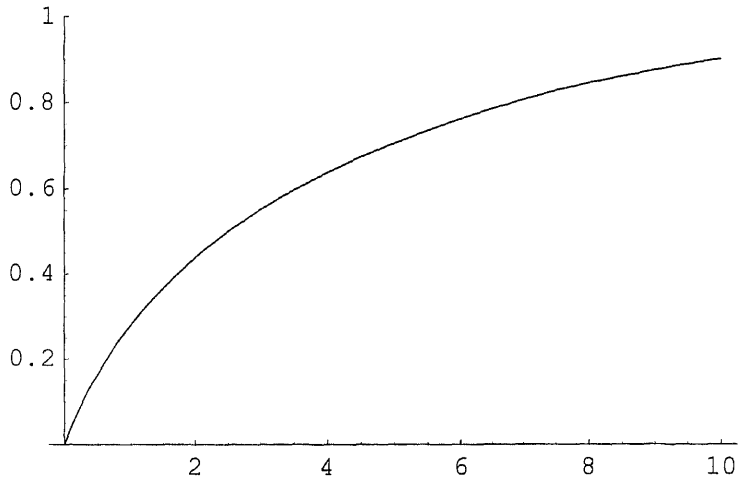

Out[30]= - Graphics -

```
In[31]:= Result2 = Table[{t, Evaluate[ξ[t] /. Sol1]}, {t, 0, 10, 0.5}];
         TableForm[Result2]
```

```
Out[31]//TableForm=
0       0.
0.5     0.159343
1.      0.252291
1.5     0.312126
2.      0.351457
2.5     0.376801
3.      0.392079
3.5     0.399877
4.      0.402003
4.5     0.399779
5.      0.394201
5.5     0.386035
6.      0.375883
6.5     0.364226
7.      0.351449
7.5     0.337865
8.      0.32373
8.5     0.309256
9.      0.294615
9.5     0.279951
10.     0.265383
```

```
In[32]:= Simulation2 = Plot[Evaluate[ξ[t] /. Sol1], {t, 0, 10},
           PlotRange → {0, 1}]
```

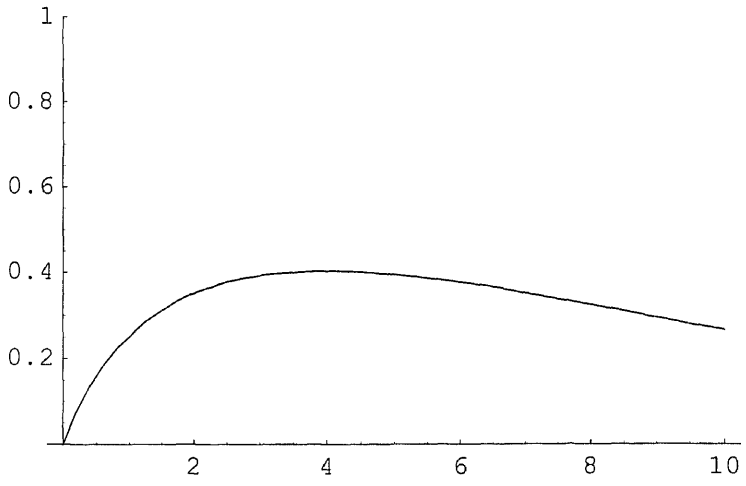


```
Out[32]= - Graphics -
```

```
In[33]:= Result3 = Table[{t, Evaluate[v[t] /. Sol1]}, {t, 0, 10, 0.5}];
         TableForm[Result3]
```

Out[33]//TableForm=

0	1.
0.5	0.999654
1.	0.998832
1.5	0.997716
2.	0.996409
2.5	0.994975
3.	0.993463
3.5	0.991907
4.	0.990331
4.5	0.988756
5.	0.987197
5.5	0.985665
6.	0.984169
6.5	0.982716
7.	0.981311
7.5	0.979958
8.	0.978659
8.5	0.977417
9.	0.976231
9.5	0.975104
10.	0.974033

```
In[34]:= Simulation3 = Plot[Evaluate[v[t] /. Sol1], {t, 0, 10}]
```

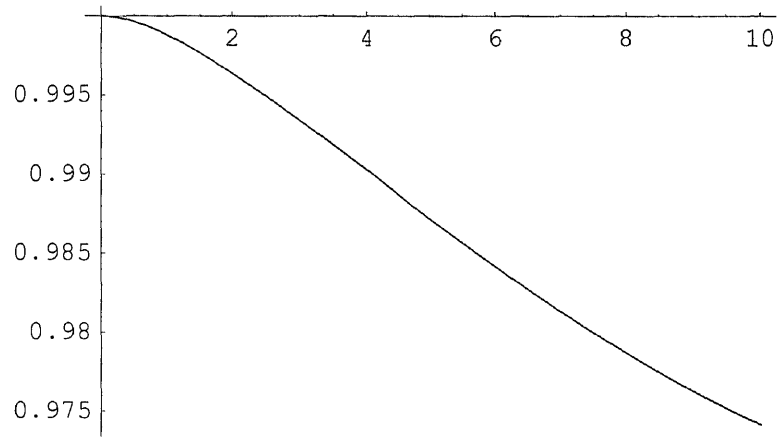


```
Out[34]= - Graphics -
```

```
In[35]:= data1 = {{0, 0}, {0.5, 0.171318}, {1, 0.275365}, {2, 0.433448},
           {3, 0.540752}, {4, 0.62297}, {5, 0.6986}, {6, 0.760346},
           {7, 0.810399}, {8, 0.843497}, {9, 0.865146}}
```

```
Out[35]= {{0, 0}, {0.5, 0.171318}, {1, 0.275365}, {2, 0.433448}, {3, 0.540752},
          {4, 0.62297}, {5, 0.6986}, {6, 0.760346}, {7, 0.810399},
          {8, 0.843497}, {9, 0.865146}}
```

```
In[36]:= dataplot1 = ListPlot[data1, Prolog -> AbsolutePointSize[4]];
```

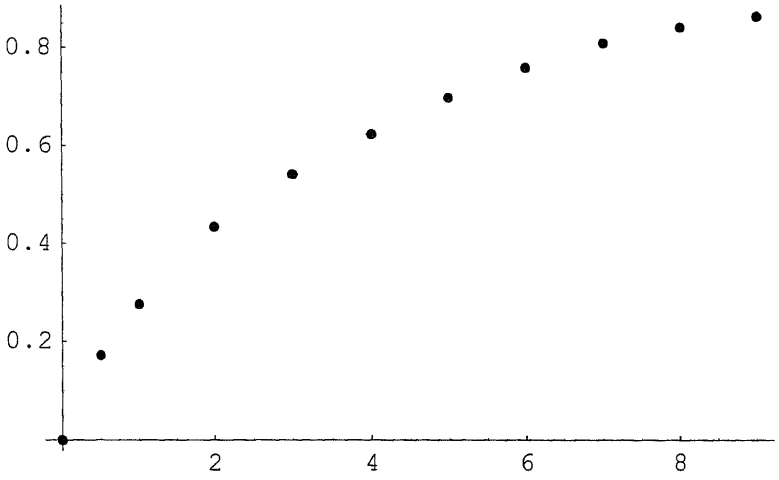


```
In[37]:= Show[dataplot1, Simulation1]
```

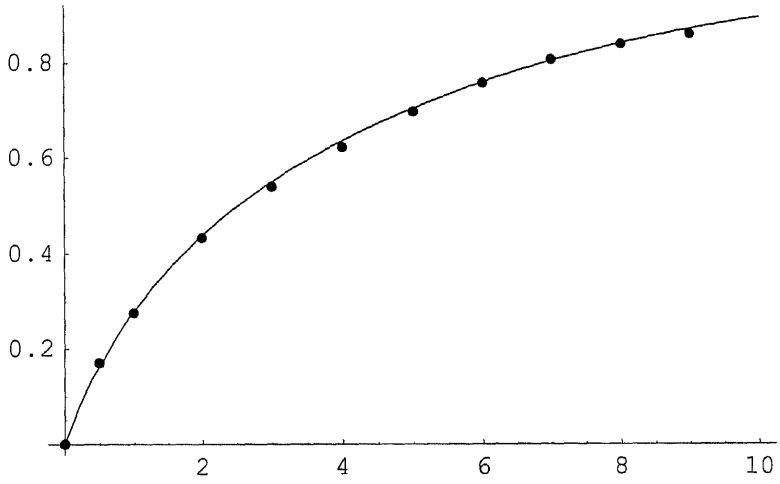


```
Out[37]= -Graphics-
```

```
In[38]:= Simulation4 = Plot[Evaluate[X[t] /. Sol1], {t, 0, 36},
           PlotRange → {0, 1}]
```

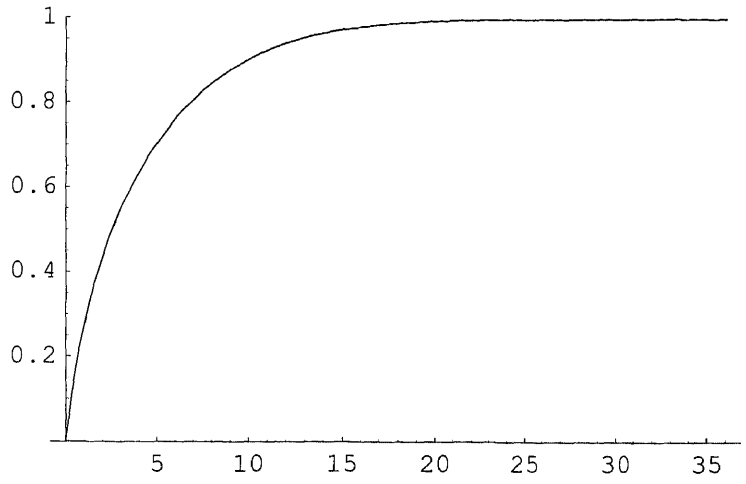


```
Out[38]= - Graphics -
```

```
In[39]:= Simulation5 = Plot[Evaluate[ξ[t] /. Sol1], {t, 0, 36},
           PlotRange → {0, 0.5}]
```

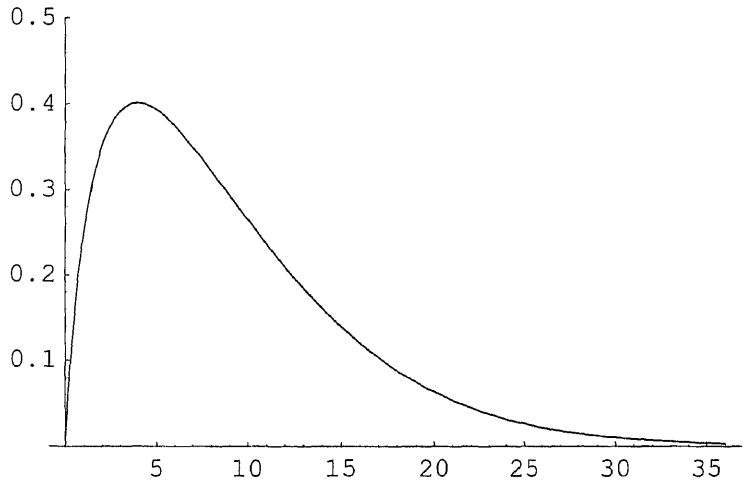


```
Out[39]= - Graphics -
```

In[40]:= **Show[Simulation$_4$, Simulation$_5$]**

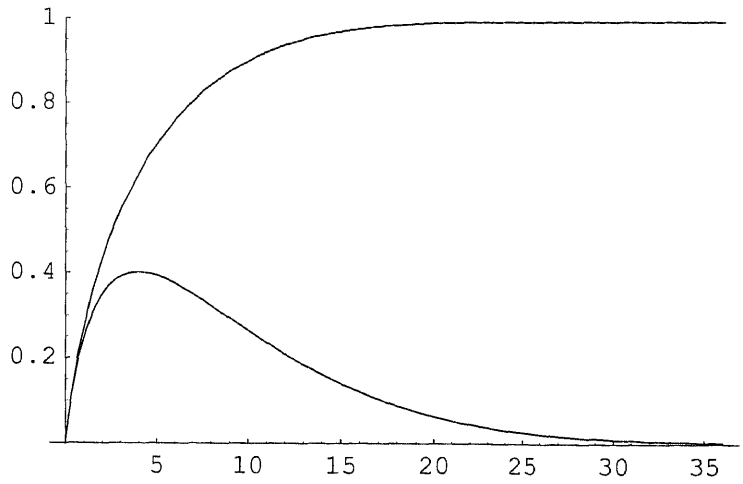

Out[40]= - Graphics -

APPENDIX C

IMPACT OF TEMPERATURE DISCREPANCY BETWEEN REACTOR VESSEL AND INTEGRATED SYSTEM ON REACTION RATE CONSTANTS

In the pervaporation-assisted esterification experiments, the temperature of the reaction mixture inside the reactor and the pervaporation unit was maintained at the same temperature. However, due to heat losses in transfer lines between the reactor and the pervaporation unit, the average temperature of the integrated system was lower than the temperature set at the reactor and the pervaporation unit.

Because of the temperature discrepancy, the rate constants obtained from the batch experiments can not be used for simulations of the pervaporation-assisted esterification performed at the same temperature. Therefore, to overcome the problem arising from temperature discrepancy, a blank experiment was carried out by using the integrated system without the membrane to obtain a value of k_{f0} at the average system temperature.

According to the Arrhenius equation (equation 4.1), the average system temperature could be estimated by employing the activation energy and frequency factor obtained from the batch experiments which were 135.09 kJ/mol and 2.667×10^{19} L/(mol.h) respectively. A sample calculation to show the impact of the temperature discrepancy is provided here for a particular pervaporation-assisted esterification experiment conducted at 341 K, $\theta_B = 8$, $C_{cat} =$ 1.10 M, and $A_m/V_0 = 65.9$ m^{-1}. A k_{f0} value of 2.52×10^{-2} L/(mol.h) was obtained by fitting the experimental data to the mathematical model. The average system temperature was calculated to be 336 K by using this k_{f0} value.

Although the temperature of the reactor and the pervaporation unit were fixed at 341 K, the calculated average system temperature was lower by 5 K. Conversion-time

profiles were simulated at 341 and 336 K to illustrate the effect of temperature discrepancy (Figure C.1).

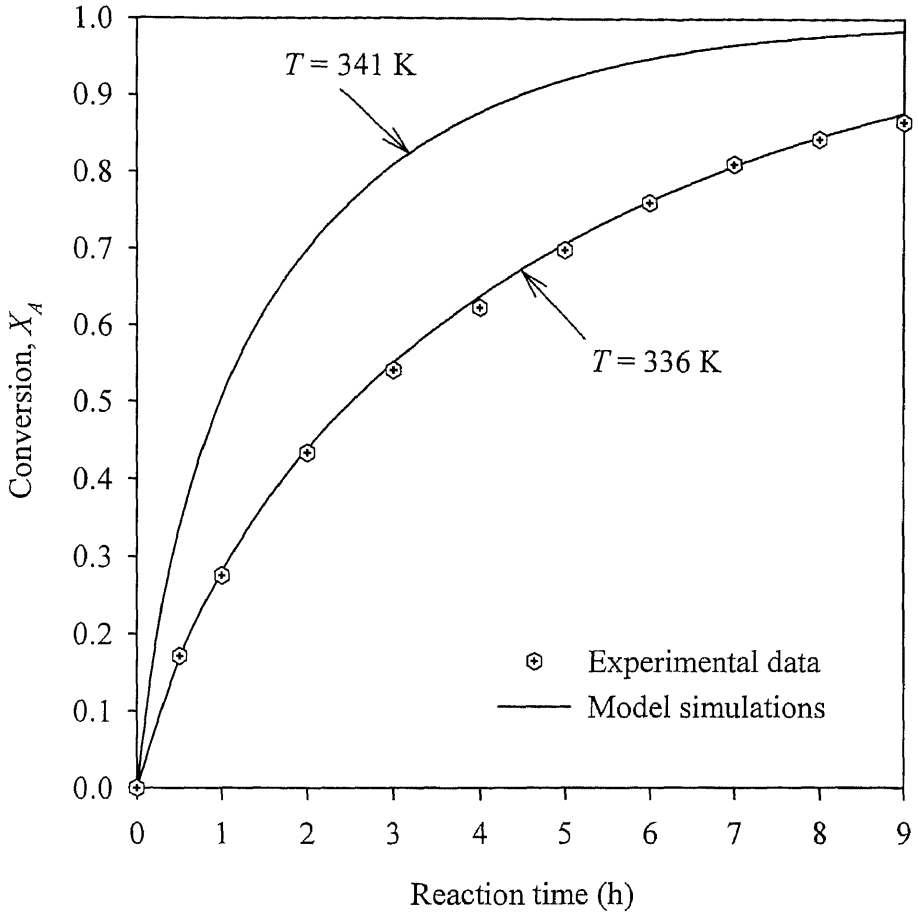

Figure C.1 Impact of Temperature Discrepancy between the Reactor Temperature and the Integrated System on Conversion-Time Profiles of the Pervaporation-Assisted Esterification

APPENDIX D

IMPACT OF METHANOL FLUX ON CALCULATED CONVERSION-TIME PROFILES OF PERVAPORATION-ASSISTED ESTERIFICATION

In the mathematical model for pervaporation-assisted esterification, the pervaporation membrane was assumed to be a perfect water permeable membrane, $J_A = J_B = J_E = 0$. However, from the analysis, the permeate consists of two components, water and methanol. Although the methanol concentration was found to be small (7.71% by volume), it may affect the calculated results for the pervaporation-assisted esterification. Therefore, a sensitivity of the methanol flux will be discussed here to determine the impact of this parameter on the model. Calculations shown here are for pervaporation-assisted esterification experiment conducted at $T = 341$ K with $\theta_B = 8$, $C_{cat} = 1.10$ M, and $A_m/V_0 = 65.9$ m^{-1}. From this experiment, the average methanol flux over a range of reaction time was calculated to be 0.1223 mol/(m^2.h).

The set of differential and algebraic equations was solved through numerical integration technique as discussed before for the set of operating parameters. One calculation was performed by setting $J_B = 0$ and another was performed by setting $J_B =$ 0.1224 mol/(m^2.h). Results of the calculations are provided in Table D.1. Errors caused by assuming $J_B = 0$ are less than –0.04%, therefore it is reasonable to use this assumption in the model.

Table D.1 Calculated Conversions for Pervaporation-Assisted Esterification at $T = 341$ K when $\theta_B = 8$, $C_{cat} = 1.10$ M, and $A_m/V_0 = 65.9$ m^{-1}

Reaction time (h)	X_A, *calc* (%) ($J_B = 0$)	X_A, *calc* (%) ($J_B = 0.1224$ mol/(m^2.h))	Percent Error
0	0.00	0.00	0.0000
1	28.09	28.09	0.0000
2	43.92	43.92	0.0000
3	55.15	55.16	-0.0181
4	63.77	63.78	-0.0157
5	70.64	70.65	-0.0142
6	76.22	76.24	-0.0262
7	80.79	80.81	-0.0247
8	84.56	84.58	-0.0236
9	87.65	87.68	-0.0342
10	90.19	90.21	-0.0222

REFERENCES

Agarwalla, S. and Lund, C. R. F., "Use of a Membrane Reactor to Improve Selectivity to Intermediate Products in Consecutive Catalytic Reaction", *J. Membrane Sci.*, **70**, 129 (1992).

Bagnell, L., Cavell, K., Hodges, A. M., Mau, A. W. H., and Seen, A. J., "The Use of Catalytically Active Pervaporation Membranes in Esterification Reactions to Simultaneously Increase Product Yield, Membrane Permselectivity and Flux", *J. Membrane Sci.*, **85**, 291 (1994).

Bart, H. J., Reidetschläger, J., Schatka, K. and Lehmann A., "Kinetics of Esterification of Levulinic Acid with n-Butanol by Homogeneous Catalysis", *Ind. Eng. Chem. Res.*, **33**, 21 (1994).

Bitterlich, S., Meissner, H. and Hefner, W., "Enhancement of the Conversion of Esterification Reactions by Non-Porous Membranes", *Proceedings of Fifth International Conference on Pervaporation Processes in the Chemical Industry* (R. Bakish, Ed.), Bakish Materials Corp., Englewood, New Jersey, 273 (1991).

Connors, K. A., The Study of Reaction Rates in Solution, Chemical Kinetics, VCH, New York, (1990).

Dams, A. and Krug, J, "Pervaporation Aided Esterification — Alternatives in Plant Extension for Existing Chemical Process", *Proceedings of Fifth International Conference on Pervaporation Processes in the Chemical Industry* (R. Bakish, Ed.), Bakish Materials Corp., Englewood, New Jersey, 338 (1991).

Dhanuka, V. R., Malshe, V. C. and Chandalia, S. B., "Kinetics of the Liquid Phase Esterification of Carboxylic Acids with Alcohols in the Presence of Acid Catalysts: Re-interpretation of Published Data", *Chem. Eng. Sci.*, **32**, 551 (1977).

DeGarmo, J. L., Parulekar, V. N., and Pinjala, V., "Consider Reactive Distillation", *Chem. Eng. Prog.*, **88**, 43 (1992).

Fogler, H. S., Elements of Chemical Reaction Engineering, PTR Prentice Hall, New Jersey, Second Edition (1992).

Gao, H., Xu, Y., Liao, S., Liu, R., Liu, L., Li, D., Yu, D., Zhao, Y. and Fan, Y., "Catalytic Polymeric Hollow Fiber Reactors for Selective Hydrogenation of Conjugated Dienes", *J. Membrane Sci.*, **106**, 213 (1995).

REFERENCES
(Continued)

Gao, H., Xu, Y., Liao, S., Liu, R., Liu, L., Li, D., and Yu, D., "Catalytic Hydrogenation and Gas Permeation Properties of Metal Containing Poly(Phenylene Oxide) and Polysulfone", *J. Appl. Polym. Sci.*, **50**, 1035 (1993).

Gao, Z., Yue, Y., and Li, W., "Application of Zeolite-Filled Pervaporation Membrane", *Zeolites*, **16**, 70 (1996).

Gobina, E. and Hughes, R., "Reaction Coupling in Catalytic Membrane Reactors", *Chem. Eng. Sci.*, **51**, 3045 (1996).

Govind, R. and Itoh, N., "Membrane Reactor Technology", *AIChE Symposium Series No. 268*, 85 (1989).

Hussain, S. Z. and Kamath, N. R., "Esterification of Salicylic Acid with Methanol: Semi-Batch Reactor Design", *Indian J. Technol.*, **5**, 92 (1967).

Huang, R. Y. M., Pervaporation Membrane Separation Processes, Elsevier, Amsterdam, (1991).

Ioannides, T. and Gavalas, G. R., "Catalytic Isobutane Dehydrogenation in a Dense Silica Membrane Reactor", *J. Membrane Sci.*, **106**, 213 (1993).

Jennings, J. F. and Binning R. C., "Organic Chemical Reactions Involving Liberation of Water", U.S. Patent 2,956,070 (1960).

Keurentjes, J. T. F., Janssen, G. H. R., and Gorissen, J. J., "The Esterification of Tartaric Acid with Ethanol: Kinetics and Shifting the Equilibrium by Means of Pervaporation", *Chem. Eng. Sci.*, **49**, 4681 (1994).

Kita, H., Tanaka, K., Okamoto, K.-I. and Yamamoto, M., "The Esterification of Oleic Acid with Ethanol Accompanied by Membrane Separation", *Chem. Lett.*, 2053 (1987).

Kita, H., Sasaki, S., Tanaka, K. Okamoto, K.-I. and Yamamoto, M., "Esterification of Carboxylic Acid With Ethanol Accompanied by Pervaporation", *Chem. Lett.*, 2025 (1988).

Kwon, S. J., Song, K. M., Hong, W. H. and Rhee, J. S., "Removal of Water Product from Lipase-Catalyzed Esterification in Organic Solvent by Pervaporation", *Biotechnol. Bioeng.*, **46**, 393 (1995).

REFERENCES
(Continued)

Leyes C. E. and Othmer, D. F., "Esterification of Butanol and Acetic Acid", *Ind. Eng. Chem.*, **37**, 968 (1945).

Mohan, K., and Govind, R., "Analysis of Equilibrium Shift in Isothermal Reactor with Permselective Wall", *AIChE J.*, **34**, 1493 (1988).

Neel, J., David, M. O., Gref, R., Nguyen, Q. T., Bruschke, H., and Schneider, W., "Esterification Reaction Assisted by Pervaporation Through a Hydrophilic Membrane", *The 1990 International Congress on Membranes and Membrane Processes*, **1**, 344 Chicago, IL (1990).

Neel, J., David, M. O., Gref, R. and Nguyen, Q. T., "Pervaporation-Esterification Coupling. I. Basic Kinetic Model", *Trans. Instn Chem. Eng.*, **69**, 335 (1991a).

Neel, J., David, M. O., Gref, R. and Nguyen, Q. T., "Pervaporation-Esterification Coupling. II. Modeling of the Influence of Different Operating Parameters", *Trans. Instn Chem. Eng.*, **69**, 341 (1991b).

Ni, X., Xu, Z. Shi, Y. and Hu, Y., "Modified Aromatic Polyimide Membrane Preparation and Pervaporation Results for Esterification System", *Water Treat.*, **10**, 115 (1995).

Okamoto, K.-I., Yamamoto, M., Otoshi, Y., Semoto, T., Yano, M., Tanaka, K., and Kita, H., "Pervaporation-Aided Esterification of Oleic Acid", *J. Chem. Eng. Japan*, **26**, 475 (1993).

Ortiz, I., Campos, D. and Irabien, J. A., "Analysis of Modeling of 1-Butyl Alcohol Esterification with Hydrobromic Acid and Sulfuric Acid as Homogeneous Catalyst," *Chem. Eng. Sci.*, **42**, 2467 (1987).

Reid, E. E., "Esterification", Unit Processes in Organic Synthesis (Edited by Groggins, P. H.), 596-642, McGraw-Hill, New York, Fourth Edition (1952).

Sanchez, N., Coteron, Martinez, M. and Aracil, J., "Kinetics Analysis and Modeling of the Esterification Reaction of Oleic Acid and Oleyl Alcohol Using Cobalt Chloride as Catalyst", *Ind. Eng. Chem. Res.*, **31**, 1985 (1992).

Sun, Y. M., Khang, S. J., "Catalytic Membrane for Simultaneous Chemical Reaction and Separation Applied to a Dehydrogenation Reaction", *Ind. Eng. Chem Res.*, **27**, 1136 (1988).

REFERENCES
(Continued)

Waldburger, R., Widmer, F., and Heinzelmann, W., "Combination of Esterification and Pervaporation in Continuous Membrane Reactor", *Chem. Ing. Technik.*, **66**, 850 (1994).

Ziaka, Z. D., Minet, R. G., and Tsotsis, T. T., "Propane Dehydrogenation in a Packed Bed Membrane Reactor", *AIChE J.*, **39**, 526 (1993a).

Ziaka, Z. D., Minet, R. G., and Tsotsis, T. T., "A high Temperature Catalytic Membrane Reactor for Propane Dehydrogenation", *J. Membrane Sci.*, **77**, 221 (1993b).

Zhu, Y., Minet, R. G. and Tsotsis, T. T., "A Continuous Pervaporation Membrane Reactor for the Study of Esterification Reactions Using a Composite Polymeric/Ceramic Membrane", *Chem. Eng. Sci.*, **51**, 4103 (1996).